Radio Science Bulletin

ISSN 1024-4530

INTERNATIONAL
UNION OF
RADIO SCIENCE

UNION
RADIO-SCIENTIFIQUE
INTERNATIONALE

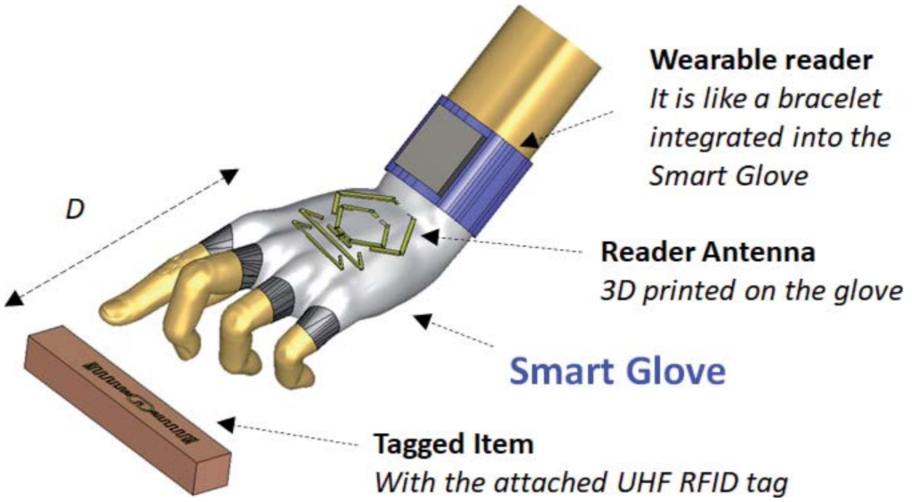

Vol. 2021, No. 377
June 2021

URSI, c/o Ghent University (INTEC)
Technologiepark - Zwijnaarde 126, B-9052 Gent (Belgium)

Contents

Cover: A schematic representation of a "smart glove" using a Yagi-like structure to create a wearable UHF-RFID antenna integrated into a glove along with a compact UHF-RFID reader. See the paper by Andrea Michel and Rajesh Kumar Singh.

Radio Science Bulletin Staff

Editor

W. R. Stone
Stoneware Limited
840 Armada Terrace
San Diego, CA 92106, USA
Tel: +1-619 222 1915, Fax: +1-619 222 1606
E-mail: r.stone@ieee.org

Editor-in-Chief

P. Van Daele
URSI Secretariat
Ghent University - INTEC
Technologiepark - Zwijnaarde 126
B-9052 Gent, BELGIUM
Tel: +32 9-264 33 20, Fax: +32 9-264 42 88
E-mail: Pet.VanDaele@UGent.be

Production Editor

I. Lievens
URSI Secretariat / Ghent University - INTEC
Technologiepark - Zwijnaarde 126
B-9052 Gent, BELGIUM
Tel: +32 9-264.33.20, Fax: +32 9-264.42.88
E-mail: ingeursi@ugent.be, info@ursi.org

Senior Associate Editor

A. Pellinen-Wannberg
Department of Physics
Umea University
BOX 812
SE-90187 Umea, SWEDEN
Tel: +46 90 786 74 92, Fax: +46 90 786 66 76
E-mail: asta.pellinen-wannberg@umu.se

Associate Editors, Commissions

Commission A

Amitava Sengupta
Department of Applied Sciences
The Northcap University, Sector 23 A, Gurgaon, Haryana
122017,India
E-mail: sengupta53@yahoo.com

Nosherwan Shoaib
Department of Electrical Engineering
National University of Sciences and Technology RIMMS,
H-12, Islamabad, Pakistan
E-mail: nosherwan.shoaib@seecs.edu.pk

Giovanna Signorile
INRiM (National Institute of Metrological Research)
Via Torrazza Piemonte 41, Turin, Italy
E-mail: g.signorile@inrim.it

Commission B

Henrik Wallén
Dept. Radio Science and Engineering
Aalto University
PO Box 13000, Otakaari 5 A, FI-00076 Aalto Finland
E-mail: henrik.wallen@aalto.fi

Dimitrios Tzarouchis
University of Pennsylvania
School of Engineering and Applied Science
220 South 33rd Street, 107 Towne Building Philadelphia,
PA 19104 USA
E-mail: dtz@seas.upenn.edu

Commission C

Pape Abdoulaye Fam
Dakar University, Senegal
E-mail: pafam@esp.sn

Ruisi He
State Key Lab of Rail Traffic Control and Safety
Beijing Jiaotong University
No. 3 Shangyuancun, Beijing 100044, China
E-mail: ruisi.he@bjtu.edu.cn

Alberto Tarable
CNR, Institute of Electronics, Information Engineering and Telecommunications
Corso Duca degli Abruzzi 24
10129 Torino, Italy
E-mail: alberto.tarable@ieiit.cnr.it

Commission D

Atsushi Kanno
Optical Access Technology Laboratory
Photonic ICT Research Center
Network Research Institute
National Institute of Information and Communications Technology
4-2-1 Nukui-kitamachi, Koganei
Tokyo 184-8795, Japan
E-mail: kanno@nict.go.jp

Commission E

Carlo Carobbi
Dipartimento di Ingegneria dell'Informazione
Università degli Studi di Firenze - UniFI
P.zza S.Marco, 4 - 50121 Firenze, Italy
E-mail: carlo.carobbi@unifi.it

Chaouki Kasmi
Directed Energy Research Center
Technology Innovation Institute
PO Box 9639, Masdar City
Abu Dhabi, United Arab Emirates
E-mail: Chaouki.Kasmi@tii.ae

Commission F

Swaroop Sahoo
Department of Electrical Engineering
Indian Institute of Technology Palakkad
Ahalia Integrated Campus
Kozhippara PO Palakkad, Kerala, India
E-mail: swaroop@iitpkd.ac.in

Commission G

Iwona Stanislawska
Polish Academy of Sciences
Space Research Centre
ul. Bartycka 18 A,00-716 Warsaw, Poland
E-mail: stanis@cbk.waw.pl

Commission H

Craig Rodger
Department of Physics
University of Otago
PO Box 56, Dunedin 9016, New Zealand
E-mail: craig.rodger@otago.ac.nz

Commission J

Richard Bradley
Technology Center
National Radio Astronomy Observatory
1180 Boxwood Estate Road
Charlottesville VA 22903, USA
E-mail: rbradley@nrao.edu

Commission K

Emily Porter
Electrical and Computer Engineering
University of Texas Austin
2501 Speedway, C0803
Austin, TX 78712 USA
E-mail: emily.e.porter@ieee.org

URSI Officers and Secretariat

Current Officers triennium 2020-2023

President

P. L. E. Uslenghi
Dept. of ECE (MC 154)
University of Illinois at Chicago 851
S. Morgan Street
Chicago, IL 60607-7053
USA
Tel: +1 312 996-6059
Fax: +1 312 996 8664
E-mail: uslenghi@uic.edu

Vice President

K. Kobayashi
Dept of Electrical, and Comm. Eng.
Chuo University
1-13-27 Kasuga, Bunkyo-ku
TOKYO, 112-8551
JAPAN
Tel. +81 3 3817 1846/69
Fax +81 3 3817 1847
E-mail kazuya@tamacc.chuo-u.ac.jp

Past President

M. Ando
Senior Executive Director
National Institute of Technology
701-2, Higashi Asakawa, Hachioji,
Tokyo 193-0834, Japan
Tel:+81-42-662-3123,
Fax: +81-42-662-3131
E-mail: ando@kosen-k.go.jp,
mando@antenna.ee.titech.ac.jp

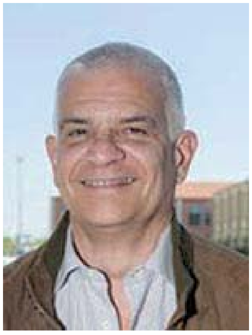

Vice President

G. Manara
Dip. di Ingegn. dell'Informazione
Universita di Pisa
Via G. Caruso 16
56122 Pisa
ITALY
Tel. +39-050-2217552
Fax +39-050-2217522
E-mail g.manara@iet.unipi.

Secretary General

P. Van Daele
URSI Secretariat
Ghent University - INTEC
Technologiepark - Zwijnaarde 126
B-9052 Gent
BELGIUM
Tel: +32 9-264 33 20
Fax: +32 9-264 42 88
E-mail: Pet.VanDaele@UGent.be

Vice President

A. Sihvola
Electronic Science Department Aalto
University
School of Electrical Engineering
PO Box 13000
FI-00076 AALTO
FINLAND
Tel: +358 50 5871286
E-mail: Ari.Sihvola@aalto.fi

Vice President

P. Doherty
Boston College
Institute for Scientific Research,
885 Centre Street
Newton, MA 2459, USA
Tel. +1 617 552 8767
Fax +1 617 552 2818
E-mail Patricia.Doherty@bc.edu

URSI Secretariat

Secretary General

P. Van Daele
URSI Secretariat
Ghent University - INTEC
Technologiepark - Zwijnaarde 126
B-9052 Gent
BELGIUM
Tel: +32 9-264 33 20
Fax: +32 9-264 42 88
E-mail: Pet.VanDaele@UGent.be

Assistant Secretary General AP-RASC

K. Kobayashi
Dept. of Electr and Commun. Eng,
Chuo University
1-13-27 Kasuga, Bunkyo-ku
Tokyo, 112-8551, JAPAN
Tel: +81 3 3817 1846/69
Fax: +81 3 3817 1847
E-mail: kazuya@tamacc.chuo-u.ac.jp

Assistant Secretary General

Stefan J. Wijnholds
Netherlands Institute for
Radio Astronomy
Oude Hoogeveensedijk 4
7991 PD Dwingeloo
The Netherlands
E-mail: wijnholds@astron.nl

Assistant Secretary General AT-RASC

W. Baan
Astron
Asserweg 45
9411 LP Beilen
THE NETHERLANDS
Tel: +31 521-595 773/100
Fax: +31 521-595 101
E-mail: baan@astron.nl

Assistant Secretary General Publications & GASS

W. R. Stone
840 Armada Terrace
San Diego, CA 92106
USA
Tel: +1-619 222 1915
Fax: +1-619 222 1606
E-mail: r.stone@ieee.org

Executive Secretary

I. Heleu
URSI Secretariat
Ghent University - INTEC
Technologiepark - Zwijnaarde 126
B-9052 Gent
BELGIUM
Tel. +32 9-264.33.20
Fax +32 9-264.42.88
E-mail info@ursi.org

Administrative Secretary

I. Lievens
URSI Secretariat
Ghent University - INTEC
Technologiepark - Zwijnaarde 126
B-9052 Gent
BELGIUM
Tel: +32 9-264.33.20
Fax: +32 9-264.42.88
E-mail: ingeursi@ugent.be

Editor's Comments

W. Ross Stone
Stoneware Limited
840 Armada Terrace
San Diego, CA 92106, USA
Tel: +1-619 222 1915, Fax: +1-619 222 1606
E-mail: r.stone@ieee.org

Special Section on 2020 URSI ITNC Young Scientist Papers

This issue contains the winner of the 2020 URSI Italian National Committee (ITNC) Young Scientist Best Paper Award "Roberto Sorrentino," and two Young Scientist papers that received Honorable Mention. These awards were presented at the annual meeting of the URSI Italian National Committee that was held virtually on November 27, 2020. A report on the meeting and an introduction to the special section is provided by Carlo Carobbi, Giuliano Manara, Giuseppe Mazzarella, and Giuseppe Schettini, who served as Guest Editors for this special section. Their efforts are gratefully acknowledged.

The paper by Jorge A. Tobon V. describes the development and testing of a prototype for a system that uses microwave imaging to monitor a brain stroke after its onset. The system used a helmet-like array of antennas, a switching system to connect the antennas to a signal-processing system, and the signal-processing system including the imaging software. The elements and operation of the system are described in detail. Considerable effort was expended in developing three-dimensional phantoms that would adequately simulate the human head and a hemorrhagic stroke environment. The experimental results validated the system's operation with different targets and positions.

Electromagnetic propagation in two-dimensional materials with thicknesses of the order of sub-nanometers is the topic of the paper by Nicola Currelia, Alessandro Fanti, Giuseppe Mazzarella, and Ilka Kriegel. Such materials have become of significant importance in a variety of device applications. This paper provides a very comprehensive overview of the various types of two-dimensional materials of importance for such applications, including a very extensive set of references to the literature on them. Optical propagation in such materials is then reviewed in depth, including in multilayer configurations. Nonlinear optics in two-dimensional materials is covered. Part of the importance of this paper is the comprehensive review and coverage of the literature it provides on the topic, along with well-written explanations of the basic physics that should be understandable by those who are not experts in the field.

Andrea Michel and Rajesh Kumar Singh have provided a paper that looks at using Yagi-like structures to create a wearable UHF-RFID antenna integrated into a glove, along with a compact UHF-RFID reader. The paper begins with a review of other "smart glove" designs, and explains the use of a power-transfer parameter to estimate the performance of a smart-glove reader antenna in terms of tag detection and reading range. A variety of Yagi-like structures, involving different combinations and numbers of directors and reflectors, was examined in an effort to optimize performance. The Specific Absorption Rate (SAR) was also calculated for the various designs. The results of the study showed that the power-transfer efficiency could be used to estimate the overall performance of such designs, and provided insight into the comparative performance of the various designs examined.

Our Other Contributions

Valerian Tatarskii was a wonderful person, and one of the founders of the theory of wave propagation in random media. Valery Zavorotny has provided us with a fascinating paper describing Prof. Tatarskii's life, career, and the development of much of his field of radio science. I urge you to read it, both as an interesting biography and as a history of the development of the theory of wave propagation in random media. The extensive list of references in this paper is of particular value.

Nosherwan Shoaib has taken over as Chair of the URSI Early Career Representative Committee, and therefore also as the ECR Associate Editor for the *Radio Science*

Bulletin. He has provided us with a report on the Young Scientist and Student Paper Competition activities at the 2021 URSI GASS.

We have very sadly lost several well-loved and respected members of our radio science community. In Memoria recognizing François Lefeuvre, Gentei Sato, Oleg A. Tretyakov, and Theodoros D. Tsiboukis appear in this issue.

Harvey Liszt has provided us with a report on the activities of IUCAF (the Scientific Committee on Frequency Allocations for Radio Astronomy and Space Science). This is an important inter-Union committee that studies and coordinates the requirements of radio-frequency spectrum allocations for passive radio sciences.

In his Telecommunications Health and Safety column, James Lin looks at the implications of 5G telecommunications technology and science for current and needed updates to health and safety regulations. This is obviously an area where ongoing efforts are needed.

In her Women in Radio Science column, Asta Pellinen Wannberg brings us a very interesting article by Dr. Rashmi Joshi, a female radio scientist from India. Dr. Joshi shares her experiences and feelings growing up and pursuing a career in science in India as a working mother in a traditional societal environment where the path she chose was anything but traditional. The sharing of her views and what she has learned along the way are greatly appreciated.

Important Deadlines Are Coming!

As the world is starting to emerge from the pandemic, conferences are starting to return to face-to-face formats. There are several important conferences for which calls for papers appear in this issue. In particular, the URSI Commissions are organizing the topics for sessions at the XXXVth General Assembly and Scientific Symposium to be held August 19-26, 2023, in Sapporo, Japan. If you have a topic you would like to see included, please contact the chair of the appropriate Commission now. The deadline for paper submissions is January 25, 2023, at www.ursi-gass2023.jp.

Maxwell Foundation Newsletter Available

The 16th Edition Part II of the James Clerk Maxwell Foundation Newsletter is available for downloading at https://clerkmaxwellfoundation.org/Newsletter_2022_Spring.pdf. The issue contains the second part of an "Homage to Heinrich Hertz" by D. O. Forfar, Trustee of the Foundation.

Introduction to the Italian Special Section: The URSI Italian National Meeting 2020

The annual meeting of the URSI Italian National Committee (ITNC) was held virtually on November 27, 2020, through a virtual platform provided by the GARR Consortium (Italian Network for Instruction and Research) of Rome, Italy. The event was held online since participation in-person was not allowed due to the Covid-19 pandemic.

The 2020 Italian URSI Meeting

The URSI ITNC meeting was co-organized with the Italian Society of Electromagnetics (SIEm), in parallel with the XXIII Riunione Nazionale di Elettromagnetismo (RiNEm – Italian National Meeting on Electromagnetics) on November 27, 2020. It was attended by several Italian researchers working in universities and research institutes.

The meeting offered a joint URSI-SIEm plenary session, and an URSI special session with three tutorials, exemplifying scientific activities in the framework of three specific URSI Commissions. As a first presentation in the URSI Special Session, the Italian Young Scientist Giulia Sacco, winner of the 2020 URSI GASS Student Paper Competition, was invited to give a speech about her awarded paper. Moreover, another URSI session was organized as the final of the 2020 URSI ITNC Young Scientist Best Paper Award, since this year named after Prof. Roberto Sorrentino, who passed away in March 2020. The final session was centered on the presentations of the selected three best papers submitted to the 2020 URSI ITNC Scientist Young Best Paper Award.

The URSI special session consisted of four presentations, three of which were contributed by URSI Scientific Commissions. It was chaired by Prof. Carlo Carobbi (University of Florence), President of the Italian URSI Committee. Prof. Carobbi briefly illustrated URSI activities in Italy and worldwide as an introduction to the session. The first presentation was given by Giulia Sacco, titled "An FMCW Radar for Localization and Vital Signs Measurement for Different Chest Orientations." In particular, she underlined that in realistic configurations for ambient assisted-living (AAL) applications, it is important to continuously and non-invasively measure the vital signals of a patient. Thanks to the ability to remotely retrieve the respiratory and heart rates, radars represent an optimal solution for this kind of application. However, during the normal daily activity, the orientation of the thorax towards the antenna is usually unknown, and it is necessary to investigate the radar performance in these conditions. More specifically, a 5.8 GHz frequency-modulated continuous wave (FMCW) radar, with ad-hoc designed wideband and low-sidelobe-level series-fed patch antennas, was used to measure vital signals. Measurements were performed in a common office environment on five volunteers having their front, left, back, and right sides facing the antenna. The signals collected by the radar were compared with those measured by a respiratory belt and a photoplethysmograph, used as references for the respiratory and heart rate, respectively. The data obtained from the five volunteers were statistically analyzed. Results revealed that independently of the orientation, the radar was able to measure the respiratory and heart rates with high accuracy.

A contribution from Commission E (Electromagnetic Noise and Interference), titled "The Threat of Radiated Intentional Electromagnetic Interference (IEMI): Deterministic and Statistical Prediction Models for Field Coupling to Cables and Systems," was then presented by Prof. Giordano Spadacini (Dipartimento di Elettronica, Informazione e Bioingegneria, Politecnico di Milano, Italy). In the presentation, it was observed that the newest technologies are pushing modern society towards an unprecedented dependence upon electronics. In this context, the protection of circuits and systems against intentional electromagnetic interference (IEMI) is gaining increasing interest. According to standard IEC 61000-2-13, IEMI exploits "intentional malicious generation of electromagnetic energy, introducing noise or signals into electric and electronic systems, thus disrupting, confusing or damaging these systems for terrorist or criminal purposes." As a special case, radiated IEMI attacks are based on the generation of electromagnetic fields with peak E-fields exceeding hundreds of V/m, made possible by high-power electromagnetic (HPEM) technology. For instance, intentional HPEM fields may encompass both narrowband waveforms having any center frequency in the GHz range, and ultra-wideband waveforms characterized by any spectral content typically above 300 MHz. After a review of the typical electromagnetic environments, the tutorial tackled the problem of modeling fields coupling to cables and systems. Many inherent uncertainties in the problem (such as the actual spectral content of the field, the direction of incidence and polarization, etc.) suggest the use of deterministic (e.g., worst-case analysis) and statistical approaches, or a combination of both, for the description of susceptibility effects.

The second tutorial was a contribution from Commission D (Electronics and Photonics). The title of the presentation was "Thermal Effects on Supermodes in Yb-Doped Multicore Fibers for High-Power Lasers." The tutorial was given by Prof. Federica Poli (Dipartimento di Ingegneria e Architettura, Università di Parma, Parma, Italy). High-power lasers, based on large-mode-area Yb-doped fibers, are becoming more and more important for many applications. The excess heat generated during the amplification process, combined with the thermo-optic effect, is responsible for an unwanted change in the fiber's refractive-index profile and, consequently, in the higher-order mode propagation in fibers that should operate in the single-mode regime. Multi-core fibers, with more than one Yb-doped core, represent a possible solution to overcome the fiber laser's output power limits caused by the thermo-optic instabilities. In particular, the impact of the thermally induced refractive-index change on the supermodes guided in Yb-doped multi-core fibers was analyzed through a finite-element-based solver with an embedded thermal model. Useful design guidelines for the choice of the core number and the core separation in the fiber's cross section were provided for different heating conditions.

The third tutorial was a contribution from Commission H, Waves in Plasmas (Including Space and Laboratory Plasmas). The title of the presentation was "RF Heating and Diagnostic Systems in Magnetic Confinement Plasma Devices for Fusion Power." It was given by Dr. Lorenzo Figini (Istituto per la Scienza e Tecnologia dei Plasmi - CNR, Milano, Italy). High-performance scenarios in magnetic-confinement plasma devices typically have a core plasma temperature of the order of tens of keV, which is in the range of plasma parameters required for fusion reactions to occur. In tokamaks, ohmic heating alone is not adequate to raise the temperature to sufficiently high values, since the plasma resistivity drops as the temperature increases. To overcome this limitation, different auxiliary plasma-heating techniques have been developed, based on either the injection of intense beams of neutral particles or the coupling of RF waves resonantly absorbed by the plasma. Each method has its own advantages and drawbacks. In this work the distinctive features of the various techniques based on RF waves were reviewed. A greater focus was put on electron cyclotron (EC) waves, which will play a major role in providing heating power to the next generation of fusion devices. In particular, the peculiarities that make EC waves attractive not only for heating, but also for the control of magneto-hydrodynamic instabilities, as well as their use as a diagnostic tool, were analyzed. Finally, it was observed that the burning plasma of future fusion reactors will also pose new challenges, demanding innovative designs for their RF-based heating systems.

The final session of the 2020 URSI ITNC Young Scientist Best Paper Award, named since this year, after Prof. Roberto Sorrentino, was chaired by Prof. Giuliano Manara (University of Pisa). Three finalists presented their papers. The judging committee was composed of Dr. Pietro Bolli (URSI Commission J), Dr. Lorenzo Crocco (URSI Commission K), and Prof. Matteo Pastorino (URSI Commission B).

The 2020 URSI ITNC Young Scientist Best Paper Award "Roberto Sorrentino" was assigned to Dr. Jorge Alberto Tobon Vasquez (Politecnico di Torino) for the paper, "A 3-D Microwave Imaging System for Brain Stroke Follow-Up: Experimental Testing." Honorary mentions were delivered to the other two finalists: Dr. Nicola Curreli for the paper, "Quadratic Gain of Optical Parametric Amplification in Artificial Crystals of WS_2," and Dr. Andrea Michel for the paper, "On the Use of Power Transfer Efficiency to Analyze the Performance of a 3D-Printed Wearable UHF RFID Antenna for Smart Gloves." The URSI award and the honorary mentions were announced during the Joint URSI-SIEm Award Ceremony.

All the participants in the Italian URSI National Meeting 2020 and XXIII RiNEm appreciated the variety of the scientific topics presented, the relevant technical applications, and the distinctive features of URSI, namely, its organization into ten Scientific Commissions with emphasis on interdisciplinarity, and its special consideration for the activities of Young Scientists.

The extended versions of the Young Scientists' papers, presented at the 2020 URSI ITNC Young Scientist Best Paper Award "Roberto Sorrentino," are published in this issue of the *Radio Science Bulletin*.

Acknowledgments

We would like to acknowledge the GARR Consortium (Italian Network for Instruction and Research) for having provided the efficient telematic wideband BlueMeet GARR system that allowed the effective participation of all the scientists registered to both the URSI Italian Meeting 2020 and the XXIII RiNEm.

Carlo Carobbi
President of the URSI Italian National Committee
E-mail: carlo.carobbi@unifi.it

Giuliano Manara
Secretary of the URSI Italian National Committee
E-mail: carlo.carobbi@unifi.it

Giuseppe Mazzarella
President of SIEm
E-mail: mazzarella@unica.it

Giuseppe Schettini
Chair of XXIII RiNEm
E-mail: giuseppe.schettini@uniroma3.it

A 3D Microwave-Imaging System for Brain Stroke Follow-Up: Review and Experimental Testing

Jorge A. Tobon V.

Department of Electronics and Telecommunications
Politecnico di Torino
10129 Turin, Italy
E-mail: jorge.tobon@polito.it

Abstract

This work describes a prototype of a novel imaging device and presents the experimental testing of it. The proposed prototype uses microwave-imaging technology to monitor a brain stroke after its onset, exploiting the different dielectric properties of human tissues. This device complements well-assessed MRI (Magnetic Resonance Imaging) and CT (Computerized Tomography), and could give clinicians fast and extra information in the decision-making stages. The system includes a helmet-like array of antennas, a switching system to connect the antennas to signal processing, the signal processing itself, and the imaging algorithm. The complete functioning prototype reconstructs the position and size of a target – representing the stroke – in a three-dimensional human-like head phantom that considers the proper tissue properties.

In this work, different sizes and positions of targets demonstrated the prototype's functioning. Although the system had low complexity, the available information guaranteed a good reconstructed image of the scenario.

1. Introduction

Accurate and fast diagnosis would improve brain-stroke treatment in the first stages. A rapid, accurate, and monitored therapy could reduce the five million deaths each year, and permanent damage in surviving patients [1].

Clinicians can follow the evolution of a first-stage patient through images of the brain or other related parameters. On the image side, the available technologies (Magnetic Resonance Imaging (MRI) or X-ray-based Computerized Tomography (CT)) provide high-resolution images of a patient's situation, with some drawbacks if we consider the first-stage constraints. These well-assessed technologies can be costly and not widely available (e.g., MRI), use ionizing radiation (CT), or require patient preparation and data-processing time. The proposed microwave-imaging (MWI) technique covers the cases where other techniques would not be available (such as bedside monitoring), or where the patient has yet to arrive at the hospital (as in an ambulance), while giving fast and continuous information on stroke evolution. It can also be a complementary imaging source while waiting for a high-resolution scan.

Microwave technology has been the core of several devices addressing brain-stroke diagnosis or monitoring developed in recent years [2-4]. There are two different approaches: a quantitative image of the brain [2], and the classification between stroke types (without imaging, directly processing the measured data) [3]. The first case requires longer computational times and a high-complexity system, while the second approach requires a large dataset of previously measured data. Recently, a quantitative imaging device was presented in [4], where a two-dimensional approach permitted the device to have lower complexity.

In this work, we present a low-complexity device designed to for brain-stroke monitoring [5] and its experimental testing. In previous work, the system was compared to a digital twin model while tested experimentally with a plastic target. Here, we go a step further towards validating the prototype in a more realistic case, considering a target that mimics a hemorrhagic stroke. The stroke monitoring goal leads to imaging a localized and "small" variation region. The proposed device creates a three-dimensional image zone of the brain affected by the stroke. The localized nature of the problem keeps complexity and processing time low. The system collects data as a scattering matrix of the complete system at two different instants. Each moment is related to a different stroke evolution. Antennas sense information related to stroke-size variation, and the system processes it through a fast linearized algorithm in a differential approach. The algorithm's linearization is possible thanks to the Born approximation [6, 7].

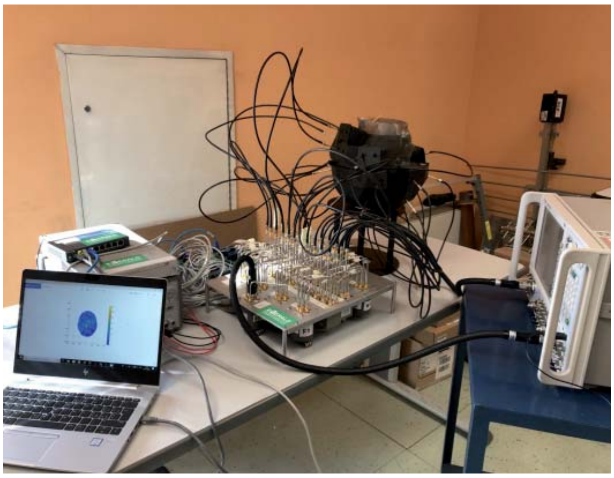

Figure 1. The complete prototype system: Control computer, vector network analyzer, switching matrix, and antenna helmet.

2. Microwave-Imaging Technique System Description

The implemented prototype, pictured in Figure 1, is comprised of four main sections: microwave sensors (antennas on the head), a switching matrix (connecting antennas to the signal source and receivers), the signal generation/acquisition system, and the control and data processing unit (where the imaging algorithm is implemented). Each section is explained in the following paragraphs.

2.1 Antenna Helmet

A rigorous method determined the number and position of the antennas around the head [7]. The proposed distribution aimed to obtain enough information from the available antennas while keeping the system's low complexity. The mentioned method also sets the system's operating frequency, trading-off between resolution (higher frequencies) and penetration (lower frequencies) in the scenario that considers a human head with layered dielectric properties. The selected frequency was 1 GHz.

The antennas were built in 24 blocks placed in contact with the head's surface (Figure 2). Each block was made of a flexible dielectric material containing a monopole printed antenna (Figure 2). The flexible material was a graphite powder and urethane rubber mix. The rubber was flexible and adaptable, and the graphite increased the permittivity. These characteristics made the material a good choice for a matching medium. The matching medium increased the signal penetration in the head, reducing the discontinuity

Figure 2a. Details of the helmet-phantom subsystem.

Figure 2b. The brick antenna.

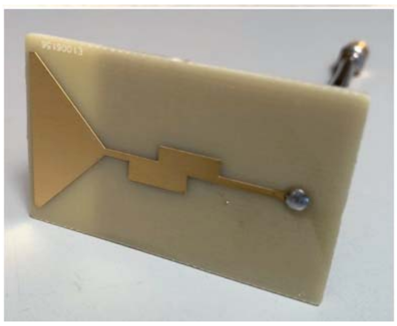

Figure 2c. The printed monopole inside the brick.

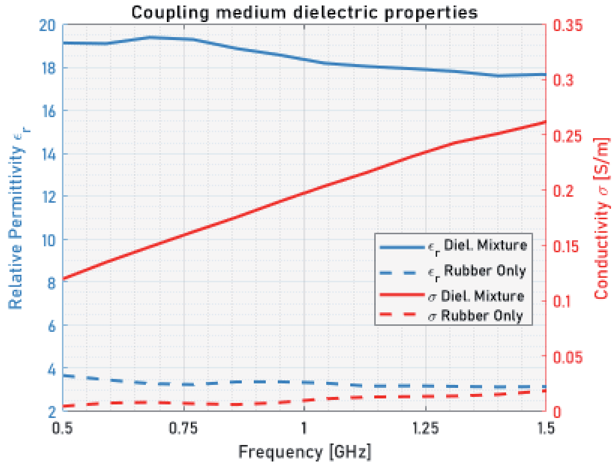

Figure 3. The measured dielectric properties of the rubber and graphite-rubber mixture.

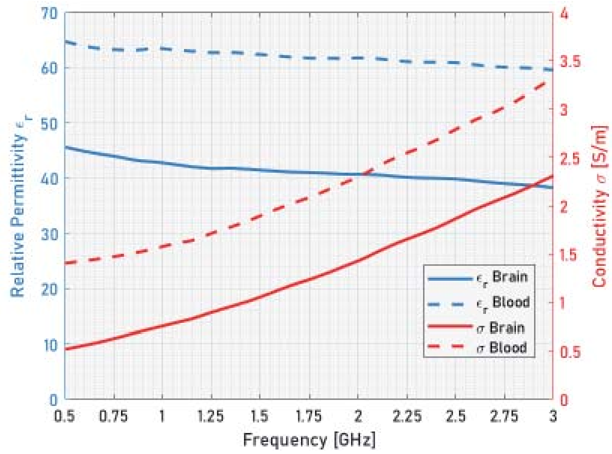

Figure 4. The measured characteristics of the liquids used in the phantom.

found by the signal that went to and from the antenna. The matching medium's dielectric properties were chosen in combination with the operating frequency, and were obtained through the proportions in the rubber-graphite mixture. The graphite presence also increased conductivity, but to levels comparable to other matching materials used in existing devices. Figure 3 depicts the dielectric properties of the mixture measured with the Keysight 85070D dielectric probe. The solid matching material had practical advantages compared to a liquid, which is the usual choice in this application.

The complete array was conformal to the head's shape, and was kept in place by a helmet made using three-dimensional printed technology (Figure 2). The antenna material system's modeling and design were made via full-wave electromagnetic software [8]. The complete prototype, and the interactions between the antennas, were also modeled through the same tool.

2.2 Generation, Acquisition, and Routing of Signals

A standard vector network analyzer (VNA) generated and received all the signals (Keysight N5227A, 10 MHz to 67 GHz). The power was set to 0 dBm, and the intermediate frequency (IF) filter was set to 10 Hz to reduce the measurement noise. Coaxial cables connected the vector network analyzer to the two ports of the switching matrix. The 2 × 24 switching matrix, made of high-isolation electromechanical coaxial switches, linked each of the 24 antennas to one of the vector network analyzer ports at different instants in time. Semi-rigid coaxial cable maximized the isolation and minimized the insertion losses in the connections between each of the routing-matrix stages. The implementation required all of the internal paths (going from each vector network analyzer port to the antennas) to have the same electrical length, avoiding different phase-shifting or attenuations for each channel [9]. Each antenna could work as a transmitter and a receiver. When one antenna was transmitting, the remaining 23 were receiving in sequence, thus obtaining a 24 × 24 scattering matrix describing the complete system. A final device implementation could substitute the vector network analyzer and switching matrix for ad hoc subsystems with, for example, off-the-shelf devices (due to their high availability and low cost in the microwave range of frequencies).

2.3 Imaging Algorithm

A personal computer (the laptop in Figure 1) was the control and processing center. Here, we focus on the processing part. The control tasks (that included switching command, vector network analyzer data acquisition, and storage) were essential for the functioning of the prototype but were not of central interest from the microwave-imaging-technique point of view.

A differential approach was a proper choice, as the application here was to monitor the stroke's time evolution [7, 9]). We will call ΔS the difference between scattering matrices collected at two separate instants, each one representing a different stroke situation. As the stroke evolves, ΔS changes, containing the information that will be our input data. The output will be a three-dimensional image of the variation of the dielectric contrast inside the brain being studied. This differential dielectric contrast, $\Delta\chi$, is defined as the ratio between the permittivity variation between two instants and the permittivity of the background at the reference instant ($\Delta\varepsilon/\varepsilon_b$). It is important to note that permittivity is in general a complex number, and that the reference instant could be related to the time where the diagnosis is first made.

The localized nature of the contrast variation permits us to take advantage of the Born approximation [10]. The relationship between ΔS and $\Delta\chi$ becomes

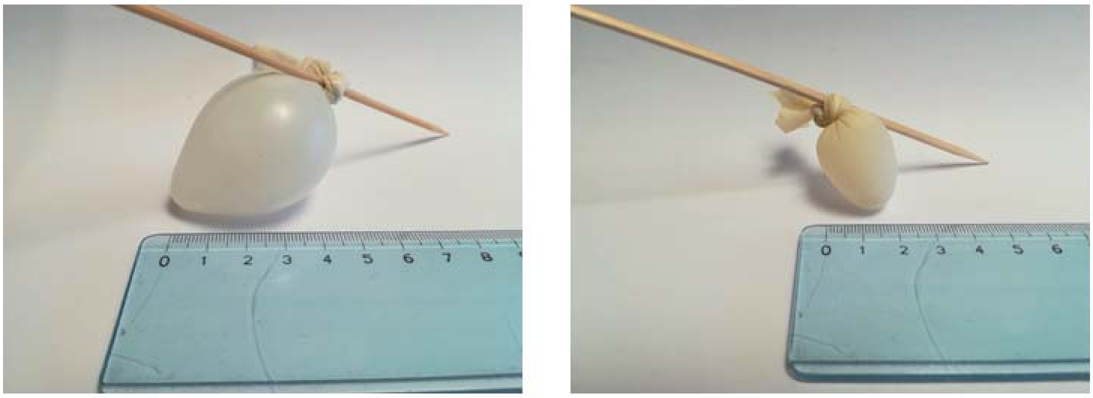

Figure 5. The blood-like targets considered. The left target is referred to in the text as the Big target. The right image is referred to as the Small target.

$$\Delta S\left(\mathbf{r}_p,\mathbf{r}_q\right)=I\left(\Delta\chi\right) \quad (1)$$

where I is a linear compact integral operator, with kernel $-j\omega\varepsilon_b / A\mathbf{E}_\mathrm{b}\left(\mathbf{r}_m,\mathbf{r}_p\right)\bullet\mathbf{E}_\mathrm{b}\left(\mathbf{r}_m,\mathbf{r}_q\right)$, where $\mathbf{r}_m$ are the points in the imaging domain, D; $\mathbf{r}_p$ and $\mathbf{r}_q$ are the positions of the transmitting and receiving antennas; and A is a "normalizing" constant related to the power applied at the antenna ports. $\omega = 2\pi f$ is the angular frequency, j is the imaginary unit, and the symbol $\bullet$ denotes the dot product between vectors $\mathbf{E}_\mathrm{b}$, the background field in the unperturbed (or reference) scenario, which is the field radiated inside the imaging domain by each element of the array. To assemble our linear operator, we calculated the background fields, $\mathbf{E}_\mathrm{b}$, using three-dimensional vectorial Finite-Element Method (FEM) full-wave simulation software. All the helmet and head geometry were modeled numerically in the mentioned software.

The inversion of Equation (1) was performed via the reliable and well-assessed truncated singular-value decomposition (TSVD) scheme [10]. We hence obtained the unknown differential contrast

$$\Delta\chi=\sum_{n=1}^{L_t}\frac{1}{\sigma_n}\left\langle\Delta S,\left[u_n\right]\right\rangle\left[v_n\right], \quad (2)$$

where $\left\langle|u|,|\sigma|,|v|\right\rangle$ are the results of a singular-value decomposition applied to the discretized operator *I*. The truncation index, L_t, is the regularization parameter to avoid the ill-poss- edness of the inverse operator, and it was selected as a trade-off between accuracy and stability.

3. Experimental Testing

The previous section described the implemented prototype and the design steps. In this section, we will present the experimental validation, starting from the phantom description.

A *phantom* is an object that mimics a body part's characteristics, permitting the device's testing before clinical-trial availability or in early-stage development. The total control of the region under test gives a high versatility during the testing, increasing the number of test cases. In this activity, we centered the interest in a human-head phantom. A three-dimensional-printed container with a human head shape was filled with a liquid mimicking the brain tissues' average characteristics. This average brain liquid was a mix of Triton x-100 (nonionic surfactant), water, and table salt. The phantom is pictured in Figure 2, while the characteristics of the liquid as a function of frequency are plotted in Figure 4. The targets used resembled a hemorrhagic stroke in size and characteristics. The dielectric properties were obtaining through another Triton x-100, water, and salt mixture that mimicked blood. The target container was a thin latex film in two different sizes, as depicted in Figure 5. At the working frequency (1 GHz), the blood-mimicking liquid characteristics were $\varepsilon_r = 63.41$ and $\sigma = 1.75$ S/m, while for the average brain-mimicking liquid they were $\varepsilon_r = 42.37$ and $\sigma = 0.77$ S/m. These values were measured in a wider frequency range using the dielectric probe Keysight 85070D already mentioned in the antenna section. The design of the phantom design and the recipes for the liquids are available in [11].

The measurements comprised two steps. In the first step, we measured our prototype-phantom system's scattering matrix with no target inside. We then put the target inside and took the second scattering-matrix measurement. The liquid nature of the phantom facilitated the insertion of the target. The transparency of the liquids and the head container permitted external confirmation that the position was the desired position. Some uncertainties in position were due to the viscosity and the difference in density between the two liquids involved (the blood-mimicking and brain-mimicking liquids), as the target tended to float and move. However, these uncertainties in the placement did not diminish system reliability. Each measured set was a complete 24 × 24 scattering matrix. The difference between the two situations was the input for the truncated singular-value decomposition algorithm.

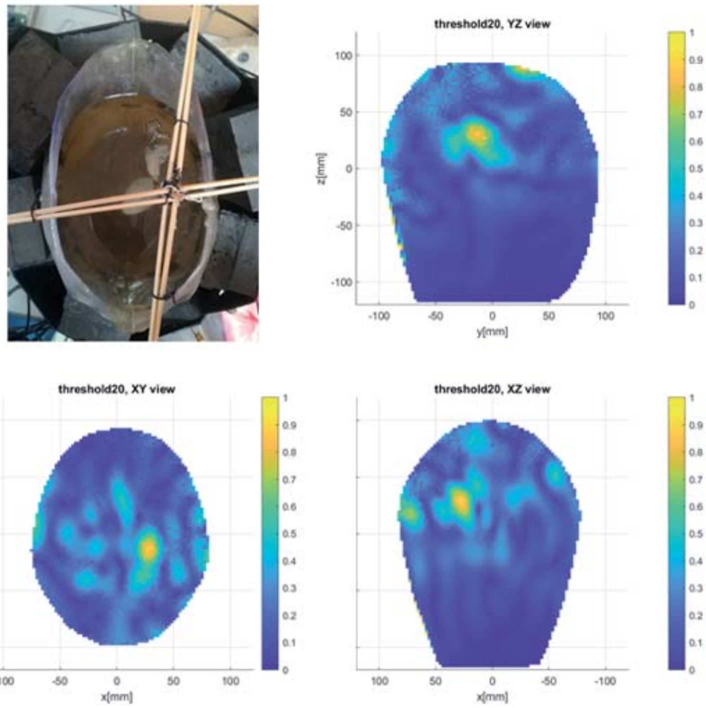

Figure 6. The reconstruction of the big target in Position 1: A photo of the real position and the three main planes centered at the reconstructed target.

The first case tested corresponded to a blood target called "Big" in the following (on the left in Figure 5). This target's size is presented here in two different positions. The results are depicted in Figures 6 and 7. The reader can find a picture of the experimental configuration and the normalized reconstructed target images in three different cuts for all the cases. Each cut is in one of the Cartesian planes that passed by the located target. A good and focalized target was reconstructed in both cases by the truncated singular-value decomposition. The size was also in agreement with the actual inserted object.

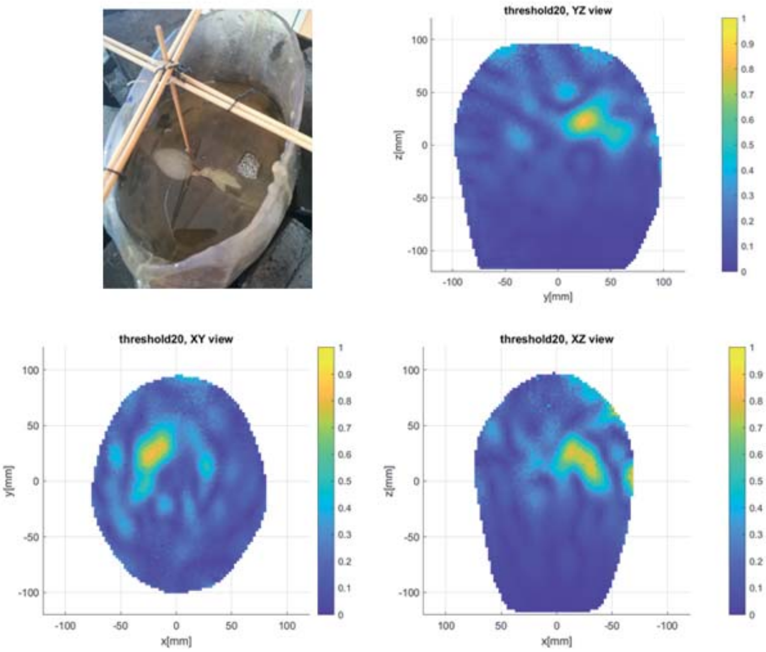

Figure 7. The reconstruction of the big target in Position 2: A photo of the real position and the three main planes centered at the reconstructed tarFigure 8. The reconstruction of the small target: A photo of the real position and the three main planes centered at the reconstructed target.

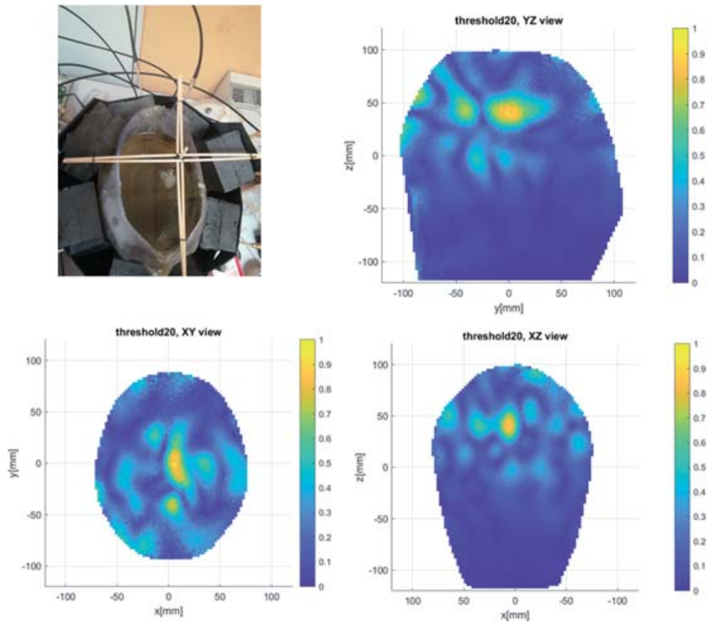

Figure 8. The reconstruction of the small target: A photo of the real position and the three main planes centered at the reconstructed target.

A smaller and more challenging blood target (called "Small" in the following, on the right in Figure 5) was reconstructed in Figure 8. In this case, the reconstruction seemed more affected by artifacts, but a well-defined target was still present. This case was considered more challenging because the reduced target size meant a lower perturbation of the field perceived by the antennas (while the contrast was the same as in the previous cases), which could be affected by noise or system inaccuracies. However, the good reconstruction confirmed that the system could also detect small intrusions.

The time required to complete the measurements and reconstruction was in line with continuous monitoring. The total scan took around four minutes for each of the differential measurements, but it could be optimized in a non-prototypal solution. The linearized operator's kernel was calculated offline, while the data processing by the truncated singular-value decomposition took less than one second.

4. Conclusions and Perspectives

Here we have described and experimentally tested a three-dimensional imaging system for brain-stroke monitoring. The device's design guarantees the adequate quantity of information needed to reconstruct the position and size of an unknown target located inside the brain. The experimental validation we presented here involved a simplified but realistic head phantom with a target representing a hemorrhagic stroke. The results presented validated the system's behavior with different targets and positions. The next steps in the research comprise the microwave-imaging technique system's testing with more-complex phantoms (considering more tissue layers), and an exhaustive measurement campaign with targets of different sizes and characteristics (such as the ischemic type of stroke).

5. Acknowledgments

This work was supported by the Italian Ministry of University and Research under the PRIN project "MiBraScan – Microwave Brain Scanner for Cerebrovascular Diseases Monitoring." The author thanks Lorenzo Crocco (Institute for the Electromagnetic Sensing of the Environment, National Research Council of Italy, Naples, Italy) and Prof. Francesca Vipiana (Department of Electronics and Telecommunications, Politecnico di Torino, Turin, Italy) for their contributions and guidance.

6. References

1. A. S. M. Alqadami, K. S. Bialkowski, A. T. Mobashsher, and A. M. Abbosh, "Wearable Electromagnetic Head Imaging System Using Flexible Wideband Antenna Array Based on Polymer Technology for Brain Stroke Diagnosis," *IEEE Trans. Biomed. Circuits Syst.*, **13**, 1, February 2019, pp. 124-134.

2. Emelia J. Benjamin, Paul Muntner, and Márcio Sommer Bittencourt, "Heart Disease and Stroke Statistics-2019 Update: A Report from the American Heart Association," *Circulation*, **139**, 10, 2019, pp. e56-e528.

3. M. Bertero and P. Boccacci, *Introduction to Inverse Problems in Imaging*, Bristol, UK, Inst. Phys., 1998.

4. Andreas Fhager, Stefan Candefjord, Mikael Elam, and Mikael Persson, “Microwave Diagnostics Ahead: Saving Time and the Lives of Trauma and Stroke Patients,” *IEEE Microwave Magazine*, **19**, 3, May 2018, pp. 78-90.

5. M. Hopfer, R. Planas, A. Hamidipour, T. Henriksson, and S. Semenov, “Electromagnetic Tomography for Detection, Differentiation, and Monitoring of Brain Stroke: A Virtual Data and Human Head Phantom Study,” *IEEE Antennas Propag. Mag.*, **59**, 5, October 2017, pp. 86-97.

6. Nadine Joachimowicz, Bernard Duchêne, Christophe Conessa, and Olivier Meyer, “Anthropomorphic Breast and Head Phantoms for Microwave Imaging,” *Diagnostics*, **85**, 8, December 2018, pp. 1-12.

7. D. O. Rodriguez-Duarte, J. A. Tobon Vasquez, R. Scapaticci, L. Crocco, and F. Vipiana, “Brick Shaped Antenna Module for Microwave Brain Imaging Systems,” IEEE Antennas and Wireless Propagation Letters, 2020.

8. R. Scapaticci, O.M. Bucci, I. Catapano, and L. Crocco, “Differential Microwave Imaging for Brain Stroke Follow Up,” *Int. J. Antennas Propag.*, 2014, 11 pages, 2014 (Article ID 312528).

9. R. Scapaticci, J. A. Tobon Vasquez, G. Bellizzi, F. Vipiana, and L. Crocco, “Design and Numerical Characterization of a Low-Complexity Microwave Device for Brain Stroke Monitoring,” *IEEE Trans. Antennas Propag.*, **66**, December 2018, pp.7328-7338.

10. Jorge A. Tobon Vasquez, R. Scapaticci, G. Turvani, G. Bellizzi, N. Joachimowicz, B. Duchêne, E. Tedeschi, M. R. Casu, L. Crocco, and F. Vipiana, “Design and Experimental Assessment of a 2D Microwave Imaging System for Brain Stroke Monitoring,” *Int. J. Antennas Propag.*, 2019 (Article ID 8065036),12 pages.

11. J. A. Tobon Vasquez, R. Scapaticci, G. Turvani, G. Bellizzi, D. O. Rodriguez-Duarte, N. Joachimowicz, B. Duchêne, E. Tedeschi, M. R. Casu, L. Crocco, and F. Vipiana, “A Prototype Microwave System for 3D Brain Stroke Imaging,” *SENSORS*, **20**, 9, 2020.

Linear and Nonlinear Optical Propagation in 2D Materials

Nicola Currelia[1], Alessandro Fanti[2], Giuseppe Mazzarella[2], and Ilka Kriegel[1]

[1]Functional Nanosystems
Istituto Italiano di Tecnologia
via Morego 30, 16163 Genova, Italy

[2]Department of Electric and Electronic Engineering
University of Cagliari
Via Marengo 2, 09123 Cagliari, Italy

Abstract

Recently, a lot of effort has been dedicated to developing next-generation optoelectronic devices based on two-dimensional materials, thanks to their unique optical properties that are significantly different from those of their bulk counterparts. In order to implement high-performance nanoscale optical devices, an in-depth study of how linear and nonlinear propagation occurs in two-dimensional materials is required. We focus here on the theory behind the propagation of electromagnetic waves in two-dimensional materials, as well as emerging applications in the fields of electronics, optics, and sensors that are summarized and discussed in the paper.

1. Introduction

Over the last 15 years, the study of two-dimensional (2D) materials has rapidly progressed in a variety of scientific and engineering subfields [1, 2]. Compared to their conventional bulk counterparts, two-dimensional materials exhibit electronic confinement effects within two dimensions because their thickness is of the order of sub-nanometers [3-5]. The types of two-dimensional materials available have been continuously growing, including insulators, semiconductors, and a plethora of metals and semimetals [6-22]. Their tunable optical and electronic properties [23-25] and their easy integration allow improving the performance of optoelectronic devices thanks to their photo response [26-32], as well as

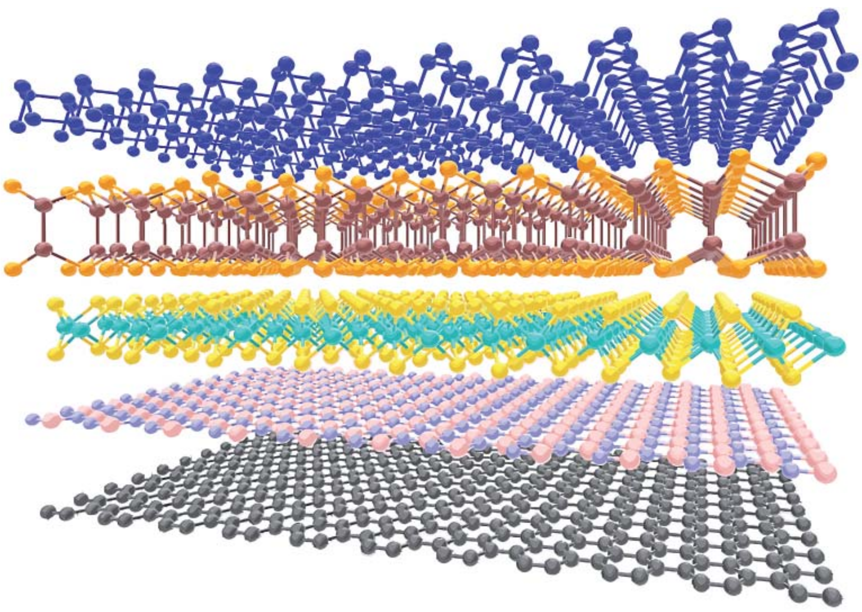

Figure 1. A sketch of several two-dimensional materials. From top to bottom: phosphorene, InSe, MoS_2, h-BN, and graphene.

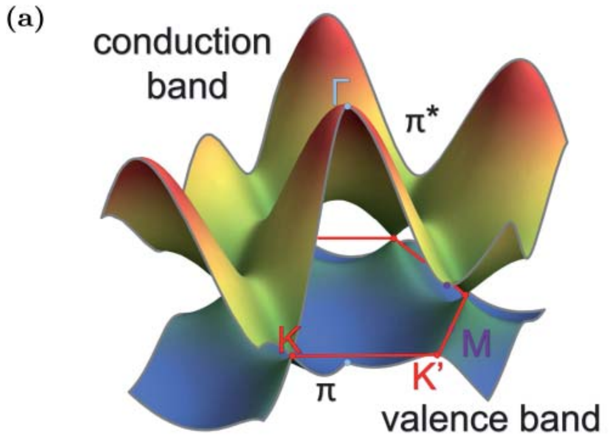

Figure 2a. The electronic energy dispersion of graphene throughout the whole region of the Brillouin zone.

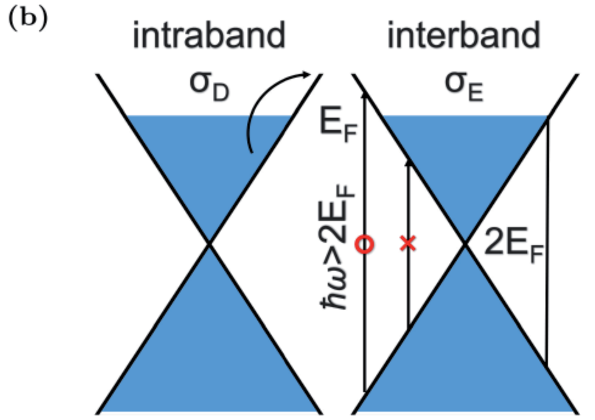

Figure 2b. The dispersion around the K point: on the left, the intraband transition of the electron, while on the right, the interband transition of the electron, which occurs if $\hbar\omega > 2E_F$.

in data-communications, telecommunications [33], and energy-storage applications [34]. In fact, the properties of two-dimensional materials are determined by their structural features, in which dimensionality plays a fundamental role [35, 36]. When approaching the two-dimensional nature of crystals – defined as an infinite crystalline in-plane periodic structure with atomic thickness – novel peculiar properties arise [37]. In addition to their unique electronic and optical properties, these materials show high mechanical strength and flexibility [38]. Quantum confinement in the direction perpendicular to two-dimensional crystal's planes promotes a longer mean free path of electrons, excitons, phonons, and ballistic in-plane transport without scattering or diffusion [35, 39, 40]. Moreover, the two-dimensional geometry is compatible with the design and implementation of optical devices finding applications in electronics, optics, and many other fields [41]. For these reasons, in this article we focus on the theoretical and experimental research of linear and nonlinear optical propagation and effects caused by different electromagnetic external stimuli in two-dimensional materials.

2. Electronic and Optical Properties of Two-Dimensional Materials

Since the discovery of graphene [42], new materials have been added to the family of two-dimensional materials at an increasing pace. Among them, the most interesting are hexagonal boron nitride (h-BN) [35, 43, 44], transition-metal dichalcogenides (TMDs, such as MoS_2, $MoSe_2$, WS_2, WSe_2) [44, 45], silicene [46, 47], germanene [48], stanene [49], phosphorene [50-52], borophene [53, 54], just to cite a few. All of these materials cover the entire spectrum of electrical conductivity, from (semi)metals (e.g., graphene and borophene) and semiconductors (e.g., TMDs) to insulators (e.g., h-BN) (Figure 1).

2.1 Graphene

Graphene is a two-dimensional crystal formed by carbon atoms arranged in a hexagonal honeycomb lattice. The electronic structure of graphene can be derived through a tight-binding model, in which Dirac cones are found at the corners of the Brillouin zone (Figure 2a) [53, 56]. In the proximity of these points, charge carriers obey a linear dispersion relation:

$$E = \pm v_F p \,, \tag{1}$$

where E and p are the energy and the momentum measured with respect to the Dirac points, $v_F = 10^6\ \mathrm{ms}^{-1}$ is the Fermi velocity, while the plus and minus signs refer to the conduction and valence bands, respectively [56]. The bands with conical dispersion intersect at the Fermi energy, thus making graphene a semimetal. As a result, an additional chiral symmetry exists, fixing a parallel or anti-parallel pseudospin to the directions of motion of the carriers [56, 57]. This contributes to peculiar effects on the electronic and optical properties of graphene. For example, for undoped samples at $0\ \mathrm{K}$, the universal optical conductivity of graphene – which links the surface-current density, $\mathbf{J}$, to the electric field, $\mathbf{E}$ ($\mathbf{J} = \bar{\sigma}\mathbf{E}$) – is independent of any material parameter:

$$\sigma_0 = \frac{e^2}{4\hbar} \sim 6.08 \times 10^{-5}\,\mathrm{S}\,, \tag{2}$$

where e is the electron's charge and $\hbar$ is the reduced Planck's constant. The transmission for a single-layer graphene is thus given as [57-60]

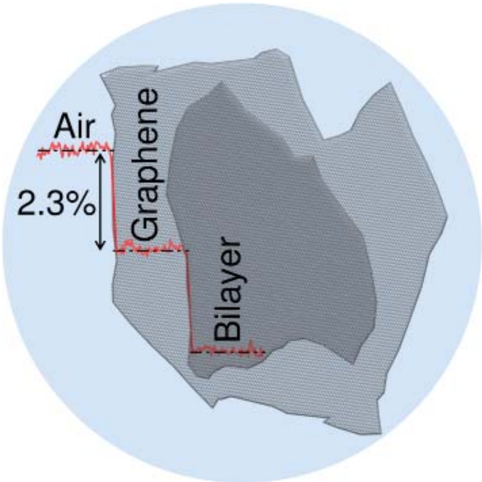

Figure 3. A schematic diagram of the intensity of white light transmitted through graphene and bilayer graphene. The dashed-line scan profile shows the intensity between layers.

$$T = (1+0.5\pi\alpha)^{-2} \sim 1-\pi\alpha \sim 97.7\% \,, \quad (3)$$

where $\alpha = e^2/(4\pi\varepsilon_0\hbar c) = \bar{\sigma}_0/(\pi\varepsilon_0 c) \sim 1/137$ is the fine-structure constant [58, 60]. Notably, the optical absorption depends only on the fine-structure constant, and is given by $A \sim 1-T \sim \pi\alpha \sim 2.3\%$, considering that for a monolayer the reflection contribution (R) is less than 0.1% (Figure 3) [60]. On the other hand, doping has a strong effect on optical properties [57, 61], because of the so-called Pauli blocking [57]. In fact, Pauli blocking ensures that photons with energy ($\hbar\omega$) less than $2E_F$ (where E_F is the Fermi energy) cannot be absorbed (Figure 2b) [56-58, 62].

The conical dispersion of low-energy carriers in graphene is very different from other materials' parabolic dispersion [55, 56]. For example, bi-layer graphene presents parabolic dispersion at the Fermi energy, and a small bandgap of up to 250 meV that can be opened with an electric field [58, 63, 64]. In the case of multiple-layer structures (such as bi-layer or few-layer graphene), it is possible to consider an optically equivalent superposition of almost non-interacting single-layer graphene flakes in which each layer can be seen as a two-dimensional electron gas with little perturbation from the adjacent layer [65]. For few-layer graphene, the contribution of the reflection becomes more prominent, reflecting $\sim 2\%$ of the incident light for ten-layer crystals [65].

Frequency-independent absorption of graphene along with extremely high carrier mobility has attracted the interest of the scientific community. In fact, graphene has rapidly established itself as a building block for optoelectronic applications, with a strong focus on various photodetection platforms. The versatility of this material enables its application in areas including ultra-fast and ultra-sensitive detection of light in the broadband spectral region between the ultraviolet and infrared frequency ranges [66, 67]. These detectors can be integrated with other photonic components based on the same material, as well as with other two-dimensional materials, such as transition metal dichalcogenides, silicon photonic, and electronic technologies [68]. Furthermore, in a single layer of graphene [69], the interband transition photoelectrons are modulated by a driving voltage over a wide band in order to obtain an optical modulator with a bandwidth in the near-infrared region of over 1 GHz [66, 70-75]. Another interesting research direction is graphene's use in flexible electronic devices, such as touch screens [58], electronic paper, organic photovoltaic cells [76] and organic light-emitting diodes [77], thanks to its flexibility as well as its low surface resistance and high transmittance.

2.2 Transition Metal Dichalchogenide Monolayers

The interesting properties of graphene have led to the discovery and study of other two-dimensional crystals and heterostructures thereof, showing exciting optical properties that differ from their bulk counterparts. Transition-metal dichalcogenides (TMDs) are probably the second-most-

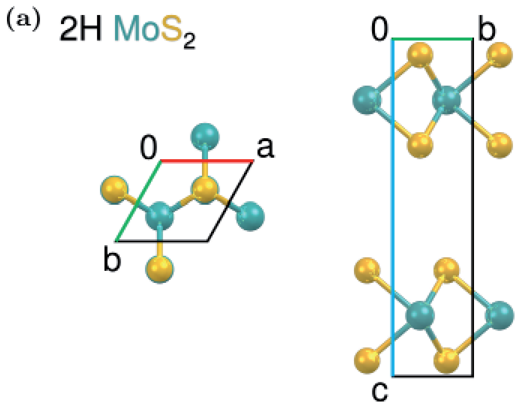

Figure 4a. The 2H crystal structure.

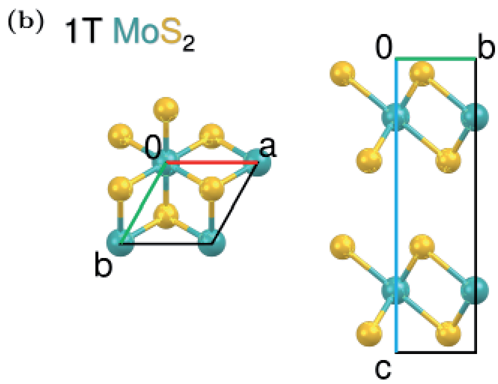

Figure 4b. The 1T MoS_2 crystal structure.

studied two-dimensional material class after graphene. They are a family of materials with MX_2 chemical formula, where M is a transition metal and X is a chalcogen such as S, Se, or Te [45, 55]. The TMDs' atomic and electronic structure consists of a layer of M atoms inserted between two atomic layers of X atoms, with a hexagonal unit cell having D_{3h} symmetry and a thickness of ~ 0.7 nm [45, 78-80]. Within the TMDs, it is possible to find metallic (e.g., VS_2 and NbS_2), semiconducting (e.g., MoS_2 and WS_2), or insulating (e.g., HfS_2) materials [45, 80]. The TMD crystals show different polyforms [45, 80]. Typical crystal structures include trigonal prismatic 1H (2H for multilayer), 1T, and 1T′ (i.e., distorted-1T) phases [37, 41, 81], as shown in Figure 4. The most stable crystalline configuration is the 2H-stacking (also known as AB-stacking) [45, 55, 82]. In particular, semiconducting 2H TMDs show peculiar optical and electronic properties, fundamentally different from their three-dimensional bulk counterparts. For example, MoS_2 [78, 79, 83], $MoSe_2$ [55, 84], WS_2, and WSe_2 [85] undergo a crossover from indirect to direct gap when going from bi-layer to monolayer form. In the case of MoS_2, bulk crystals have an indirect bandgap of the order of 1.29 eV, while in its two-dimensional form, MoS_2 presents a direct bandgap [57, 83] of ~ 1.9 eV around the K points of the Brillouin zone. This leads to pronounced luminescence enhancement [78].

2.3 Other Two-Dimensional Materials

Similarly, layered post-transition metal chalcogenides of group-III, such as GaS, GaSe, SnS, SnS_2, and InSe, are also being explored due to their high mobilities, large photo responses, and in-plane anisotropy [82, 86]. They present different polytypes that vary with respect to their layer-stacking configuration, namely, the group-IV monochalcogenides (e.g., SnS and GeSe) [87] or the 1T dichalcogenides (e.g., SnS_2) [82]. Moreover, there is also the family of two-dimensional transition metal carbides, nitrides, and carbonitrides, which are known as MXenes with the following chemical formulas: M_2X, M_3X_2, and M_4X_3, where M is an early transition metal and X is a carbon or a nitrogen atom [88]. They exhibit interesting mechanical properties as well as good thermal and electrical conductivity [82].

In addition, wide-bandgap two-dimensional materials play a key role in device implementation. For example, thanks to its inert nature, insulating characteristics, and ultra-flat structure, hexagonal boron nitride (h-BN) acts as a substrate or sacrificial layer for high-mobility two-dimensional crystal-based devices [89].

Other wide-bandgap materials, including transition metal oxides (TMO: e.g., MoO_2 with 2H-phase, MnO_2 with 1T-phase, and á-MoO_3) and chromium oxide (i.e., Cr_2O_3), known for its multiferroic properties [90], exhibit hyperbolic optical behavior [82, 91]. Other examples of layered materials include elementary two-dimensional materials, such as phosphorus allotropes (e.g., black and blue phosphorus) [51], silicene [92], germanene [93], tellurene [94], gallenene [95], antimonene [96], and borophene [97], which range from metallic to semiconductor as well as topological insulators (for example, Bi_2Se_3 and Sb_2Se_3), known for their topologically protected and spin-momentum-locked electronic transport [82, 98].

3. Optical Propagation in Two-Dimensional Materials

In this section, the electromagnetic surface wave [99] that propagates in a direction parallel to the two-dimensional material layer, as well as the transmission and reflection of electromagnetic waves by a periodic structure consisting of *N* layers, will be investigated.

3.1 The Electromagnetic Surface Wave in Two-Dimensional Materials

An electromagnetic surface wave is a field configuration essentially confined in a small region close to the interface between two dielectric media, and propagating in the direction along the interface itself [100-106]. Here, we consider only plane interfaces and choose a Cartesian reference frame with the z axis normal to the interface (Figure 5). In order to model the linear optical description of single-layer crystals, two possible approaches can be followed. The first approach consists of treating a two-dimensional material as a real two-dimensional layer, which imposes a discontinuity on the in-plane magnetic field: $\Delta H_{\parallel} = \bar{\sigma}(\omega) E_{\perp}$. Here, subscripts $\parallel$ and $\perp$ denote in-plane and out-of-plane field components, respectively, and $\bar{\sigma}(\omega)$ refers to the complex optical conductivity. In this case, the system is intrinsically anisotropic with both null out-of-plane surface susceptibility ($\chi_{\perp}$) and conductivity ($\sigma_{\perp}$) [107-111]. A second approach consists of treating the two-dimensional material as an equivalent three-dimensional layer having an out-of-plane dielectric constant of the bulk crystal, and an in-plane dielectric constant. In the case of graphene, the in-plane dielectric constant is given by [112]

$$\varepsilon_G(\omega) = 1 + i\frac{\bar{\sigma}(\omega)}{\omega \varepsilon_0 t_G}, \tag{4}$$

with ω being the optical angular frequency and $t_G = 0.34$ nm being the thickness of the graphene mono-layer [113]. Previous works numerically verified that the two approaches lead to indistinguishable results [114-116]. For this reason, the first approach was analyzed in this review. However, it is worth noting that the out-of-plane optical constants of two-dimensional materials have proven to be experimentally elusive, and the established models that make use of an exclusively in-plane surface current are not sufficient to

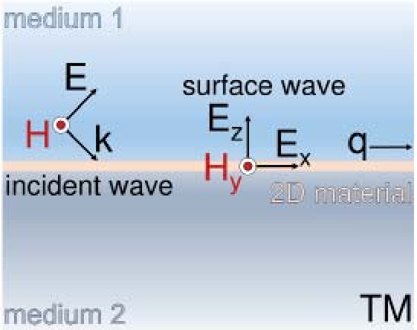

Figure 5a. A TM surface wave in two-dimensional materials. The two-dimensional material is shown as the orange color with negligible thickness.

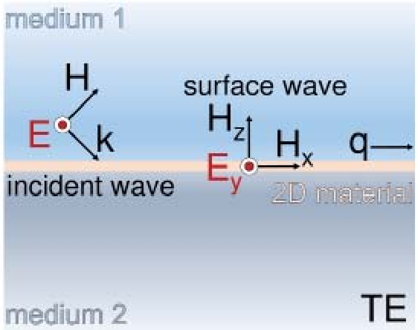

Figure 5b. A TE surface wave in two-dimensional materials. The two-dimensional material is shown as the orange color with negligible thickness.

correctly describe a two-dimensional crystal [117]. By our convention, the surface wave propagates in the x direction and the field decays in the z direction. The basic principle behind the phenomenon of the surface waves is the solution of Maxwell's equations at the interface. From this, it is possible to obtain the result that surface waves are excited by external incident electromagnetic waves [100, 106, 118]. Surface plasmon polaritons (SPPs) are a particular type of electromagnetic surface wave traveling along a metal-dielectric or metal-air interface in the infrared or visible-frequency range. The physical characteristics of surface plasmon polaritons in metals are determined by their intrinsic properties and the geometry of the material. The thickness plays a very important role in the physical propagation of surface plasmon polaritons. In fact, more recently it has been found that two-dimensional materials inserted at the interface between dielectrics support surface plasmon polaritons thanks to the strongly confined electric field as the thickness approaches the atomic level and light is being confined to dimensions two to three orders of magnitude smaller than that of the free-space wavelength [119]. The polarization of the incident waves determines the polarization of surface waves. It is therefore possible to find transverse-magnetic (TM) and transverse-electric (TE) surface waves, determining the components of the field for each surface wave. In the TM surface wave, the incident field has a component of a magnetic field perpendicular to the incidence plane (Figure 5a), while in the TE surface wave, the incident field has a component of an electric field perpendicular to the incidence plane (Figure 5b).

3.1.1 Field Configuration at TM Surface Wave

For a TM surface wave, E_x, E_z, H_y field components are considered, and it is assumed that the two-dimensional material is surrounded by two dielectric media, 1 and 2, as shown in Figure 5a. The TM surface wave propagates on the surface of the two-dimensional material in the x direction with wave vector in the direction of propagation ($\overline{q} = q\overline{x}$). In medium 1, the electromagnetic fields of the TM surface wave are given by [100]

$$E_x^{(1)} = E_1 e^{iqx} e^{-\kappa_1 z},$$

$$E_z^{(1)} = \frac{iq}{\kappa_1} E_x^{(1)}, \tag{5}$$

$$H_y^{(1)} = -\frac{i\omega\varepsilon_0\varepsilon_1}{\kappa_1} E_x^{(1)},$$

while in medium 2,

$$E_x^{(2)} = E_2 e^{iqx} e^{\kappa_2 z},$$

$$E_z^{(2)} = -\frac{iq}{\kappa_2} E_x^{(2)}, \tag{6}$$

$$H_y^{(2)} = \frac{i\omega\varepsilon_0\varepsilon_1}{\kappa_2} E_x^{(2)},$$

where $E_x^{(i)}$, $E_z^{(i)}$, and $H_y^{(i)}$ are the electric fields in the x, y, and z directions, respectively; E_i is the amplitude of the electric field in the x direction for the ith medium ($i = 1, 2$); ε_0 and ε_1 are the dielectric constants of the vacuum and the medium, respectively; and κ_i is the decay constant of the fields inside the ith medium, given by

$$\kappa_i = \sqrt{q^2 - \omega^2 \varepsilon_i / c^2}\,. \tag{7}$$

The magnetic and the electric fields are related by the following relations:

$$E_x^{(i)} = -\frac{i}{\omega\varepsilon_0\varepsilon_i} H_y^{(i)} z, \tag{8}$$

$$E_z^{(i)} = -q / (\omega \varepsilon_0 \varepsilon_i) H_y^{(i)} , \tag{9}$$

which can be derived from Maxwell's equations [100]. Due to the presence of surface currents that flow on the two-dimensional material, the magnetic-field components are not continuous. The boundary conditions of the electromagnetic wave on the surface of the two-dimensional material are therefore given by

$$E_x^{(1)} = E_x^{(2)} , \tag{10}$$

$$H_y^{(1)} - H_y^{(2)} = -J , \tag{11}$$

where $J = \bar{\sigma}(\omega) E_x^{(2)}$ is the surface current on the two-dimensional material, and $\bar{\sigma}(\omega)$ is the complex optical conductivity of the two-dimensional material. Since a two-dimensional material presents a negligible thickness when compared to the wavelength in the materials, J appears only in the boundary conditions.

In the case of graphene, there are two contributions to $\bar{\sigma}(\omega)$, corresponding to two possible optical scatterings or excitations of electrons by photons. These are the intraband transition (within the same conduction band) and the interband transition (from valence to conduction band), as shown in Figure 2b. The real and imaginary parts of $\bar{\sigma}(\omega)$ are related by the closed formula for the complex optical conductivity, given by the following equation [108, 112]:

$$\bar{\sigma}(\omega) \equiv \sigma_D + \mathrm{Re}\{\sigma_E\} + i\,\mathrm{Im}\{\sigma_E\} = \tag{12}$$

$$= i \frac{4\bar{\sigma}_0}{\pi} \frac{E_F}{\hbar\omega + i\Gamma}$$

$$+ \frac{\bar{\sigma}_0}{2} \left[tanh\left(\frac{\hbar\omega + 2E_F}{4k_B T} \right) + tanh\left(\frac{\hbar\omega - 2E_F}{4k_B T} \right) \right]$$

$$- i \frac{\bar{\sigma}_0}{2\pi} \ln\left[\frac{(\hbar\omega + 2E_F)^2}{(\hbar\omega - 2E_F)^2 + (2k_B T)^2} \right] ,$$

where $k_B T$ is the product of the Boltzmann constant, k_B and the temperature, T. The first term in Equation (12), σ_D, is the intraband conductivity (or Drude conductivity) [120-122], while the second and the third terms correspond to the real part and the imaginary part of interband conductivity (σ_E), respectively [121-123]. The spectral width (Γ) is a parameter that describes the scattering rate with phonons due to the impurities and depends on the Fermi level **(E_F) as**

$$\Gamma = \hbar e v_F^2 \big/ \mu E_F , \tag{13}$$

where $v_F = 10^6$ m/s is the Fermi velocity of graphene and $\mu = 10^4\ \mathrm{cm}^2/\mathrm{Vs}$ is the mobility for ideal graphene [120]. For simplicity, it is possible to consider the limiting case for $T \to 0$ [120-125]:

$$\bar{\sigma}(\omega)|_{T=0} = i \frac{4\bar{\sigma}_0}{\pi} \frac{E_F}{\hbar\omega + i\Gamma} \tag{14}$$

$$+ \bar{\sigma}_0 \delta_{-1}\left(\hbar\omega - 2E_F\right) - i \frac{\bar{\sigma}_0}{\pi} \ln\left| \frac{\hbar\omega + 2E_F}{\hbar\omega - 2E_F} \right| ,$$

where $\delta_{-1}(x)$ is the Heaviside step function. For $\hbar\omega < 2E_F$, the intraband transition is dominant and the optical transition of the electron with $q \neq 0$ is possible due to the additional scattering of an electron by an impurity or a phonon, which might modify the momentum of the electron. On the other hand, the interband transition from the valence to conduction band is dominant for $\hbar\omega > 2E_F$ [122]. For a two-dimensional electron gas system (e.g., GaAs/AlGaAs quantum-well structure), the optical conductivity is described by [123, 126]

$$\bar{\sigma}_{2Dgas} = i \frac{ne^2}{m(\omega + i\gamma)} , \tag{15}$$

where n, m, and γ are the density, effective mass, and scattering rate of the two-dimensional electron gas system. The dispersion of a TM surface wave is obtained by substituting Equations (5) and (6) into the boundary conditions Equations (10) and (11). In addition, the following equation is a requirement to have a TM surface wave in the two-dimensional material [120, 121, 123, 127]:

$$\frac{\varepsilon_1}{\kappa_1} + \frac{\varepsilon_2}{\kappa_2} + \frac{i\bar{\sigma}(\omega)}{\omega\varepsilon_0} = 0 , \tag{16}$$

where ε_i, ($i = 1,2$) is the dielectric constant of the *i*th medium that surrounds the two-dimensional material. Consider that $\varepsilon_i > 0$ and $\kappa_i > 0$. In order to satisfy Equation (16), the imaginary part of $\bar{\sigma}(\omega)$ should be positive ($\mathrm{Im}\{\bar{\sigma}(\omega)\} > 0$). This requirement is satisfied by the conventional two-dimensional electron gas system, since $\mathrm{Im}\left\{\bar{\sigma}_{2Dgas}\right\} = ne^2\omega \Big/ \left[m\left(\gamma^2 + \omega^2\right) \right] > 0$ [123], and in the case of graphene, $\mathrm{Im}\left\{\bar{\sigma}(\omega)\right\} > 0$ for $\hbar\omega < 1.667 E_F$

By solving Equation (16), it is possible to derive the dispersion relation of the TM surface wave for graphene. If $\hbar\omega \ll 2E_F$ (with $E_F = 0.64\,eV$), it is obtained that $\bar{\sigma}(\omega) \sim \sigma_D(\omega)$ and Γ can be ignored, since it gives only the spectral broadening of the TM surface wave. When the velocity of light can be considered to be much larger than the group velocity of the surface plasmon, v_{sp}, and thus $q \gg \omega/c$, resulting in $\kappa_1 = \kappa_2 = q$ in Equation (7). This condition is called the non-retarded regime [105, 120, 128]. By substituting σ_D in Equations (14) to (16) and solving for ω, a square-root dependence ($\omega \propto \sqrt{q}$) of the dispersion relation is obtained [105, 120, 128, 129]:

$$\omega = \frac{1}{\hbar}\sqrt{\frac{E_F e^2 q}{\pi\varepsilon_0\left(\varepsilon_1 + \varepsilon_2\right)}} \,. \tag{17}$$

The aforementioned relation can be also obtained for a conventional two-dimensional electron gas by substituting Equation (15) into Equation (16) and solving for ω finding that $\omega \propto \sqrt{q}$ dependence is a characteristic of surface plasmon polaritons in two-dimensional materials [105, 120, 124, 128]. Considering graphene as a medium, the long-wavelength plasmon dispersion can be calculated by looking for zeros of the dynamical dielectric function ($\varepsilon_g(q,\omega) = 0$) [124, 128].

3.1.2 Field Configuration at TE Surface Wave

For a TE surface wave (Figure 5b), the field components are E_y, H_x, H_z. In medium 1, the electromagnetic fields of the TE surface wave are given by

$$H_x^{(1)} = H_1 e^{iqx} e^{-\kappa_1 z} \,,$$

$$H_z^{(1)} = \frac{iq}{\kappa_1} H_x^{(1)} \,, \tag{18}$$

$$E_y^{(1)} = \frac{i\omega\mu_0}{\kappa_1} H_x^{(1)} \,,$$

and in medium 2,

$$H_x^{(2)} = H_2 e^{iqx} e^{\kappa_2 z} \,,$$

$$H_z^{(2)} = -\frac{iq}{\kappa_2} H_x^{(2)} \,, \tag{19}$$

$$E_y^{(2)} = -\frac{i\omega\mu_0}{\kappa_2} H_x^{(2)} \,,$$

where μ_0 is the permeability of the vacuum. Similarly for the TM surface wave, the magnetic and the electric fields are related by the following relations:

$$H_x^{(i)} = \frac{i}{\omega\mu_0}\frac{\partial E_y^{(i)}}{\partial z} \,, \tag{20}$$

$$H_z^{(i)} = q\big/\left(\omega\mu_0\right) E_y^{(i)} \,, \tag{21}$$

and, by using the boundary conditions of the electromagnetic field at the surface $z = 0$, which are related to the case of the TM surface wave given in Equations (10) and (11),

$$E_y^{(1)} = E_y^{(2)} \,, \tag{22}$$

$$H_x^{(1)} - H_x^{(2)} = -J \,, \tag{23}$$

at $z = 0$, where $J = \bar{\sigma}(\omega) E_y^{(2)}$ and assuming that the two dielectric media are vacuum ($\varepsilon_1 = \varepsilon_2 = 1$), thus $\kappa_1 = \kappa_2 = \sqrt{q^2 - (\omega/c)^2} \equiv \kappa$, the following equation is obtained [123, 130]:

$$2 - \frac{i\bar{\sigma}(\omega)\omega\mu_0}{\kappa} = 0 \,. \tag{24}$$

The concepts of surface-plasmon dispersion and the non-retarded regime [120, 128] were introduced in Equations (16) and Equation (17). For small q, the non-retarded approximation cannot be used because the group velocity of the surface plasmon (v_{sp}) is comparable to the velocity of light. This case is the so-called retarded regime [128], in which the dispersion of the surface plasmon is linear ($\omega \propto q$). From Equation (7) and solving Equation (16) (supposing that $\varepsilon_1 = \varepsilon_2 = \varepsilon$) for the retarded regime the following is obtained:

$$\omega \sim \frac{c}{\sqrt{\varepsilon}} q \,. \tag{25}$$

For a conventional two-dimensional electron gas system, $\mathrm{Im}\left\{\bar{\sigma}_{2Dgas}\right\} > 0$, as given by Equation (15) [123]. The TE surface wave hence cannot be supported by a normal bulk metal or any other common material found in nature, since $\omega > 0$, and Equation (25) requires $\mathrm{Im}\left\{\bar{\sigma}\right\} < 0$ [101, 123]. However, it is possible to obtain artificial materials that possess a negative permeability (e.g., metamaterials [131], generally not easy to fabricate, and two-dimensional materials [132]). For example, in the case of graphene, $\mathrm{Im}\{\bar{\sigma}(\omega)\} < 0$ for $\hbar\omega < 2E_F$. This unusual property has enabled graphene to have a TE surface wave, although a TE surface wave in doped graphene occurs only for a narrow frequency range of $1.667E_F < \hbar\omega < 2E_F$ [101, 121, 123, 133]. Similarly, in [134], a single-layer h-BN crystal was predicted to support a TE non-radiating surface mode in the visible spectrum.

3.2 The Optical Absorption, Reflection, and Transmission Spectra in Two-Dimensional Materials

To describe the optical spectra of the electromagnetic wave incident on a two-dimensional material, Maxwell's equations with boundary conditions were first evaluated, considering the two-dimensional material between two dielectric media. Subsequently, using the transfer-matrix method, optical spectra were obtained in the case of a two-dimensional material within a multilayer of dielectric media.

3.2.1 Two-Dimensional Material Between Two Dielectric Media

The probabilities for absorption, reflection, and transmission of an electromagnetic wave penetrating two-dimensional materials can be obtained by solving Maxwell's equations for an electromagnetic wave with boundary conditions. A two-dimensional material having a negligible thickness is placed between two dielectric media, as shown in Figure 6. It is modeled as a conducting interface with a conductivity $\bar{\sigma}$ between two dielectric media with dielectric constants ε_1 and ε_2. Considering the TM polarization of the electromagnetic wave, as shown in Figure 6, it is possible to obtain two boundary conditions for the electric field, $E^{(i)}$, and the magnetic field, $H^{(i)}$ ($i = 1, 2$), as follows:

$$E_+^{(1)} \cos\vartheta + E_-^{(1)} \cos\vartheta = E_+^{(2)} \cos\phi , \qquad (26)$$

$$H_+^{(2)} - \left[H_+^{(1)} - H_-^{(1)} \right] = -\bar{\sigma} E_+^{(2)} \cos\phi , \qquad (27)$$

where the +(-) index indicates the bottom- (top-) going waves according to Figure 6, ϑ is the incident and reflection angle, and ϕ is the refraction angle. The E and H fields are related to each other in terms of the electromagnetic wave impedance for each medium:

$$Z_i = \frac{E_i}{H_i} = \frac{377}{\sqrt{\varepsilon_i}} \Omega \ (i = 1, 2) , \qquad (28)$$

where the constant $377\,\Omega$ is the impedance of vacuum

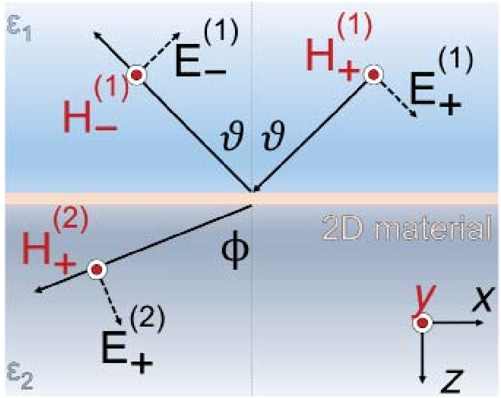

Figure 6. A two-dimensional material is placed between two dielectric media with dielectric constants ε_1 and ε_2. The thickness of the two-dimensional material is neglected. The incident EM wave comes at an angle ϑ in medium 1 (top) and is transmitted at an angle ϕ in medium 2 (bottom).

($Z_0 = \sqrt{\mu_0/\varepsilon_0}$). The quantities ϕ, ϑ, and Z_i are related by Snell's law ($Z_2 \sin\vartheta = Z_1 \sin\phi$). Solving Equations (26) to (28), the reflection (R), transmission (T), and absorption (A) probabilities of the electromagnetic wave are obtained as follows:

$$R = \left| \frac{E_1^{(-)}}{E_1^{(+)}} \right|^2 = \left| \frac{Z_2 \cos\phi - Z_1 \cos\vartheta - Z_1 Z_2 \bar{\sigma} \cos\vartheta \cos\phi}{Z_2 \cos\phi + Z_1 \cos\vartheta + Z_1 Z_2 \bar{\sigma} \cos\vartheta \cos\phi} \right|^2 ,$$

$$T = \frac{\cos\phi}{\cos\vartheta} \frac{Z_1}{Z_2} \left| \frac{E_2^{(+)}}{E_1^{(+)}} \right|^2$$

$$= \frac{4 Z_1 Z_2 \cos\vartheta \cos\phi}{\left| Z_2 \cos\phi + Z_1 \cos\vartheta + Z_1 Z_2 \bar{\sigma} \cos\vartheta \cos\phi \right|^2} , \qquad (29)$$

$$A = 1 - \mathrm{Re}\{R\} - \mathrm{Re}\{T\}$$

$$= \frac{4 Z_1 Z_2^2 \cos\vartheta \left| \cos\phi \right|^2 \mathrm{Re}\{\bar{\sigma}\}}{\left| Z_2 \cos\phi + Z_1 \cos\vartheta + Z_1 Z_2 \bar{\sigma} \cos\vartheta \cos\phi \right|^2} ,$$

where the values of R, T, and A are real quantities and are denoted in terms of percentages (0% to 100%).

3.2.2 Multilayer Configuration

The configuration described in the previous section can be generalized to a multilayer configuration in which two-dimensional and standard dielectric slabs alternate. This structure can be modeled using the formalism of the equivalent chain of transmission lines [135], and then analyzed using the wave-amplitude transmission matrix (WATM) [136]. The latter is very effective when, as in our case, we are mainly interested in an input-output description of the structure. It has already been used in the present context [137-139]. Assuming N two-dimensional materials inside a multilayer dielectric media, spaced apart from each other by a distance $z = d$, the wave-amplitude transmission matrix method [140] relates the electromagnetic fields at all interfaces in a multi-layered system. For simplicity, a system with two two-dimensional material layers placed between three dielectric slabs (media 1, 2, and 3 with dielectric constants ε_1, ε_2, and ε_3, respectively) can be assumed as a first approximation (Figure 7). The incident electromagnetic wave with TM polarization comes from medium 1 with angle ϑ_1 and it propagates through medium 2 with angle ϑ_2 and medium 3 with angle ϑ_3. By adopting the polarization TM of the incident electromagnetic wave between two dielectric media ($0 < z < d$), the electromagnetic fields are related to each other through the boundary conditions obtained from Maxwell's equations. It is therefore possible to define the boundary conditions of the monolayer interface of the electric field, $E^{(i)}$, and of the magnetic field, $H^{(i)}$, ($i = 1,2$), as follows:

$$E_x^{(1)} = E_x^{(2)}, \tag{30}$$

$$H_y^{(2)} - H_y^{(1)} = -\bar{\sigma} E_x^{(2)}. \tag{31}$$

Considering a thickness of the two-dimensional material sufficiently small compared to the wavelength of the incident light ($d \ll \lambda$), the electric and magnetic fields in medium 1 can be described as follows:

$$E_x^{(1)}(z) = E_{x+}^{(1)}(z) + E_{x-}^{(1)}(z) = E_{x_0+}^{(1)} e^{i\kappa_1 z} + E_{x_0-}^{(1)} e^{-i\kappa_1 z}, \tag{32}$$

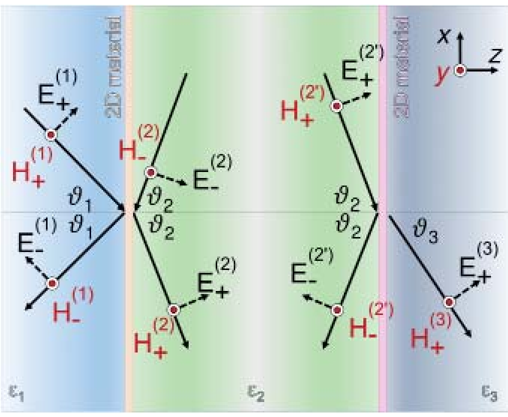

Figure 7. The wave propagation through three media and two different two-dimensional materials.

$$H_y^{(1)}(z) = \frac{\omega \varepsilon_0 \varepsilon_1}{\kappa_1}\left[E_{x_0+}^{(1)} e^{i\kappa_1 z} - E_{x_0-}^{(1)} e^{-i\kappa_1 z}\right], \tag{33}$$

and for medium 2,

$$E_x^{(2)}(z) = E_{x+}^{(2)}(z) + E_{x-}^{(2)}(z) = E_{x_0+}^{(2)} e^{i\kappa_2 z} + E_{x_0-}^{(2)} e^{-i\kappa_2 z} \tag{34}$$

$$H_y^{(2)}(z) = \frac{\omega \varepsilon_0 \varepsilon_1}{\kappa_2}\left[E_{x_0+}^{(2)} e^{i\kappa_2 z} - E_{x_0-}^{(2)} e^{-i\kappa_2 z}\right], \tag{35}$$

where $E_x^{(i)}$ is the amplitude of the electric field along the x axis inside medium i, ε_i is the dielectric constant of the ith medium, ω is the angular frequency of the electromagnetic wave, and k_i is the wave vector in the z direction, which is defined as

$$k_i = \frac{2\pi}{\lambda}\sqrt{\varepsilon_i}\cos\vartheta_i, \tag{36}$$

where λ is the wavelength of the electromagnetic wave. The amplitudes of the electric field of the electromagnetic wave are $E_{x_0+}^{(i)}$ and $E_{x_0-}^{(i)}$ going to the z direction. The reflected wave at the second interface with medium 3 inside the medium 2 is described by $E_{x_0-}^{(2)}$. The relationship between H_y and E_x comes from the following equation:

$$H_y^{(i)} = i\omega\varepsilon_0\varepsilon_i \int E_x^{(i)} dz. \tag{37}$$

The corresponding angle of propagation of the electromagnetic wave inside each dielectric medium, measured from the z axis, is ϑ_i ($i = 1,2$). Quantities ϑ_i and ε_i between two dielectric media are related by Snell's law ($\varepsilon_1 \sin\vartheta_1 = \varepsilon_2 \sin\vartheta_2$). Using Equations (30) through (35), solving for E_{x_0+} and E_{x_0-} explicitly at the boundary, it is possible to write the following matrix:

$$\begin{bmatrix} E_{x_0+}^{(1)} \\ E_{x_0-}^{(1)} \end{bmatrix} = [M_1][T_1][M_2][T_2]\ldots[T_{N-2}][M_{N-1}]\begin{bmatrix} E_{x_0+}^{(N)} \\ 0 \end{bmatrix} \tag{38}$$

where

$$M_i = \frac{1}{2}\begin{bmatrix} 1+\Delta_i+G_i & 1-\Delta_i+G_i \\ 1-\Delta_i-G_i & 1+\Delta_i-G_i \end{bmatrix}, \tag{39}$$

$$T_i = \begin{bmatrix} e^{-i\kappa_{i+1}d} & 0 \\ 0 & e^{i\kappa_{i+1}d} \end{bmatrix}. \tag{40}$$

Equation (39) describes the electromagnetic waves in medium i as a function of the electromagnetic waves in medium $i+1$ at the first boundary, where α_i and β_i are

$$G_i = \frac{\kappa_i \bar{\sigma}}{\omega \varepsilon_0 \varepsilon_i}, \tag{41}$$

$$\Delta_i = \frac{\kappa_i}{\kappa_{i+1}} \frac{\varepsilon_{i+1}}{\varepsilon_i}.$$

Equation (40) describes the propagation of the wave through the medium $i+1$, where d is the length of the medium $i+1$.

The total reflection (ρ_{total}) and transmission (τ_{total}) coefficients are

$$\begin{bmatrix} E_{x_0+}^{(1)} \\ E_{x_0-}^{(1)} \end{bmatrix} = \begin{bmatrix} \xi & \zeta \\ \gamma & \delta \end{bmatrix} \begin{bmatrix} E_{x_0+}^{(3)} \\ 0 \end{bmatrix}, \tag{42}$$

$$\rho_{total} = \frac{E_{x_0-}^{(1)}}{E_{x_0+}^{(1)}} = \frac{\gamma}{\xi}, \tag{43}$$

$$\tau_{total} = \frac{E_{x_0+}^{(3)}}{E_{x_0+}^{(1)}} = \frac{1}{\xi},$$

where ξ, ζ, γ, and δ are the components of the total matrix (Equation (38)), resulting in

$$R = \left| \rho_{total} \right|^2, \tag{44}$$

$$T = \frac{\sqrt{\varepsilon_3} \cos \vartheta_1}{\sqrt{\varepsilon_1} \cos \vartheta_3} \left| \tau_{total} \right|^2,$$

$$A = 1 - \mathrm{Re}\{R\} - \mathrm{Re}\{T\},$$

where R, T, and A are reflection, transmission, and absorption probabilities of the electromagnetic wave, respectively. In the case of the absence of a two-dimensional material at the interface, $\alpha_i = 0$ can be set in the matching matrix of the corresponding interface.

With this theoretical background, it is possible to optimize the design of optical devices (e.g., optical absorbers). For example, considering a device consisting of N two-dimensional materials and respective media, the number and position of the absorption peaks can be tuned a priori, thus providing the theoretical basis for the study and design of the device and its application.

3.3 Nonlinear Optics in Two-Dimensional Materials

In the previous section, we discussed optical propagation in a two-dimensional material. We have dealt with the problem of a linear dielectric medium impinged upon by an electromagnetic wave. In this context, a linear dielectric medium was characterized by a linear relation between the polarization density (P) and the electric field (E) [141]:

$$\mathbf{P} = \varepsilon_0 \chi \mathbf{E}, \tag{45}$$

where ε_0 is the permittivity of free space and ÷ is the electric susceptibility of the medium. The relationship between $\mathbf{P}$ and $\mathbf{E}$ expressed by Equation (45) describes the conventional linear optical effects, such as refraction and absorption, and occurs when $\mathbf{E}$ is small. However, it becomes nonlinear when $\mathbf{E}$ acquires values comparable to interatomic electric fields, which are typically $\sim 10^5 - 10^8$ Vm^{-1}. Since externally applied optical electric fields are typically small in comparison with characteristic interatomic or crystalline fields, even when focused laser light is used, the nonlinearity is usually weak. A nonlinear anisotropic dielectric medium is characterized by a tensor relation that can be expanded in a Taylor series [141]:

$$P_i = \varepsilon_0 \left(\sum_j \chi_{ij} E_j + \sum_{jk} \chi_{ijk}^{(2)} E_j E_k + \sum_{jkl} \chi_{ijkl}^{(3)} E_j E_k E_l + \ldots \right) \tag{46}$$

where $i, j, k, l = 1, 2, 3$ and the coefficients χ_{ij}, $\chi_{ijk}^{(2)}$, and $\chi_{ijkl}^{(3)}$ represent the tensor components of the nth-order nonlinearity. These coefficients are characteristic constants of the medium, and may be originated by microscopic or macroscopic phenomena. In particular, the $\div^{(2)}$ coefficient of the second term in Equation (46) gives rise to a second-order nonlinearity (three-wave mixing), including second-harmonic generation (SHG), sum- and difference-frequency generation (SFG, DFG), and optical parametric interaction (optical parametric amplification, OPA, and optical parametric oscillation, OPO). Third-order nonlinear effects, which usually arise from the susceptibility of third-order nonlinear optics ($\div^{(3)}$), include third-harmonic generation (THG), four-wave mixing (FWM), intensity-dependent refractive index changes (optical Kerr effect and saturable absorption, SA), and two-photon excitation fluorescence (TPEF). The higher-order coefficients ($\div^{(n)}$) represent the susceptibility of higher-order nonlinear optics, namely the higher-order multiphoton scattering/absorption/luminescence and the high-harmonic generation (HHG). Since the interaction intensity of nonlinear processes usually decreases with n [142, 143], the effects of nonlinear higher-order effects (including HHG) have very low intensity, therefore typically $\div^{(n)} \sim 0$ for $n > 3$. In the case of bulk crystals, the generation of nonlinear effects occurs when the phase-matching condition is satisfied in order to maximize the intensity of the nonlinear optical signal. According to quantum mechanics, the phase-matching condition is satisfied when the photon's momentum and energy are simultaneously conserved before and after the nonlinear process [143]. For this reason, the path of the incident light and the orientation of the crystal must be carefully designed in order to optimize the nonlinear effects [144]. However, in the case of a medium with reduced thickness – comparable to the sub-wavelength range and shorter than the coherence length – the phase-matching condition is easily achieved. This allows for obtaining strong nonlinear effects [144]. Nonlinear optical properties of single-layer and few-layer atomic crystals have been recently investigated [145]. The theory of Bloembergen and Pershan [146] for the light waves at the boundary of nonlinear media can be extended to a nonlinear two-dimensional crystal placed between linear bulk media. In this case, the two-dimensional crystal is treated as a zero-thickness interface, i.e., a real two-dimensional system [145]. The crystalline structure of the material strongly influences nonlinear processes. In fact, thanks to the high values of the tensors $\div^{(2)}$ and $\div^{(3)}$ some materials show an anisotropic nonlinear response [147] even if the linear optical response is isotropic. This allows characterizing the orientation of the crystal with very high sensitivity [142, 143].

Since the susceptibility, $\div^{(2)}$, is a third-rank tensor of even parity under inversion, $\div^{(2)}$ vanishes for media with inversion symmetry. Namely, in centrosymmetric media that have inversion symmetry, the properties of the medium are not altered by the transformation $\mathbf{r} \to -\mathbf{r}$ [141]; the $\mathbf{P}-\mathbf{E}$ function must have odd symmetry so that the reversal of $\mathbf{E}$ results in the reversal of $\mathbf{P}$ without any other change:

$$\mathbf{P} = \varepsilon_0 \left[\div\mathbf{E} + \div^{(2)}\mathbf{E}^2 + \div^{(3)}\mathbf{E}^3 \right] \quad (47)$$

$$= \varepsilon_0 \left[\div(-\mathbf{E}) + \div^{(2)}(-\mathbf{E})^2 + \div^{(3)}(-\mathbf{E})^3 \right] = -\mathbf{P}\,.$$

In order to verify the latter, the second-order nonlinear susceptibility coefficient must be zero ($\div^{(2)} = 0$). In contrast, odd-order nonlinearity (i.e., $\div^{(3)}$) is allowed in any material, regardless of whether the material is centrosymmetric, such as third-harmonic generation and four-wave mixing [143].

Given a plane wave of amplitude $E(\omega)$ traveling in a nonlinear medium (in this case, a non-centrosymmetric two-dimensional material) in the direction of its q vector (Figure 8), a polarization is generated at the second-harmonic frequency as follows:

$$P(2\omega) = \varepsilon_0 \chi^{(2)} E^2(\omega) = 2\varepsilon_0 d_{eff} E^2(\omega)\,, \quad (48)$$

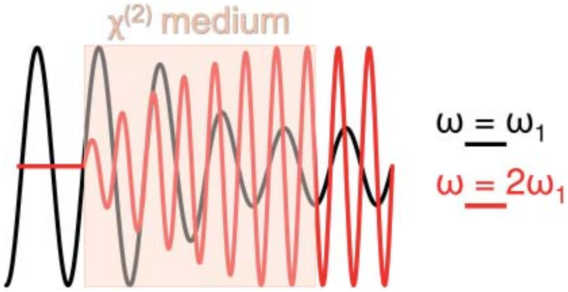

Figure 8. A diagram of second-harmonic generation with perfect phase matching.

where d_{eff} is the effective nonlinear optical coefficient, which depends on $\chi^{(2)}$.

If the slowly varying envelope approximation is applied [148],

$$\left| \frac{\partial^2 E(z,\omega)}{\partial z^2} \right| \ll k \left| \frac{\partial E(z,\omega)}{\partial z} \right|, \quad (49)$$

and assuming negligible losses, the wave equation at 2ω is

$$\frac{\partial E(z,2\omega)}{\partial z} = -\frac{i\omega}{n_{2\omega} c} d_{eff} E^2(z,\omega) e^{i\Delta q z}\,, \quad (50)$$

where $\Delta q = q(2\omega) - 2q(\omega)$. Considering the low conversion efficiency assumption ($E(2\omega) \ll E(\omega)$), which is a valid condition when the conversion to the second harmonic is not significant, the amplitude, $E(\omega)$, remains constant over the thickness of the nonlinear medium, t. By using the boundary condition $E(2\omega, z=0) = 0$, we hence get

$$E(2\omega, z=t) = -\frac{i\omega}{n_{2\omega} c} d_{eff} E^2(z,\omega) \int_0^t e^{i\Delta q z} dz$$

$$= -\frac{i\omega}{n_{2\omega} c} d_{eff} E^2(\omega) t \frac{\sin(\Delta q t/2)}{\Delta q t/2} c^{\Delta q t/2} \quad (51)$$

In terms of the optical intensity,

$$I(2\omega,t) = \left| E(2\omega,t) \right|^2 = \frac{2\omega^2 d_{eff}^2 t^2}{n_{2\omega} n_{\omega}^2 c^3 \varepsilon_0} \left[\frac{\sin(\Delta q t/2)}{\Delta q t/2} \right]^2 I^2(\omega) \quad (52)$$

The intensity $I(2\omega)$ is maximized for the phase-matched condition $\Delta q = 0$. Equation (52) shows that $I(2\omega,t) = 0$ when $d_{eff} \propto \chi^{(2)} = 0$ for media presenting inversion symmetry. For example, the natural vertical stacking of

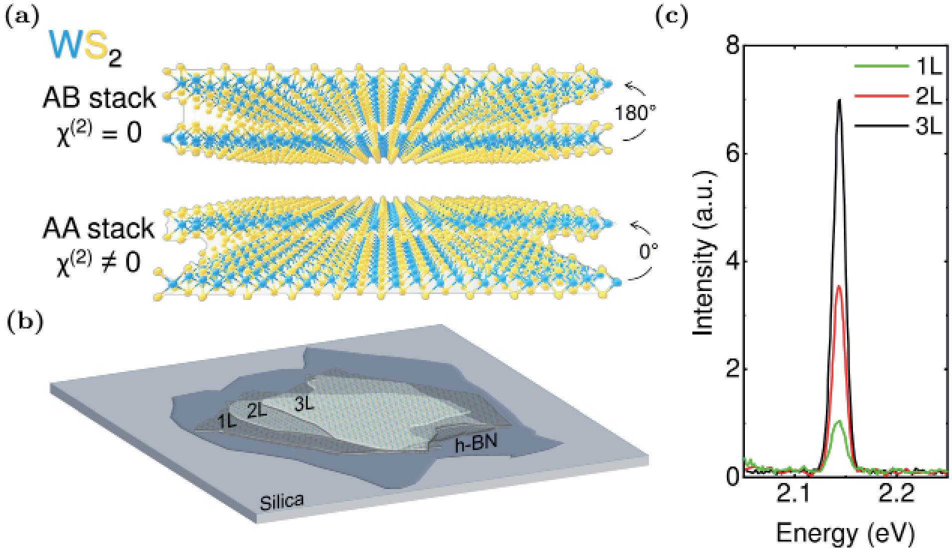

Figure 9 a) (upper left) Schematics of a natural centrosymmetric AB structure with an interlayer twist angle of 180° ($\chi^{(2)} = 0$) and an artificial non-centrosymmetric AA configuration with 0° twist angle ($\chi^{(2)} \neq 0$). b) (lower left) A sketch of the WS_2 AA stack sample. c) (right) The photoluminescence spectra as a function of the number of layers (data from [148]).

the most commonly used transition metal dichalcogenide semiconductors, TMDS (2H polytype), is constituted by monoatomic layers rotated by 180° with respect to their next neighbors, forming the so-called AB stack [149]. As a direct consequence, the inversion symmetry is present for even layers ($\chi^{(2)} = 0$), preventing the observation of any second-order nonlinear process [?]. However, TMDS can be reduced to nanometric thickness ($t \sim 1$ nm) due to the weak van der Waals interlayer forces, showing a non-centrosymmetric structure ($\chi^{(2)} \neq 0$) in their monolayer form. In this case, the medium is usually presented without any phase factor ($\Delta q = 0$) due to the atomically thin nature [151, 152], and hence

$$E(2\omega) = -\frac{i\omega}{n_{2\omega}c} d_{eff} E^2(\omega) t \,. \tag{53}$$

However, the crystal structure is very important for symmetry reasons, and it is possible to find bulk crystals of TMDS possessing a $\chi^{(2)} \neq 0$. For example, in [152] the authors probe the SHG generated from the noncentrosymmetric $3R$ crystal phase of MoS_2. Instead, Trovatello et al. [148] showed that artificial crystals with vertically stacked WS_2 monolayers, with interlayer $\sim 0°$ crystal angle alignment, forming the so-called AA stack [149], preserved the broken inversion symmetry ($\chi^{(2)} \neq 0$), as shown in Figure 9a. In both cases, if no strong interactions are assumed between the layers and each layer is treated as optically independent, it is possible to model the individual electric field from any layer as

$$E(N,2\omega) \propto e^{i\Delta q(N-1)t} e^{-\alpha(N-1)t/2} \,, \tag{54}$$

where N is the number of the layers and ($N-1$) results due to the indexing of the crystal, i.e., the top-most layer is 1, so the subsequent intensity is normalized to 1, and t is the crystal thickness. To account for the re-absorption of the second-harmonic light, it is introduced an exponential loss factor, α . This is the attenuation factor at the second-harmonic energy extracted from the single-layer linear-absorption spectrum (i.e., $\gamma = 1 - I_{abs} = e^{-\alpha t}$). It is possible to write the total SH light from N layers as

$$I(N,2\omega) \propto \left| \sum_{M=1}^{N} e^{i\Delta q(M-1)t} e^{-\alpha(M-1)t/2} \right|^2 . \tag{55}$$

From Equation (55), it is clear that the intensity scales quadratically with N in the case of a non-centrosymmetric crystal of N layers. This has been observed experimentally, performing a proof-of-principle demonstration. As shown in Figure (9b), three layers of manually AA stacked WS_2, sitting on top of a h-BN flake, were identified by photoluminescence characterization, demonstrating that artificial stacking of AA aligned WS_2 monolayers provides a route for quadratic scaling of the efficiency with the layers' numbers (Figure 9c).

4. Conclusion

Two-dimensional materials offer compelling perspectives for implementing devices with new capabilities over those based on conventional materials. In non-interacting two-dimensional material layers, the transfer-matrix method can be used to obtain their reflectance, transmittance, and absorbance spectra. In this way, photonic-band structures for periodical two-dimensional material layers can be studied in a simple way. Another key feature of two-dimensional nonlinear materials is their non-centrosymmetry, which can be easily realized in two-dimensional materials. For example, WS_2 becomes non-centrosymmetric when its bulk counterpart is thinned into a monolayer. These properties demonstrate that these effects greatly improve performance in two-dimensional-material-based devices. It is hence of great importance to pursue appropriate two-dimensional crystals without thickness limitations, which can provide more opportunities to obtain high-performance optoelectronic devices. All this research paves the way for optical devices ranging from sensors to modulators to isolators, serving as a versatile tool for studying optical properties in two-dimensional materials.

5. References

1. K. S. Novoselov and A. Geim, "The Rise of Graphene," *Nature Materials*, **6**, 3, 2007, pp. 183-191.

2. A. C. Ferrari, F. Bonaccorso, V. Fal'ko, K. S. Novoselov, S. Roche, P. Bøggild, S. Borini, F. H. L. Koppens, V. Palermo, N. Pugno, J. A. Garrido, R. Sordan, A. Bianco, L. Ballerini, M. Prato, E. Lidorikis, J. Kivioja, C. Marinelli, T. Ryhänen, A. Morpurgo, J. N. Coleman, V. Nicolosi, L. Colombo, A. Fert, M. Garcia-Hernandez, A. Bachtold, G. F. Schneider, F. Guinea, C. Dekker, M. Barbone, Z. Sun, C. Galiotis, A. N. Grigorenko, G. Konstantatos, A. Kis, M. Katsnelson, L. Vandersypen, A. Loiseau, V. Morandi, D. Neumaier, E. Treossi, V. Pellegrini, M. Polini, A. Tredicucci, G. M. Williams, B. Hee Hong, J.-H. Ahn, J. Min Kim, H. Zirath, B. J. van Wees, H. van der Zant, L. Occhipinti, A. Di Matteo, I. A. Kinloch, T. Seyller, E. Quesnel, X. Feng, K. Teo, N. Rupesinghe, P. Hakonen, S. R. T. Neil, Q. Tannock, T. Löfwander and J. Kinaret, "Science and Technology Roadmap for Graphene, Related Two-Dimensional Crystals, and Hybrid Systems," *Nanoscale*, **7**, 11, 2015, pp. 4598-4810.

3. H. Wang, H. Yuan, S. S. Hong, Y. Li, and Y. Cui, "Physical and Chemical Tuning of Two-Dimensional Transition Metal Dichalcogenides," *Chemical Society Reviews*, **44**, 9, 2015, pp. 2664-2680.

4. Q. Ma, G. Ren, K. Xu, and J. Z. Ou, "Tunable Optical Properties of 2D Materials and Their Applications," *Advanced Optical Materials*, **9**, 2, 2021, p. 2001313.

5. A. J. Mannix, B. Kiraly, M. C. Hersam, and N. P. Guisinger, "Synthesis and Chemistry of Elemental 2D Materials," *Nature Reviews Chemistry*, **1**, 2, 2017, pp. 1-14.

6. Z. W. Seh, K. D. Fredrickson, B. Anasori, J. Kibsgaard, A. L. Strickler, M. R. Lukatskaya, Y. Gogotsi, T. F. Jaramillo, and A. Vojvodic, "Two Dimensional Molybdenum Carbide (MXene) as an Efficient Electrocatalyst for Hydrogen Evolution," *ACS Energy Letters*, **1**, 3, 2016, pp. 589-594.

7. Z. Li, L. Wang, D. Sun, Y. Zhang, B. Liu, Q. Hu, and A. Zhou, "Synthesis and Thermal Stability of Two-Dimensional Carbide MXene Ti_3C_2," *Materials Science and Engineering: B*, **191**, 2015, pp. 33-40.

8. P. Urbankowski, B. Anasori, T. Makaryan, D. Er, S. Kota, P. L. Walsh, M. Zhao, V. B. Shenoy, M. W. Barsoum, and Y. Gogotsi, "Synthesis of Two-Dimensional Titanium Nitride Ti_4N_3 (MXene)," *Nanoscale*, **8**, 22, 2016, pp. 11385-11391.

9. X. Han, D. Xu, L. An, C. Hou, Y. Li, Q. Zhang, and H. Wang, "WO_3/g-C_3N_4 Two-Dimensional Composites for Visible-Light Driven Photocatalytic Hydrogen Production," *International Journal of Hydrogen Energy*, **43**, 10, 2018, pp. 4845-4855.

10. H. Min, E. Hwang, and S. D. Sarma, "Ferromagnetism in Chiral Multilayer Two-Dimensional Semimetals," *Physical Review B*, **95**, 15, 2017, p. 155414.

11. K. Kalantar-Zadeh and J. Z. Ou, "Biosensors Based on Two-Dimensional MoS_2," *ACS Sensors*, **1**, 1, 2016, pp. 5-16.

12. X. Zhang, J. Grajal, J. L. Vazquez-Roy, U. Radhakrishna, X. Wang, W. Chern, L. Zhou, Y. Lin, P.-C. Shen, X. Ji, X. Ling, A. Zubair, Y. Zhang, H. Wang, M. Dubey, J. Kong, M. Dresselhaus and T. Palacios, "Two-Dimensional MoS_2-Enabled Flexible Rectenna for Wi-Fi-Band Wireless Energy Harvesting," *Nature*, **566**, 7744, 2019, pp. 368-372.

13. A. Branny, S. Kumar, R. Proux, and B. D. Gerardot, "Deterministic Strain-Induced Arrays of Quantum Emitters in a Two-Dimensional Semiconductor," *Nature Communications*, **8**, 1, 2017, pp. 1-7.

14. K. Zhang, Y. Feng, F. Wang, Z. Yang, and J. Wang, "Two Dimensional Hexagonal Boron Nitride (2D-hBN): Synthesis, Properties and Applications," *Journal of Materials Chemistry C*, **5**, 46, 2017, pp. 11992-12022.

15. M.Y. Li, C. H. Chen, Y. Shi, and L. J. Li, "Heterostructures Based on Two-Dimensional Layered Materials and Their Potential Applications," *Materials Today*, **19**, 6, 2016, pp. 322-335.

16. G. R. Bhimanapati, Z. Lin, V. Meunier, Y. Jung, J. Cha, S. Das, D. Xiao, Y. Son, M. S. Strano, V. R. Cooper, L. Liang, S. G. Louie, E. Ringe, W. Zhou, S. S. Kim, R. R. Naik, B. G. Sumpter, H. Terrones, F. Xia, Y. Wang, J. Zhu, D. Akinwande, N. Alem, J. A. Schuller, R. E. Schaak, M. Terrones and J. A. Robinson, "Recent Advances in Two-Dimensional Materials Beyond Graphene," *ACS nano*, **9**, 12, 2015, pp. 11509-11539.

17. W. Zheng, T. Xie, Y. Zhou, Y. L. Chen, W. Jiang, S. Zhao, J. Wu, Y. Jing, Y. Wu, G. Chen, Y. Guo, J. Yin, S. Huang, H. Q. Xu, Z. Liu and H. Peng, "Patterning Two-Dimensional Chalcogenide Crystals of Bi_2Se_3 and In_2Se_3 and Efficient Photodetectors," *Nature Communications*, **6**, 1, 2015, pp. 1-8.

18. S. S. Sunku, D. Halbertal, R. Engelke, H. Yoo, N. R. Finney, N. Curreli, G. Ni, C. Tan, A. S. McLeod, C. F. B. Lo, C. R. Dean, J. C. Hone, P. Kim, and D. N. Basov, "Dual-Gated Graphene Devices for Near-Field Nano-Imaging," *Nano Letters*, **21**, 4, 2021, pp. 1688-1693.

19. N. Curreli, M. Serri, M. I. Zappia, D. Spirito, G. Bianca, J. Buha, L. Najafi, Z. Sofer, R. Krahne, V. Pellegrini, and F. Bonaccorso, "Liquid-Phase Exfoliated Gallium Selenide for Light-Driven Thin-Film Transistors," *Advanced Electronic Materials*, **7**, 3, 2021, p. 2001080.

20. N. Curreli, M. Serri, D. Spirito, E. Lago, E. Petroni, B. Martín-García, A. Politano, B. Gürbulak, S. Duman, R. Krahne, V. Pellegrini and F. Bonaccorso, "Liquid Phase Exfoliated Indium Selenide Based Highly Sensitive Photodetectors," *Advanced Functional Materials*, **30**, 13, 2020, p. 1908427.

21. A. Capasso, S. Bellani, A. L. Palma, L. Najafi, A. E. Del Rio Castillo, N. Curreli, L. Cinà, V. Miseikis, C. Coletti, G. Calogero, V. Pellegrini, A. Di Carlo and F. Bonaccorso, "CVD Graphene/Graphene Flakes Dual-Films as Advanced DSSC Counter Electrodes," *2D Materials*, **6**, 3, 2019, p. 035007.

22. S. Bellani, E. Petroni, A. E. Del Rio Castillo, N. Curreli, B. Martìn-Garcìa, R. Oropesa-Nunez, M. Prato, and F. Bonaccorso, "Scalable Production of Graphene Inks via Wet-Jet Milling Exfoliation for Screen-Printed Micro-Supercapacitors," *Advanced Functional Materials*, **29**, 14, 2019, p. 1807659.

23. M. Velicky and P. S. Toth, "From Two-Dimensional Materials to their Heterostructures: An Electrochemist's Perspective," *Applied Materials Today*, **8**, 2017, pp. 68-103.

24. A. Nemilentsau, T. Low, and G. Hanson, "Anisotropic 2D Materials for Tunable Hyperbolic Plasmonics," *Physical Review Letters*, **116**, 6, 2016, p. 066804.

25. Y. L. Huang, Y. Chen, W. Zhang, S. Y. Quek, C.-H. Chen, L.-J. Li, W.-T. Hsu, W.-H. Chang, Y. J. Zheng, W. Chen and A. T. S. Wee, "Bandgap Tunability at Single-Layer Molybdenum Disulphide Grain Boundaries," *Nature Communications*, **6**, 1, 2015, pp. 1-8.

26. Z. Qiu, M. Trushin, H. Fang, I. Verzhbitskiy, S. Gao, E. Laksono, M. Yang, P. Lyu, J. Li, J. Su, M. Telychko, K. Watanabe, T. Taniguchi, J. Wu, A. H. C. Neto, L. Yang, G. Eda, S. Adam and J. Lu, "Giant Gate-Tunable Bandgap Renormalization and Excitonic Effects in a 2D Semiconductor," *Science Advances*, **5**, 7, 2019, p. eaaw2347.

27. J. Wang, Z. Cheng, Z. Chen, X. Wan, B. Zhu, H. K. Tsang, C. Shu, and J. Xu, "High-Responsivity Graphene-on-Silicon Slot Waveguide Photodetectors," *Nanoscale*, **8**, 27, 2016, pp. 13206-13211.

28. T. Wang, S. Hu, B. Chamlagain, T. Hong, Z. Zhou, S. M. Weiss, and Y. Q. Xu, "Visualizing Light Scattering in Silicon Waveguides with Black Phosphorus Photodetectors," *Advanced Materials*, **28**, 33, 2016, pp. 7162-7166.

29. E. Lee, S. G. Lee, W. H. Lee, H. C. Lee, N. N. Nguyen, M. S. Yoo, and K. Cho, "Direct CVD Growth of a Graphene/MoS_2 Heterostructure with Interfacial Bonding for Two-Dimensional Electronics," *Chemistry of Materials*, **32**, 11, 2020, pp. 4544-4552.

30. L. Wu, J. Guo, Q. Wang, S. Lu, X. Dai, Y. Xiang, and D. Fan, "Sensitivity Enhancement by Using Few-Layer Black Phosphorus-Graphene/TMDCs Heterostructure in Surface Plasmon Resonance Biochemical Sensor," *Sensors and Actuators B: Chemical*, **249**, 2017, pp. 542-548.

31. J. C. Song, M. S. Rudner, C. M. Marcus, and L. S. Levitov, "Hot Carrier Transport and Photocurrent Response in Graphene," *Nano Letters*, **11**, 11, 2011, pp. 4688-4692.

32. I. Goykhman, U. Sassi, B. Desiatov, N. Mazurski, S. Milana, D. de Fazio, A. Eiden, J. Khurgin, J. Shappir, U. Levy and A. C. Ferrari, "On-Chip Integrated, Silicon–Graphene Plasmonic Schottky Photodetector with High Responsivity and Avalanche Photogain," *Nano Letters*, **16**, 5, 2016, pp. 3005-3013.

33. M. Romagnoli, V. Sorianello, M. Midrio, F. H. Koppens, C. Huyghebaert, D. Neumaier, P. Galli, W. Templ, A. D'Errico, and A. C. Ferrari, "Graphene-Based Integrated Photonics for Next-Generation Datacom and Telecom," *Nature Reviews Materials*, **3**, 10, 2018, pp. 392-414.

34. M. Ghini, N. Curreli, A. Camellini, M. Wang, A. Asaithambi, and I. Kriegel, "Photodoping of Metal Oxide Nanocrystals for Multi-Charge Accumulation and Light-Driven Energy Storage," *Nanoscale*, **13**, 19, 2021, pp. 8773-83.

35. Q. Weng, G. Li, X. Feng, K. Nielsch, D. Golberg, and O. G. Schmidt, "Electronic and Optical Properties of 2D Materials Constructed from Light Atoms," *Advanced Materials*, **30**, 46, 2018, p. 1801600.

36. A. Gupta, T. Sakthivel, and S. Seal, "Recent Development in 2D Materials Beyond Graphene," *Progress in Materials Science*, **73**, 2015, pp. 44-126.

37. K. Khan, A. K. Tareen, M. Aslam, R. Wang, Y. Zhang, A. Mahmood, Z. Ouyang, H. Zhang, and Z. Guo, "Recent Developments in Emerging Two-Dimensional Materials and Their Applications," *Journal of Materials Chemistry C*, **8**, 2, 2020, pp. 387-440.

38. Q. H. Wang, K. Kalantar-Zadeh, A. Kis, J. N. Coleman, and M. S. Strano, "Electronics and Optoelectronics of Two-Dimensional Transition Metal Dichalcogenides," *Nature Nanotechnology*, **7**, 11, 2012, pp. 699-712.

39. F. Xia, H. Wang, D. Xiao, M. Dubey, and A. Ramasubramaniam, "Two-Dimensional Material Nanophotonics," *Nature Photonics*, **8**, 12, 2014, pp. 899-907.

40. F. Yang, S. Cheng, X. Zhang, X. Ren, R. Li, H. Dong, and W. Hu, "2D Organic Materials for Optoelectronic Applications," *Advanced Materials*, **30**, 2, 2018, p. 1702415.

41. M. Xu, T. Liang, M. Shi, and H. Chen, "Graphene-Like Two-Dimensional Materials," *Chemical Reviews*, **113**, 5, 2013, pp. 3766-3798.

42. K. S. Novoselov, A. K. Geim, S. V. Morozov, D. Jiang, Y. Zhang, S. V. Dubonos, I. V. Grigorieva, and A. A. Firsov, "Electric Field Effect in Atomically Thin Carbon Films," *Science*, **306**, 5696, 2004, pp. 666-669.

43. D. Golberg, Y. Bando, Y. Huang, T. Terao, M. Mitome, C. Tang, and C. Zhi, "Boron Nitride Nanotubes and Nanosheets," *ACS Nano*, **4**, 6, 2010, pp. 2979-2993.

44. J. N. Coleman, M. Lotya, A. O'Neill, S. D. Bergin, P. J. King, U. Khan, K. Young, A. Gaucher, S. De, R. J. Smith, I. V. Shvets, S. K. Arora, G. Stanton, H.-Y. H.-Y. Kim, K. Lee, G. T. Kim, G. S. Duesberg, T. Hallam, J. J. Boland, J. J. Wang, J. F. Donegan, J. C. Grunlan, G. Moriarty, A. Shmeliov, R. J. Nicholls, J. M. Perkins, E. M. Grieveson, K. Theuwissen, D. W. McComb, P. D. Nellist, V. Nicolosi, A. O'Neill, S. D. Bergin, P. J. King, U. Khan, K. Young, A. Gaucher, S. De, R. J. Smith, I. V. Shvets, S. K. Arora, G. Stanton, H.-Y. H.-Y. Kim, K. Lee, G. T. Kim, G. S. Duesberg, T. Hallam, J. J. Boland, J. J. Wang, J. F. Donegan, J. C. Grunlan, G. Moriarty, A. Shmeliov, R. J. Nicholls, J. M. Perkins, E. M. Grieveson, K. Theuwissen, D. W. McComb, P. D. Nellist and V. Nicolosi, "Two-Dimensional Nanosheets Produced by Liquid Exfoliation of Layered Materials," *Science*, **331**, 6017, 2011, pp. 568-571.

45. M. Chhowalla, H. S. Shin, G. Eda, L.-J. Li, K. P. Loh, and H. Zhang, "The Chemistry of Two-Dimensional Layered Transition Metal Dichalcogenide Nanosheets," *Nature Chemistry*, **5**, 4, 2013, pp. 263-275.

46. L. Tao, E. Cinquanta, D. Chiappe, C. Grazianetti, M. Fanciulli, M. Dubey, A. Molle, and D. Akinwande, "Silicene Field-Effect Transistors Operating at Room Temperature," *Nature Nanotechnology*, **10**, 3, 2015, pp. 227-231.

47. J. Zhao, H. Liu, Z. Yu, R. Quhe, S. Zhou, Y. Wang, C. C. Liu, H. Zhong, N. Han, J. Lu, Y. Yao and K. Wu, "Rise of Silicene: A Competitive 2D Material," *Progress in Materials Science*, **83**, 2016, pp. 24-151.

48. M. Davila, L. Xian, S. Cahangirov, A. Rubio, and G. Le Lay, "Germanene: a Novel Two-Dimensional Germanium Allotrope Akin to Graphene and Silicene," *New Journal of Physics*, **16**, 9, 2014, p. 095002.

49. S. Balendhran, S. Walia, H. Nili, S. Sriram, and M. Bhaskaran, "Elemental Analogues of Graphene: Silicene, Germanene, Stanene, and Phosphorene," *Small*, **11**, 6, 2015, pp. 640-652.

50. L. Li, Y. Yu, G. J. Ye, Q. Ge, X. Ou, H. Wu, D. Feng, X. H. Chen, and Y. Zhang, "Black Phosphorus Field-Effect Transistors," *Nature Nanotechnology*, **9**, 5, 2014, p. 372.

51. H. Liu, A. T. Neal, Z. Zhu, Z. Luo, X. Xu, D. Tomanek, and P. D. Ye, "Phosphorene: An Unexplored 2D Semiconductor with a High Hole Mobility," *ACS Nano*, **8**, 4, 2014, pp. 4033-4041.

52. J. Pang, A. Bachmatiuk, Y. Yin, B. Trzebicka, L. Zhao, L. Fu, R. G. Mendes, T. Gemming, Z. Liu, and M. H. Rummeli, "Applications of Phosphorene and Black Phosphorus in Energy Conversion and Storage Devices," *Advanced Energy Materials*, **8**, 8, 2018, p. 1702093.

53. A. J. Mannix, X.-F. Zhou, B. Kiraly, J. D. Wood, D. Alducin, B. D. Myers, X. Liu, B. L. Fisher, U. Santiago, J. R. Guest et al., "Synthesis of Borophenes: Anisotropic, Two-Dimensional Boron Polymorphs," *Science*, **350**, 6267, 2015, pp. 1513-1516.

54. B. Feng, J. Zhang, Q. Zhong, W. Li, S. Li, H. Li, P. Cheng, S. Meng, L. Chen, and K. Wu, "Experimental Realization of Two-Dimensional Boron Sheets," *Nature Chemistry*, **8**, 6, 2016, pp. 563-568.

55. M. Bernardi, C. Ataca, M. Palummo, and J. C. Grossman, "Optical and Electronic Properties of Two-Dimensional Layered Materials," *Nanophotonics*, **6**, 2, 2017, pp. 479-493.

56. A. C. Neto, F. Guinea, N. M. Peres, K. S. Novoselov, and A. K. Geim, "The Electronic Properties of Graphene," *Reviews of Modern Physics*, **81**, 1, 2009, p. 109.

57. A. Grigorenko, M. Polini, and K. Novoselov, "Graphene Plasmonics," *Nature Photonics*, **6**, 11, 2012, pp. 749-758.

58. F. Bonaccorso, Z. Sun, T. Hasan, and A. Ferrari, "Graphene Photonics and Optoelectronics," *Nature Photonics*, **4**, 9, 2010, p. 611.

59. A. B. Kuzmenko, E. Van Heumen, F. Carbone, and D. Van Der Marel, "Universal Optical Conductance of Graphite," *Physical Review Letters*, **100**, 11, 2008, p. 117401.

60. R. R. Nair, P. Blake, A. N. Grigorenko, K. S. Novoselov, T. J. Booth, T. Stauber, N. M. Peres, and A. K. Geim, "Fine Structure Constant Defines Visual Transparency of Graphene," *Science*, **320**, 5881, 2008, pp. 1308-1308.

61. Z. Li, E. A. Henriksen, Z. Jiang, Z. Hao, M. C. Martin, P. Kim, H. Stormer, and D. N. Basov, "Dirac Charge Dynamics in Graphene by Infrared Spectroscopy," *Nature Physics*, **4**, 7, 2008, pp. 532-535.

62. Q. Bao, H. Zhang, Y. Wang, Z. Ni, Y. Yan, Z. X. Shen, K. P. Loh, and D. Y. Tang, "Atomic-Layer Graphene as a Saturable Absorber for Ultrafast Pulsed Lasers," *Advanced Functional Materials*, **19**, 19, 2009, pp. 3077-3083.

63. X. Sun, Z. Liu, K. Welsher, J. T. Robinson, A. Goodwin, S. Zaric, and H. Dai, "Nano-Graphene Oxide for Cellular Imaging and Drug Delivery," *Nano Research*, **1**, 3, 2008, pp. 203-212.

64. Z. Luo, P. M. Vora, E. J. Mele, A. C. Johnson, and J. M. Kikkawa, "Photoluminescence and Band Gap Modulation in Graphene Oxide," *Applied Physics Letters*, **94**, 11, 2009, p. 111909.

65. C. Casiraghi, A. Hartschuh, E. Lidorikis, H. Qian, H. Harutyunyan, T. Gokus, K. S. Novoselov, and A. Ferrari, "Rayleigh Imaging of Graphene and Graphene Layers," *Nano Letters*, **7**, 9, 2007, pp. 2711-2717.

66. M. Liu, X. Yin, E. Ulin-Avila, B. Geng, T. Zentgraf, L. Ju, F. Wang, and X. Zhang, "A Graphene-Based Broadband Optical Modulator," *Nature*, **474**, 7349, 2011, pp. 64-67.

67. A. Pospischil, M. Humer, M. M. Furchi, D. Bachmann, R. Guider, T. Fromherz, and T. Mueller, "CMOS-Compatible Graphene Photodetector Covering all Optical Communication Bands," *Nature Photonics*, **7**, 11, 2013, pp. 892-896.

68. F. Koppens, T. Mueller, P. Avouris, A. Ferrari, M. Vitiello, and M. Polini, "Photodetectors Based on Graphene, Other Two-Dimensional Materials and Hybrid Systems," *Nature Nanotechnology*, **9**, 10, 2014, pp. 780-793.

69. F. Wang, Y. Zhang, C. Tian, C. Girit, A. Zettl, M. Crommie, and Y. R. Shen, "Gate-Variable Optical Transitions in Graphene," *Science*, **320**, 5873, 2008, pp. 206-209.

70. F. Xia, T. Mueller, Y.-m. Lin, A. Valdes-Garcia, and P. Avouris, "Ultrafast Graphene Photodetector," *Nature Nanotechnology*, **4**, 12, 2009, pp. 839-843.

71. A. Urich, K. Unterrainer, and T. Mueller, "Intrinsic Response Time of Graphene Photodetectors," *Nano Letters*, **11**, 7, 2011, pp. 2804-2808.

72. V. Sorianello, M. Midrio, G. Contestabile, I. Asselberghs, J. Van Campenhout, C. Huyghebaert, I. Goykhman, A. Ott, A. Ferrari, and M. Romagnoli, "Graphene-Silicon Phase Modulators with Gigahertz Bandwidth," *Nature Photonics*, **12**, 1, 2018, pp. 40-44.

73. D. Schall, E. Pallecchi, G. Ducournau, V. Avramovic, M. Otto, and D. Neumaier, "Record High Bandwidth Integrated Graphene Photodetectors for Communication Beyond 180 Gb/s," in *Optical Fiber Communication Conference*, Optical Society of America, 2018, pp. M2I-4.

74. P. Ma, Y. Salamin, B. Baeuerle, A. Josten, W. Heni, A. Emboras, and J. Leuthold, "Plasmonically Enhanced Graphene Photodetector Featuring 100 Gbit/s Data Reception, High Responsivity, and Compact Size," *ACS Photonics*, **6**, 1, 2018, pp. 154-161.

75. J. E. Muench, A. Ruocco, M. A. Giambra, V. Miseikis, D. Zhang, J. Wang, H. F. Watson, G. C. Park, S. Akhavan, V. Sorianello et al., "Waveguide Integrated, Plasmonic Enhanced Graphene Photodetectors," *Nano Letters*, **19**, 11, 2019, pp. 7632-7644.

76. S. W. Tong, Y. Wang, Y. Zheng, M.-F. Ng, and K. P. Loh, "Graphene Intermediate Layer in Tandem Organic Photovoltaic Cells," *Advanced Functional Materials*, **21**, 23, 2011, pp. 4430-4435.

77. J. Wu, M. Agrawal, H. A. Becerril, Z. Bao, Z. Liu, Y. Chen, and P. Peumans, "Organic Light-Emitting Diodes on Solution-Processed Graphene Transparent Electrodes," *ACS Nano*, **4**, 1, 2010, pp. 43-48.

78. A. Splendiani, L. Sun, Y. Zhang, T. Li, J. Kim, C.-Y. Chim, G. Galli, and F. Wang, "Emerging Photoluminescence in Monolayer MoS_2," *Nano Letters*, **10**, 4, 2010, pp. 1271-1275.

79. T. Cheiwchanchamnangij and W. R. Lambrecht, "Quasiparticle Band Structure Calculation of Monolayer, Bilayer, and Bulk MoS_2," *Physical Review B*, **85**, 20, 2012, p. 205302.

80. C. Ataca, H. Sahin, and S. Ciraci, "Stable, Single-Layer MX_2 Transition-Metal Oxides and Dichalcogenides in a Honeycomb-Like Structure," *The Journal of Physical Chemistry C*, **116**, 16, 2012, pp. 8983-8999.

81. J. A. Wilson and A. Yoffe, "The Transition Metal Dichalcogenides Discussion and Interpretation of the Observed Optical, Electrical and Structural Properties," *Advances in Physics*, **18**, 73, 1969, pp. 193-335.

82. A. Chaves, J. Azadani, H. Alsalman, D. R. da Costa, R. Frisenda, A. Chaves, S. H. Song, Y. Kim, D. He, J. Zhou *et al.*, "Bandgap Engineering of Two-Dimensional Semiconductor Materials," *npj 2D Materials and Applications*, **4**, 1, 2020, pp. 1-21.

83. K. F. Mak, C. Lee, J. Hone, J. Shan, and T. F. Heinz, "Atomically Thin MoS_2: A New Direct-Gap Semiconductor," *Physical Review Letters*, **105**, 13, 2010, p. 136805.

84. Y. Zhang, T.-R. Chang, B. Zhou, Y.-T. Cui, H. Yan, Z. Liu, F. Schmitt, J. Lee, R. Moore, Y. Chen et al., "Direct Observation of the Transition from Indirect to Direct Bandgap in Atomically thin Epitaxial $MoSe_2$," *Nature Nanotechnology*, **9**, 2, 2014, p. 111.

85. W. Zhao, Z. Ghorannevis, L. Chu, M. Toh, C. Kloc, P.-H. Tan, and G. Eda, "Evolution of Electronic Structure in Atomically Thin Sheets of WS_2 and WSe_2," *ACS Nano*, **7**, 1, 2013, pp. 791-797.

86. S. Lei, L. Ge, Z. Liu, S. Najmaei, G. Shi, G. You, J. Lou, R. Vajtai, and P. M. Ajayan, "Synthesis and Photoresponse of Large GaSe Atomic Layers," *Nano Letters*, **13**, 6, 2013, pp. 2777-2781.

87. L. Li, Z. Chen, Y. Hu, X. Wang, T. Zhang, W. Chen, and Q. Wang, "Single-Layer Single-Crystalline SnSe Nanosheets," *Journal of the American Chemical Society*, **135**, 4, 2013, pp. 1213-1216.

88. B. Anasori, M. R. Lukatskaya, and Y. Gogotsi, "2D Metal Carbides and Nitrides (MXenes) for Energy Storage," *Nature Reviews Materials*, **2**, 2, 2017, pp. 1-17.

89. C. R. Dean, A. F. Young, I. Meric, C. Lee, L. Wang, S. Sorgenfrei, K. Watanabe, T. Taniguchi, P. Kim, K. L. Shepard et al., "Boron Nitride Substrates for High-Quality Graphene Electronics," *Nature Nanotechnology*, **5**, 10, 2010, pp. 722-726.

90. A. Lodesani, A. Picone, A. Brambilla, D. Giannotti, M. S. Jagadeesh, A. Calloni, G. Bussetti, G. Berti, M. Zani, M. Finazzi, L. Duò and F. Ciccacci, "Graphene as an Ideal Buffer Layer for the Growth of High-Quality Ultrathin Cr_2O_3 Layers on Ni(111)," *ACS Nano*, **13**, 4, 2019, pp. 4361-4367.

91. W. Ma, P. Alonso-González, S. Li, A. Y. Nikitin, J. Yuan, J. Martín-Sánchez, J. Taboada-Gutiérrez, I. Amenabar, P. Li, S. Vélez, C. Tollan, Z. Dai, Y. Zhang, S. Sriram, K. Kalantar-Zadeh, S.-T. Lee, R. Hillenbrand and Q. Bao, "In-Plane Anisotropic and Ultra-Low-Loss Polaritons in a Natural van der Waals Crystal," *Nature*, **562**, 7728, 2018, pp. 557-562.

92. P. Vogt, P. De Padova, C. Quaresima, J. Avila, E. Frantzeskakis, M. C. Asensio, A. Resta, B. Ealet, and G. Le Lay, "Silicene: Compelling Experimental Evidence for Graphene-Like Two-Dimensional Silicon," *Physical Review Letters*, **108**, 15, 2012, p. 155501.

93. L. Li, S. Z. Lu, J. Pan, Z. Qin, Y. Q. Wang, Y. Wang, G. Y. Cao, S. Du, and H. J. Gao, "Buckled Germanene Formation on Pt (111)," *Advanced Materials*, **26**, 28, 2014, pp. 4820-4824.

94. Z. Zhu, X. Cai, S. Yi, J. Chen, Y. Dai, C. Niu, Z. Guo, M. Xie, F. Liu, J.-H. Cho et al., "Multivalency-Driven Formation of Te-Based Monolayer Materials: a Combined First-Principles and Experimental Study," *Physical Review Letters*, **119**, 10, 2017, p. 106101.

95. V. Kochat, A. Samanta, Y. Zhang, S. Bhowmick, P. Manimunda, S. A. S. Asif, A. S. Stender, R. Vajtai, A. K. Singh, C. S. Tiwary and P. M. Ajayan, "Atomically Thin Gallium Layers from Solid-Melt Exfoliation," *Science Advances*, **4**, 3, 2018, p. e1701373.

96. J. Ji, X. Song, J. Liu, Z. Yan, C. Huo, S. Zhang, M. Su, L. Liao, W. Wang, Z. Ni, Y. Hao and H. Zeng, "Two-Dimensional Antimonene Single Crystals Grown by van der Waals Epitaxy," *Nature Communications*, **7**, 1, 2016, pp. 1-9.

97. R. Wu, I. K. Drozdov, S. Eltinge, P. Zahl, S. Ismail-Beigi, I. Bozovic, and A. Gozar, "Large-Area Single-Crystal Sheets of Borophene on Cu (111) Surfaces," *Nature Nanotechnology*, **14**, 1, 2019, pp. 44-49.

98. L. Fu and C. L. Kane, "Superconducting Proximity Effect and Majorana Fermions at the Surface of a Topological Insulator," *Physical Review Letters*, **100**, 9, 2008, p. 096407.

99. C. A. Balanis, *Advanced Engineering Electromagnetics*, John Wiley & Sons, 2012.

100. S. A. Maier, *Plasmonics: Fundamentals and Applications,* New York, NY, Springer US, 2007.

101. S. G. Menabde, D. R. Mason, E. E. Kornev, C. Lee, and N. Park, "Direct Optical Probing of Transverse Electric Mode in Graphene," *Scientific Reports*, **6**, 1, 2016, p. 21523.

102. J. Weiner and F. Nunes, *Light-Matter Interaction: Physics and Engineering at the Nanoscale,* Oxford University Press, 2017.

103. C. H. Lee, *Light-Matter Interaction: Atoms and Molecules in External Fields and Nonlinear Optics,* New York, John Wiley & Sons, 2008.

104. Y. V. Bludov, A. Ferreira, N. M. R. Peres, and M. I. Vasilevskiy, "A Primer on Surface Plasmon-Polaritons in Graphene," *International Journal of Modern Physics B*, **27**, 10, 2013, p. 1341001.

105. F. Ramos-Mendieta, J. A. Hernandez-Lòpez, and M. Palomino-Ovando, "Transverse Magnetic Surface Plasmons and Complete Absorption Supported by Doped Graphene in Otto Configuration," *AIP Advances*, **4**, 6, 2014, p. 067125.

106. J. B. Pendry, L. Martìn-Moreno, and F. J. Garcia-Vidal, "Mimicking Surface Plasmons with Structured Surfaces," *Science*, **305**, 5685, 2004, pp. 847-848.

107. M. Merano, "Fresnel Coefficients of a Two-Dimensional Atomic Crystal," *Physical Review A*, **93**, 1, 2016, p. 013832.

108. Y. C. Chang, C. H. Liu, C. H. Liu, Z. Zhong, and T. B. Norris, "Extracting the Complex Optical Conductivity of Mono- and Bilayer Graphene by Ellipsometry," *Applied Physics Letters*, **104**, 26, 2014, p. 261909.

109. G. W. Hanson, "Dyadic Green's Functions and Guided Surface Waves for a Surface Conductivity Model of Graphene," *Journal of Applied Physics*, **103**, 6, 2008, p. 064302.

110. L. Falkovsky and S. Pershoguba, "Optical Far-Infrared Properties of a Graphene Monolayer and Multilayer," *Physical Review B*, **76**, 15, 2007, p. 153410.

111. L. Zhou, Y. Wang, and G. Cao, "Estimating the Elastic Properties of Few-Layer Graphene from the Free-Standing Indentation Response," *Journal of Physics: Condensed Matter*, **25**, 47, 2013, p. 475301.

112. V. Sorianello, M. Midrio, and M. Romagnoli, "Design Optimization of Single and Double Layer Graphene Phase Modulators in SOI," *Optics express*, **23**, 5, 2015, pp. 6478-6490.

113. F. Wang, Y. Zhang, C. Tian, C. Girit, A. Zettl, M. Crommie, and Y. R. Shen, "Gate-Variable Optical Transitions in Graphene," *Science*, **320**, 5873, 2008, pp. 206-209.

114. T. G. Pedersen, "Analytic Calculation of the Optical Properties of Graphite," *Physical Review B*, **67**, 11, 2003, p. 113106.

115. V. Sorianello, G. De Angelis, T. Cassese, M. Midrio, M. Romagnoli, M. Mohsin, M. Otto, D. Neumaier, I. Asselberghs, J. Van Campenhout and C. Huyghebaert, "Complex Effective Index in Graphene-Silicon Waveguides," *Optics Express*, **24**, 26, 2016, pp. 29984-29993.

116. P. R. Wallace, "The Band Theory of Graphite," *Physical Review*, **71**, 9, 1947, p. 622.

117. Z. Xu, D. Ferraro, A. Zaltron, N. Galvanetto, A. Martucci, L. Sun, P. Yang, Y. Zhang, Y. Wang, Z. Liu, J. D. Elliott, M. Marsili, L. Dell'Anna, P. Umari and M. Merano, "Optical Detection of the Susceptibility Tensor in Two-Dimensional Crystals," *Communications Physics*, **4**, 1, 2021, pp. 1-8.

118. S. A. Maier, M. L. Brongersma, P. G. Kik, S. Meltzer, A. A. G. Requicha, and H. A. Atwater, "Plasmonics – A Route to Nanoscale Optical Devices," *Advanced Materials*, **13**, 19, 2001, pp. 1501-1505.

119. T. Low, A. Chaves, J. D. Caldwell, A. Kumar, N. X. Fang, P. Avouris, T. F. Heinz, F. Guinea, L. Martin-Moreno, and F. Koppens, "Polaritons in Layered Two-Dimensional Materials," *Nature Materials*, **16**, 2, 2017, pp. 182-194.

120. M. Jablan, H. Buljan, and M. Soljacic, "Plasmonics in Graphene at Infrared Frequencies," *Physical Review B*, **80**, 24, 2009, p. 245435.

121. G. W. Hanson, "Dyadic Green's Functions and Guided Surface Waves for a Surface Conductivity Model of Graphene," *Journal of Applied Physics*, **103**, 6, 2008, p. 64302.

122. L. A. Falkovsky and A. A. Varlamov, "Space-Time Dispersion of Graphene Conductivity," *The European Physical Journal B*, **56**, 4, 2007, pp. 281-284.

123. S. A. Mikhailov and K. Ziegler, "New Electromagnetic Mode in Graphene," *Physical Review Letters*, **99**, 1, 2007, p. 16803.

124. E. H. Hwang and S. D. Sarma, "Dielectric Function, Screening, and Plasmons in Two-Dimensional Graphene," *Physical Review B*, **75**, 20, 2007, p. 205418.

125. M. S. Ukhtary, E. H. Hasdeo, A. R. T. Nugraha, and R. Saito, "Fermi Energy-Dependence of Electromagnetic Wave Absorption in Graphene," *Applied Physics Express*, **8**, 5, 2015, p. 55102.

126. C. Kittel, P. McEuen, and P. McEuen, *Introduction to Solid State Physics*, New York, Wiley, 1996, **8**.

127. M. Jablan, M. Soljacic, and H. Buljan, "Plasmons in Graphene: Fundamental Properties and Potential Applications," *Proceedings of the IEEE*, **101**, 7, 2013, pp. 1689-1704.

128. H. Y. Deng and K. Wakabayashi, "Retardation Effects on Plasma Waves in Graphene, Topological Insulators, and Quantum Wires," *Physical Review B*, **92**, 4, 2015, p. 45434.

129. A. Vakil and N. Engheta, "Transformation Optics Using Graphene," *Science*, **332**, 6035, 2011, pp. 1291-1294.

130. M. S. Ukhtary, A. R. Nugraha, E. H. Hasdeo, and R. Saito, "Broadband Transverse Electric Surface Wave in Silicene," *Applied Physics Letters*, **109**, 6, 2016, p. 063103.

131. D. Sarid and W. A. Challener, *Modern Introduction to Surface Plasmons: Theory, Mathematical Modeling, and Applications*, Cambridge University Press, 2010.

132. X. Zhang, H. Hu, X. Lin, L. Shen, B. Zhang, and H. Chen, "Confined Transverse-Electric Graphene Plasmons in Negative Refractive-Index Systems," *npj 2D Materials and Applications*, **4**, 1, 2020, pp. 1-6.

133. Y. V. Bludov, D. A. Smirnova, Y. S. Kivshar, N. Peres, and M. I. Vasilevskiy, "Nonlinear TE-Polarized Surface Polaritons on Graphene," *Physical Review B*, **89**, 3, 2014, p. 035406.

134. M. Merano, "Transverse Electric Surface Mode in Atomically Thin Boron-Nitride," *Optics Letters*, **41**, 11, 2016, pp. 2668-2671.

135. G. Franceschetti, *Electromagnetics: Theory, Techniques, and Engineering Paradigms*, Berlin, Springer Science & Business Media, 2013.

136. R. E. Collin, *Foundations for Microwave Engineering*, New York, John Wiley & Sons, 2007.

137. C. B. Reynolds, M. S. Ukhtary, and R. Saito, "Absorption of THz Electromagnetic Wave in Two Mono-layers of Graphene," *Journal of Physics D: Applied Physics*, **49**, 19, 2016, p. 195306.

138. A. G. Hammid, R. Gnawali, P. P. Banerjee, L. Sun, J. Slagle, and D. Evans, "2 × 2 Anisotropic Transfer Matrix Approach for Optical Propagation in Uniaxial Transmission Filter Structures," *Optics Express*, **28**, 24, 2020, pp. 35761-35783.

139. T. Zhan, X. Shi, Y. Dai, X. Liu, and J. Zi, "Transfer Matrix Method for Optics in Graphene Layers," *Journal of Physics: Condensed Matter*, **25**, 21, 2013, p. 215301.

140. M. B. Lodi, N. Curreli, A. Fanti, C. Cuccu, D. Pani, A. Sanginario, A. Spanu, P. M. Ros, M. Crepaldi, D. Demarchi and G. Mazzarella, "A Periodic Transmission Line Model for Body Channel Communication," *IEEE Access*, **8**, 2020, pp. 160099-160115.

141. B. E. A. Saleh and M. C. Teich, *Fundamentals of Photonics*, Wiley Series in Pure and Applied Optics **5**, New York, USA, John Wiley & Sons, Inc., 1991.

142. W. Welford, "The Principles of Nonlinear Optics," *Physics Bulletin*, **36**, 4, 1985, p. 178.

143. R. Boyd, *Nonlinear Optics, Third Edition*, New York, Elsevier, 2008.

144. C. Manzoni and G. Cerullo, "Design Criteria for Ultrafast Optical Parametric Amplifiers," *Journal of Optics*, **18**, 10, 2016, p. 103501.

145. M. Merano, "Nonlinear Optical Response of a Two-Dimensional Atomic Crystal," *Optics Letters*, **41**, 1, 2016, pp. 187-190.

146. N. Bloembergen and P. Pershan, "Light Waves at the Boundary of Nonlinear Media," *Physical Review*, **128**, 2, 1962, p. 606.

147. J. Sipe, D. Moss, and H. Van Driel, "Phenomenological Theory of Optical Second-and Third-Harmonic Generation from Cubic Centrosymmetric Crystals," *Physical Review B*, **35**, 3, 1987, p. 1129.

148. C. Trovatello, A. Marini, X. Xu, C. Lee, F. Liu, N. Curreli, C. Manzoni, S. Dal Conte, K. Yao, A. Ciattoni et al., "Optical Parametric Amplification by Monolayer Transition Metal Dichalcogenides," *Nature Photonics*, **15**, 1, 2021, pp. 6-10.

149. J. He, K. Hummer, and C. Franchini, "Stacking Effects on the Electronic and Optical Properties of Bilayer Transition Metal Dichalcogenides MoS_2, $MoSe_2$, WS_2, and WSe_2," *Physical Review B - Condensed Matter and Materials Physics*, **89**, 7, 2014, p. 075409.

150. Y. Li, Y. Rao, K. F. Mak, Y. You, S. Wang, C. R. Dean, and T. F. Heinz, "Probing Symmetry Properties of Few-Layer MoS_2 and h-BN by Optical Second-Harmonic Generation," *Nano Letters*, **13**, 7, 2013, pp. 3329-3333.

151. N. Kumar, S. Najmaei, Q. Cui, F. Ceballos, P. M. Ajayan, J. Lou, and H. Zhao, "Second Harmonic Microscopy of Monolayer MoS_2," *Physical Review B*, **87**, 16, 2013, p. 161403.

152. M. Zhao, Z. Ye, R. Suzuki, Y. Ye, H. Zhu, J. Xiao, Y. Wang, Y. Iwasa, and X. Zhang, "Atomically Phase-Matched Second-Harmonic Generation in a 2DCrystal," *Light: Science & Applications*, **5**, 8, 2016, pp. e16131-e16131.

On the Use of Power-Transfer Efficiency to Analyze the Performance of a 3D-Printed Wearable UHF-RFID Antenna

Andrea Michel[1] and Rajesh Kumar Singh[2]

[1]Department of Information Engineering
University of Pisa
Pisa, Italy
E-mail: andrea.michel@unipi.it

[2]Defence Institute of Advanced Technology Girinagar, Pune, Maharashtra

Abstract

Novel Yagi-like antenna structures were investigated here to design a UHF-RFID wearable antenna. The textile antennas were designed to be integrated into a smart glove, together with a compact UHF-RFID reader. Parasitic elements, acting as either a reflector or directors, were included to focus the field out of the operator's hand, thereby limiting the radiation toward undesired directions. To predict and compare the performance of the proposed near-field antennas, the power-transfer efficiency was numerically computed as a function of the reader-tag distance.

1. Introduction

The connection of humans with machines has become one of the most relevant topics in current and future scientific research. The aim of Internet of Things (IoT) applications is to connect things to the Internet and to provide access from anywhere. The use of radio-frequency identification (RFID) technology helps in connecting and identifying objects or people through tagging. RFID is often seen as a requirement for the IoT [1]. An RFID reader communicates with the tags or tagged objects using radio waves. In previous years, RFID technology has attracted interest in wearable applications such as warehouse and inventory environments. For example, in warehouses, human operators use an RFID reader to detect tagged objects and to collect information. A wearable, portable RFID reader helps the user to reduce his/her effort compared to a situation where the human holds the reader in one of his/her hands every time during the tasks. This might cause an uncomfortable situation, because users have only one hand to perform their own tasks. The user's hand would be free for doing other tasks if an RFID reader could be in a wearable form, such as reader integrated into a hand glove: the so-called *smart glove*.

By integrating the RFID reader into a smart glove, the human will not face any inconvenience due to the presence of the reader. As an example, in [2] a low-frequency RFID reader and a specific antenna were integrated into a cloth. The RFID reader was integrated into small housing with a belt clip. The glove antenna was connected to the reader with a wire, and the reading range was limited by the length of the wire. Another solution was reported in [3], facing the same problem because of the wired connection between glove antenna and the reader. In [4], a miniature RFID reader, power supply, and wireless unit were integrated into surgical gloves and bracelets. There were various other solutions of RFID smart gloves previously reported in the low-frequency (LF), high-frequency (HF), and ultra-high-frequency (UHF) RFID bands for various applications, such as gesture or activity recognition [5, 6], activity tracking in car manufacturing [7], rehabilitation [8], medical [9, 10], etc.

In [11], a compact wearable RFID reader was integrated into a glove to help workers in warehouses. Reading distances from 0.8 cm to 3.5 cm, depending on the tag type, were obtained. An evaluation to increase the support to humans in factory environments using a smart glove was done in [12]. Smart gloves with an efficient reader antenna are more popular, especially in the UHF RFID band, where the reader and the antenna are both placed close to the human body [13, 14]. In this structure, there are several challenges that arise in realizing wearable antennas while maintaining the expected performance. This is because the performance of the wearable antennas is affected by the dielectric properties of the human body. Wearable antennas must be highly immune and robust to the presence of the human body. Their performance must not be affected when they are in proximity to the human body. Numerical analysis is therefore necessary to evaluate human-body proximity and to optimize the antenna's performance in the operating frequency band.

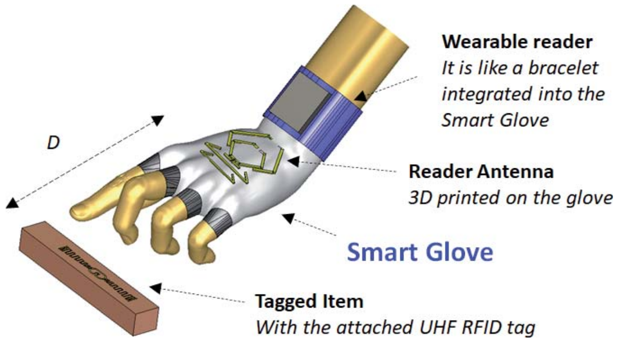

Figure 1a. A schematic representation of the operating scenario.

Figure 1b. Possible positions of UHF-RFID reader antennas designed for smart gloves around the wrist.

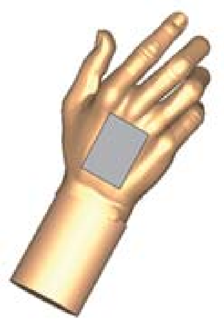

Figure 1c. Possible positions of UHF-RFID reader antennas designed for smart gloves on the hand's palm.

Specifically, a UHF-RFID smart glove is needed to detect tags or tagged objects that are close to the human hand, and to avoid the detection of tagged objects positioned at a farther distance (false positives). For the given requirements, especially in warehouses, an RFID smart glove needs to allow for the detection of tagged objects placed at a distance up to 30 cm to 40 cm from the human hand. Given the typical size of an antenna integrated into a glove, the far-field region starts beyond 70 cm to 80 cm, and this means that the tagged objects and glove-reader antennas are in the near-field region of each other, as schematically represented in Figure 1a. In such an operating scenario, the conventional far-field antenna parameters, such as radiation pattern, radiation efficiency, and antenna gain, cannot be considered as effective figures of merit [14-17]. In some papers, the electric- and magnetic-field distributions were considered as key performance parameters to optimize the near-field antenna. However, they are not directly related to the characteristics of the tag's antenna, which can be of different shapes and sizes. For these reasons, new parameters have been proposed, such as the power-transfer efficiency (PTE). As demonstrated in [18], the power-transfer efficiency is a good candidate for qualitatively predicting the RSSI (received signal-strength indicator) distribution, and then the overall system performance. The power-transfer efficiency can be estimated by means of numerical tools, and it depends on antenna shapes of the reader and tag, as well as on the surrounding environment.

An efficient reader antenna, integrated into a smart glove, can provide identification of tagged objects within the detection area (within 30 cm to 40 cm) with relatively low power. In such compact solutions, a small battery is attached to provide power to the reader antenna. An efficient antenna would thus be a suitable candidate to save battery power, and it can be used for long hours. Reader antennas integrated into smart gloves are typically designed either around the wrist (Figure 1b), or on the back of a hand (Figure 1c). The reader antennas presented in [19-21] were made around the wrist, as a bracelet. These antennas consisted of loops or segmented solenoids. Loop and solenoid antennas excite a uniform and strong magnetic field along the axis of the solenoid/loop, and radiate bi-directionally (with a symmetric field distribution), as shown in Figure 2. When these antennas are used as bracelet antennas, there is a consequent waste of energy along the human arm, because the detection area is near the hand's palm or along the hand's fingers.

On the other hand, antennas integrated on the back of a hand's palm [22, 23] are advantageous over solenoid or loop antennas integrated around the wrist, because the latter obstruct the field more compared to those designed on the back of a hand's palm. A specific antenna layout could be a better candidate to limit field radiation toward the human arm. Among others, Yagi-Uda antennas are effective in directing fields along a particular direction. A compact quasi-Yagi antenna for a portable RFID reader

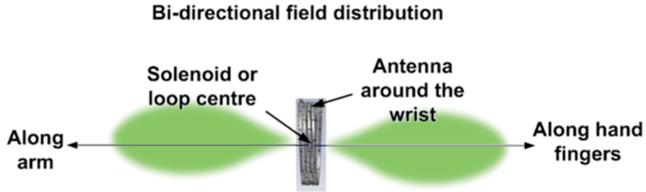

Figure 2a. A schematic representation of the field distributions: a solenoid or loop radiates a bi-directional field.

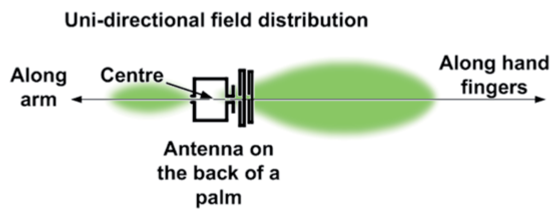

Figure 2b. A schematic representation of the field distributions: Yagi-like structures radiate more in one direction and less in other directions

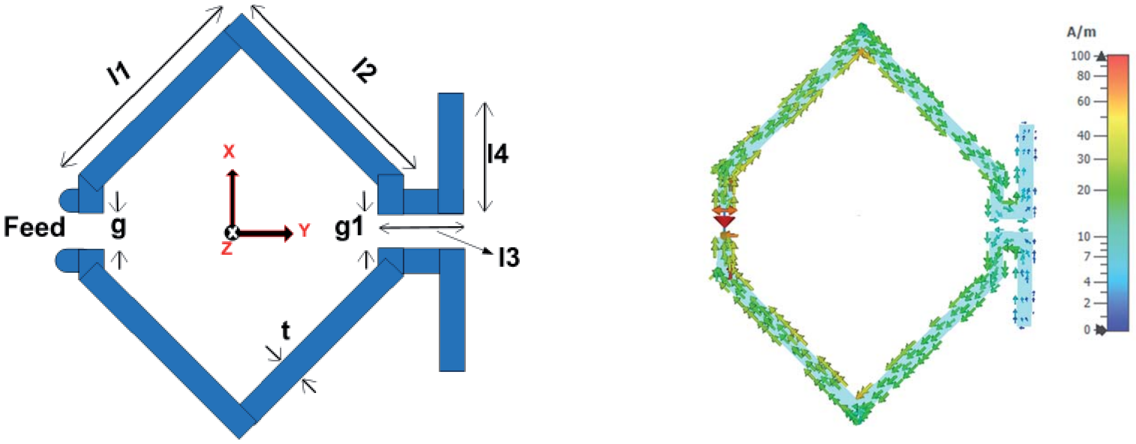

Figure 3. (a) A folded dipole (as a magnetic open loop) as a driving element for a quasi-Yagi antenna geometry; (b) the surface-current distribution; dimensions: $l1 = 3.3$ cm, $l2 = 3.5$ cm, $l3 = 0.35$ cm, $l4 = 1.05$ cm, $g = 0.2$ cm, $g1 = 0.2$ cm, $t = 0.3$ cm.

could be a valuable candidate for UHF near-field RFID applications [24-28]. An approach for combining loop and dipole antennas into a Yagi-like structure was presented in [26]. A dual-band version operating for UHF-RFID and 2.4 GHz applications was also described in [27, 28].

In this paper, the power-transfer efficiency parameter is considered to qualitatively estimate the performance of a smart glove reader antenna in terms of tag detection and reading range. Different layouts of compact and wearable quasi-Yagi structures for a UHF-RFID portable reader were investigated. The power-transfer efficiency was estimated for a set of quasi-Yagi structures (with one or two directors, with one reflector, with one reflector and one director, and with one reflector and two directors). In Section 2, a quasi-Yagi antenna is described, while in Section 3, a detailed analysis of the power-transfer efficiency is discussed. Preliminary results are also presented in Section 3. Conclusions are drawn in Section 4.

2. Smart Glove Reader Antennas

Typically, a Yagi-Uda antenna consists of a single driven element (a dipole or a folded dipole), a reflector, and one or more directors. Since the application focuses only on detecting tagged objects close to the human hand (inside the antenna's near-field region) – so as to avoid the detection of tags placed beyond the target's region – a modified layout must be designed to maximize the fields in the proximity of the smart glove, and to limit the radiation in the far field. In Figure 3a, a folded dipole is illustrated derived from a straight dipole to make current in-phase on the periphery of the folded arms. The antenna was designed for 868 MHz (the European UHF-RFID band). The total length of one arm of the rhombus-shaped folded dipole was 8.26 cm ($l1 + l2 + l3 + l4$), which was close to a quarter wavelength at the design frequency ($\lambda_0/4 = 8.63$ cm at 866 MHz). The antenna was simulated with full-wave electromagnetic-field-simulation software. The surface current flowed in one direction (in-phase current) along the folded dipole, as shown in Figure 3b. It generated a uniform magnetic field distributed above the open-loop section, with a maximum field at the center of the loop. Here, the folded dipole can be treated as a magnetic open loop.

Furthermore, to increase the field along the hand's fingers, a Yagi-like structure was adopted by adding one parasitic element to the rhombus-shaped folded dipole, as shown in Figure 4a. The director element was meandered to keep the size of the structure as compact as possible. An equivalent human-hand model was considered in the numerical analysis (Figure 5), so the lengths of the driven and parasitic elements of the antenna were optimized by considering the electrical properties of the human body. The thicknesses and electrical properties of the multilayer planar human hand model are given in Table 1.

A photo of the fabricated prototype is depicted in Figure 4b. A photo of a glove-integrated antenna worn on a hand is shown in Figure 4c. Antennas for smart gloves were made of conductive threads or by plating a non-conductive fabric with metal or alloy. Here, stretchable fabric was used as a dielectric material, and metallic parts were made on this fabric. The plain conductive fabric had a finite resistivity of 0.6 Ω/sq. This allowed for better stability of the antenna's parameters. The antenna was fed through a coaxial balun,

Table 1. Thicknesses and electrical properties of the multilayer planar human hand model.

Tissue Layer	Thickness (mm)	Conductivity @ 866 MHz (S/m)	Dielectric Constant @ 866 MHz
Skin	2 mm	0.85	41
Fat	2 mm	0.05	5.46
Muscle	2 mm	0.93	55
Bone	10 mm	0.14	12.5

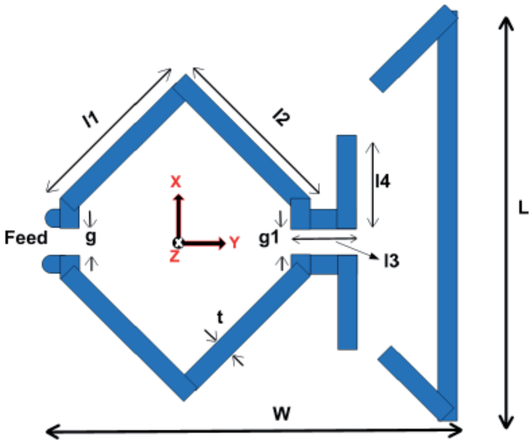

Figure 4a. The geometry of a quasi-Yagi layout with one director.

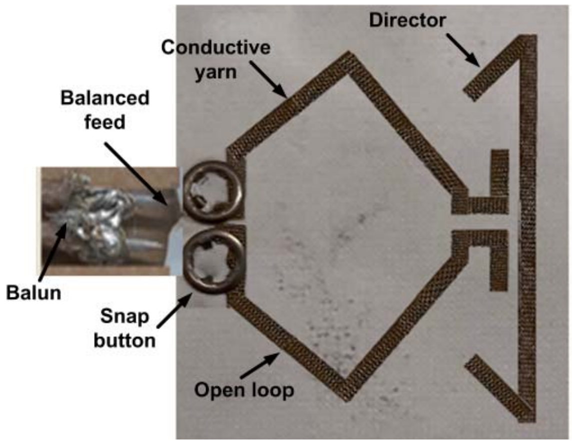

Figure 4b. A photo of a quasi-Yagi layout with one director.

Figure 4c. A photo of a glove-integrated antenna worn on the hand.

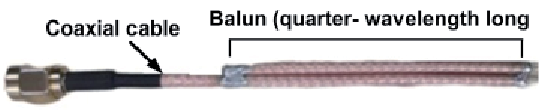

Figure 4d. A photo of a fabricated coaxial balun; dimensions: $W = 4.8$ cm, $L = 5.5$ cm.

as shown in Figure 4d. Snap buttons were attached to the antenna instead of soldering. Soldering is not possible for such fabrics. Both simulated and measured reflection coefficients are plotted in Figure 6, when the antenna was integrated into the glove, with and without the presence of the human hand. Quite good agreement between simulation and measurement results was obtained. A small shift in the resonance toward lower frequencies was due to the presence of the human hand. The measured impedance bandwidth of the fabricated antenna was larger compared to that obtained with the full-wave analysis because of the sheet resistance of the conductive material. This made the antenna suitable for RFID applications at ETSI (865 MHz to 868 MHz) and FCC (902 MHz to 928 MHz) bands. In [26], the effect of bending on the antenna performance was also discussed. Indeed, the textile antenna may be subjected to bending due to hand movement, which leads to a variation of the antenna's layout (e.g., the distance between elements may become larger), and thus to new antenna performance. However, thanks to the mechanical elasticity of the textile conductive fabric, a negligible variation in terms of input impedance could be observed while moving the hand from "closed" to "open."

The specific absorption rate (SAR) was calculated. Here, the European limit on SAR, which is 2 W/kg averaged over 10 g of tissue, was considered. The SAR-compliant transmission power was calculated to be 27.8 dBm. A reader power of 16.5 dBm was used in the measurement, which is well below the allowed limit. The received signal-strength indicator (RSSI) was measured, and then the reading range was calculated along the hand's fingers and along the arm. Preliminary results are discussed in the next section.

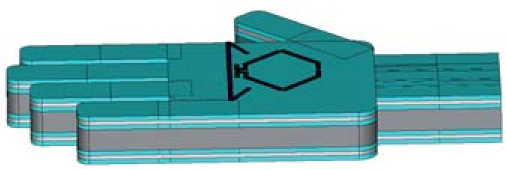

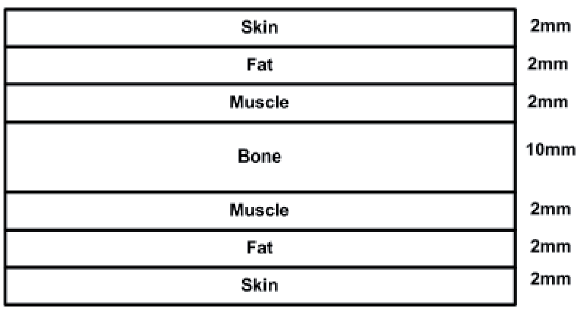

Figure 5. A multilayer model of a human hand: (a) the hand model with the antenna, and (b) the multilayer model including skin, fat, muscle, and cortical bone.

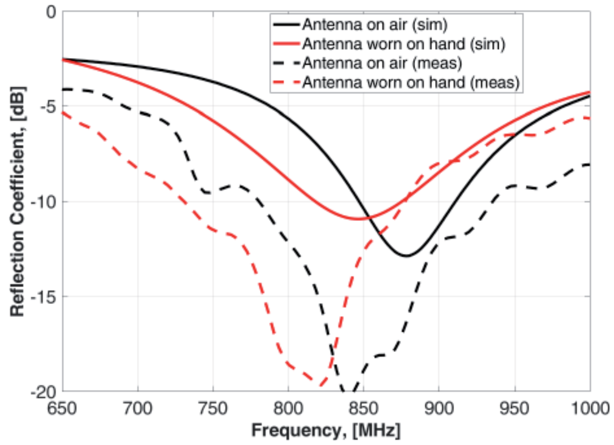

Figure 6. A comparison between the measured and simulated reflection coefficients.

3. Preliminary Results

Typically, a UHF-RFID system's performance in terms of reading range and reading rate is numerically estimated by assuming free-space propagation and local plane-wave illumination conditions. However, in some specific applications, these conditions are not satisfied, and novel propagation models must be developed. Such models are then exploited to deduce new system and antenna requirements. In the HF band, the power transmission from the reader antenna to the tag is basically an inductive coupling between loop antennas, and the equivalent circuit is represented by two coupled inductors and a mutual inductance. At the UHF band, both electric- and magnetic-energy-density distributions exhibit one or more peaks in the tag's near-field region. At the UHF band, a more-complex model is therefore needed, accounting for both electric and magnetic coupling [29-36].

Without loss of generality, the overall system can be fully characterized and described by means of a two-port equivalent network, which takes into account the reader and tag antenna characteristics, as well as the propagation channel and the presence of the human body (Figure 7). Specifically, the tag and reader antennas, and the space between them, were considered as a linear two-port network. The numerical evaluation of the entries of the impedance matrix, $\underline{\underline{Z}}$, was performed through the commercial numerical tool, CST *Microwave Studio*®.

A commercial tag layout (LAB-ID UH100) was imported into the numerical model, together with the proposed antenna. The wireless power-transfer efficiency between the reader and the tag was thus computed to qualitatively estimate the power delivered to the tag's chip when varying the tag position. The *power-transfer efficiency* was defined as the ratio between the power dissipated in the load of the tag's antenna (chip), P_T, and the input power accepted by the reader's antenna, P_R:

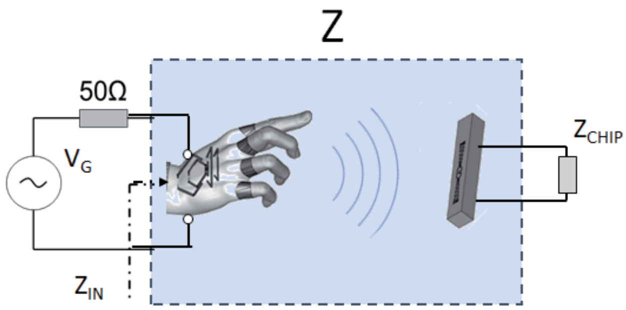

Figure 7. A schematic representation of a near-field UHF-RFID system consisting of a reader antenna and a tag antenna connected to the RFID chip.

$$PTE = \frac{P_T}{P_R}$$

$$= \frac{\frac{1}{2}\Re\{Z_L\}|I_2|^2}{\frac{1}{2}\Re\{Z_{IN}\}|I_1|^2}$$

$$= |Z_{21}|^2 \frac{\Re\{Z_L\}/\Re\{Z_{IN}\}}{|Z_L + Z_{22}|^2} \quad (1)$$

where Z_{in} is the input impedance of the two-port network when the latter is connected to Z_L. As apparent from Equation (1), the *power-transfer efficiency* expression is given by the square of the mutual-impedance amplitude (proportional to the open-circuit voltage at the tag's antenna) times a coefficient that includes the tag's loading.

To validate the effectiveness of the power-transfer efficiency for the qualitative estimation of the tag's detection performance of the reader's antenna, numerical simulations were carried out by varying the distance between the tag and

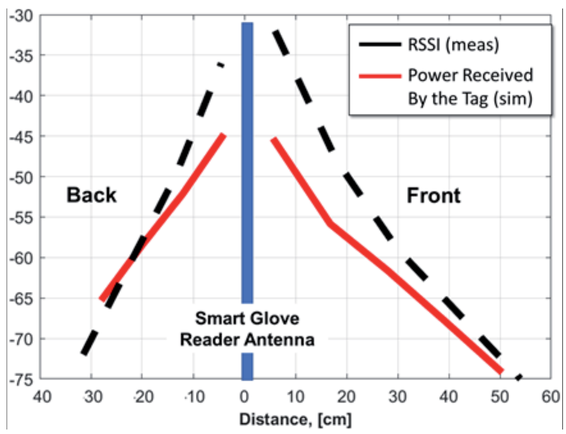

Figure 8. A comparison between the estimated power received by the tag and the measured RSSI as a function of the distance from the antenna.

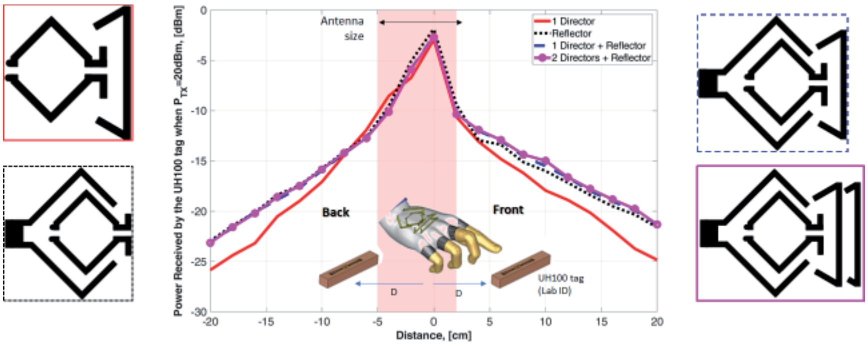

Figure 9. A comparison between the estimated power received by the tag and the measured RSSI as a function of the distance from the antenna.

the reader when the tag was both in front and in back of the antenna. Such power-transfer efficiency values were used to estimate the power received by the tag when the transmitting power was set to 20 dBm. This was then compared with the RSSI measurements obtained by means of a commercial UHF-RFID reader (CAEN RFID Ion, Model R4301P), when the reader output power was equal to 20 dBm. Preliminary results are shown in Figure 8. Even though the two curves were not perfectly overlapped, it could be observed that by using the power-transfer efficiency parameter, it was possible to estimate an asymmetric behavior of the reader antenna's radiated properties, since higher values were obtained in front of the hand with respect to the back: this was due to the Yagi-like structure.

Different layouts of Yagi-like smart-glove antennas have been also compared in terms of power-transfer efficiency as a function of the distance, by considering the same UH100 tag. In Figure 9, the simulated powers received by the tag when the transmitted power was set to 20 dBm are shown as a function of the distance in the front and rear directions. Four versions of the wearable antenna were considered, as shown in Figure 9:

- Antenna with only one director version (red solid line)
- Antenna with only reflector (black dotted line)
- Antenna with reflector and one director (blue dashed line)
- Antenna with reflector and two directors (magenta solid line with markers)

From this simulated analysis, some considerations can be drawn, predicting the real measured performance in terms of RSSI. First, the antenna version with only one director seemed to perform slightly worse than the other solutions. Indeed, by fixing one distance in the front or rear direction, the power received by the UH100 tag was lower than that achieved with the other reader-antenna layouts. The reading range was thus expected to be lower, since the UHF-RFID tag was activated when the received power was higher than the RFID chip's sensitivity, which was typically of the order of −23 dBm (this depends on the specific RFID chip mounted on the RFID tag). On the other hand, the antenna with a reflector in place of a single director was more effective in increasing the reading range of a few centimeters. Moreover, the reflector allowed for a lower reading range toward the rear direction, thus limiting the exposure of the human arm to the radiated electromagnetic fields. A slight improvement could be obtained by including both reflector and one director. In this case, a slight increase of the reading range was obtained in the front direction when both reflector and one director were contemporarily used. Given the overall available space on the back of the hand, a second director is not useful since it doesn't significantly impact the antenna's performance.

3. Conclusion

Typical parameters, such as radiation pattern, gain, or directivity, can not be used to estimate the reading range of UHF-RFID antennas for near-field applications, since the reader and tag antennas are not in the far-field region with respect to each other. Efforts are consequently being made to find new key parameters useful to predict the antenna's performance by means of numerical analysis. Among others, the power-transfer efficiency (PTE) represents an interesting parameter for taking into account during the design process in order to qualitatively estimate the final RFID system's performance. In this paper, various wearable Yagi-like reader-antenna layouts were presented and compared in terms of power-transfer efficiency, demonstrating the effectiveness of such a parameter for near-field antennas.

4. References

1. X. Jia, Q. Feng, T. Fan and Q. Lei, "RFID Technology and its Applications in Internet of Things (IoT)," 2012 2nd International Conference on Consumer Electronics, Communications and Networks (CECNet), Yichang, China, 2012, pp. 1282-1285.

2. A. Schmidt, H. Gellersen and C. Merz, "Enabling Implicit Human Computer Interaction: A Wearable RFID-Tag Reader," Digest of Papers. Fourth International Symposium on Wearable Computers, Atlanta, GA, USA, 2000, pp. 193-194.

3. M. Konkel, et al., "Tagaboo: A Collaborative Children's Game Based Upon Wearable RFID Technology," *Pers Ubiquit Comput*, **8**, pp. 382-384, 2004.

4. K. P. Fishkin, M. Philipose and A. Rea, "Hands-On RFID: Wireless Wearables for Detecting Use of Objects," Ninth IEEE International Symposium on Wearable Computers (ISWC'05), Osaka, Japan, 2005, pp. 38-41.

5. D. J. Patterson, D. Fox, H. Kautz and M. Philipose, "Fine-Grained Activity Recognition by Aggregating Abstract Object Usage," Ninth IEEE International Symposium on Wearable Computers (ISWC'05), Osaka, Japan, 2005, pp. 44-51.

6. T. Chouhan, A. Panse, A. K. Voona and S. M. Sameer," Smart Glove with Gesture Recognition Ability for the Hearing and Speech Impaired," 2014 IEEE Global Humanitarian Technology Conference - South Asia Satellite (GHTC-SAS), Trivandrum, 2014, pp. 105-110.

7. T. Stiefmeier, D. Roggen, G. Ogris, P. Lukowicz and G. Tröster, "Wearable Activity Tracking in Car Manufacturing," *IEEE Pervasive Computing*, **7**, 2, April-June 2008, pp. 42-50.

8. R. V. Aroca, R. S. Inoue, L. M. Pedro, G. A. P. Caurin and D. V. Magalhaes, "Towards a Battery-Free Wireless Smart Glove for Rehabilitation Applications Based on RFID," 2015 IEEE Brazil RFID, Sao Paulo, 2015, pp. 1-5.

9. K. Niazmand, K. Tonn, A. Kalaras, U. M. Fietzek, J. H. Mehrkens and T. C. Lueth, "Quantitative Evaluation of Parkinson's Disease Using Sensor Based Smart Glove," 2011 24th International Symposium on Computer-Based Medical Systems (CBMS), Bristol, 2011, pp. 1-8.

10. N. Popescu, D. Popescu, M. Poboroniuc and C. D. Popescu, "Intelligent Haptic Robotic Glove for Patients Diagnosed with Cerebrovascular Accidents," 2013 17th International Conference on System Theory, Control and Computing (ICSTCC), Sinaia, 2013, pp. 717-721.

11. L. Muguira, J. I. Vazquez, A. Arruti, J. R. d. Garibay, I. Mendia and S. Renteria, "RFID Glove: A Wearable RFID Reader," 2009 IEEE International Conference on e-Business Engineering, Macau, China, 2009, pp. 475-480.

12. C. Scheuermann, M. Strobel, B. Bruegge and S. Verclas, "Increasing the Support to Humans in Factory Environments Using a Smart Glove: An Evaluation," 2016 Intl IEEE Conferences on Ubiquitous Intelligence & Computing, Advanced and Trusted Computing, Scalable Computing and Communications, Cloud and Big Data Computing, Internet of People, and Smart World Congress, Toulouse, 2016, pp. 847-854.

13. D. Patron, et al., "On the Use of Knitted Antennas and Inductively Coupled RFID Tags for Wearable Applications," *IEEE Trans. Biomedical Circuits Systems*, **10**, 6, December 2016, pp. 1047-1057.

14. S. Rao, et al., "Miniature Implantable and Wearable On-Body Antennas: Towards the New Era of Wireless Body-Centric Systems [Antenna Applications Corner]," *IEEE Antennas Propag. Mag.*, **56**, 1, February 2014, pp. 271-291.

15. M. Daiki, E. Perret and S. Tedjini, "Design of Near Field UHF-RFID Reader Antenna Integrated into Clothing," 2014 IEEE RFID Technology and Applications Conference (RFID-TA), Tampere, 2014, pp. 261-265.

16. A. Michel and P. Nepa, "UHF-RFID Desktop Reader Antennas: Performance Analysis in the Near-Field Region," *IEEE Antennas Wireless Propag. Lett.*, **15**, 2016, pp. 1430-1433.

17. A. Michel, P. Nepa, X. Qing, and Z. N. Chen, "Considering High Performance Near-Field Reader Antennas: Comparisons of Proposed Antenna Layouts for Ultrahigh-Frequency Near-Field Radio-Frequency Identification," *IEEE Antennas Propag. Mag.*, **60**, 1, February 2018, pp. 14-26.

18. A. Michel, M. Rodriguez Pino and P. Nepa, "Reconfigurable Modular Antenna for NF UHF RFID Smart Point Readers," *IEEE Trans. Antenna Propag.*, **65**, 2, February 2017, pp. 498-506.

19. M. Daiki and E. Perret, "Segmented Solenoid Coil Antenna for UHF-RFID Near-Field Reader Applications," *IEEE Journal of Radio Frequency Identification*, **2**, 4, December 2018, pp. 210-218.

20. M. Daiki, E. Perret, and S. Tedjini, "Antenna Design for UHF-RFID Near-Field Applications," Proc. IEEE Int. Conf. RFID, Orlando, FL, USA, 2013.

21. R. K. Singh, A. Michel, P. Nepa and A. Salvatore, "Glove Integrated Solenoid Antennas for Near-Field UHF RFID Applications," IEEE Indian Conference on Antennas and Propagation (InCAP), Ahmedabad, India, 2019, pp. 1-4.

22. S. Ahmed, S. M. M. Rehman, L. Ukkonen and T. Björninen, "Glove-Integrated Slotted Patch Antenna for Wearable UHF-RFID Reader," 2018 IEEE International Conference on RFID Technology & Application (RFID-TA), Macau, 2018, pp. 1-5.

23. R. K. Singh, A. Michel, P. Nepa and A. Salvatore, "Design of a Compact Yagi-Uda Antenna for Near Field UHF-RFID Smart gloves," 2019 IEEE International Conference on RFID Technology and Applications (RFID-TA), Pisa, Italy, 2019, pp. 453-457.

24. R. K. Singh, A. Michel, P. Nepa and A. Salvatore, "Compact Quasi-Yagi Reader Antenna for UHF RFID Smart-Glove," IEEE International conference on Smart and Sustainable Technologies, Croatia, September 23-26 2020.

25. R. K. Singh, A. Michel, P. Nepa and A. Salvatore, "Modified Yagi-Uda Reader Antenna for UHF RFID Smart-Glove," 14th European Conference on Antennas and Propagation (EUCAP), Copenhagen, Denmark, 2020, pp. 1-4.

26. R. K. Singh, A. Michel, P. Nepa, A. Salvatore, M. Terraroli and P. Perego, "Compact and Wearable Yagi-Like Textile Antennas for Near-Field UHF-RFID Readers," *IEEE Trans. Antennas Propag*., **69**, 3, March 2021, pp. 1324-1333.

27. R. K. Singh, A. Michel, P. Nepa and A. Salvatore, "Glove Integrated Dual-Band Yagi Reader Antenna for UHF RFID and Bluetooth Application," International Workshop on Antenna Technology (iWAT), Bucharest, Romania, 2020, pp. 1-4.

28. R. K. Singh, A. Michel, P. Nepa and A. Salvatore, "Wearable Dual-Band Quasi-Yagi Antenna for UHF-RFID and 2.4 GHz Applications," *IEEE Journal of Radio Frequency Identification*, **4**, 4, December 2020, pp. 420-427.

29. A. Buffi, A. Michel, P. Nepa, and G. Manara, "Numerical Analysis of Wireless Power Transfer in Near-Field UHF-RFID Systems," *Wireless Power Transfer*, 1-12, 2017.

30. A. Michel, M. Rodriguez Pino, G. Alvarez Narciandi, M. Arrebola, and P. Nepa, "Using the Power Transfer Efficiency for RFID detection in Unusual Scenarios," Proceedings of 2019 URSI International Symposium on Electromagnetic Theory (EMTS), San Diego, CA, USA, 27-31 May, 2019.

31. G. Manara, A. Michel and P. Nepa, "Near-field Coupling in Wireless Systems," 2019 URSI Asia-Pacific Radio Science Conference (AP-RASC), New Delhi, India, 2019, pp. 1-1.

32. A. Michel, A. Buffi, P. Nepa, and G. Manara, "Wireless Power Transfer in UHF RFID Printer Encoder," 2017 International Conference on Electromagnetics in Advanced Applications (ICEAA), Verona, 2017.

33. A. Michel, M. Rodriguez Pino, P. Nepa and G. Manara, "On the Tag Detection in Near-Field UHF RFID Applications," 2017 XXXIInd General Assembly and Scientific Symposium of the International Union of Radio Science (URSI GASS), Montreal, QC, 2017, pp. 1-3.

34. A. Michel, A. Buffi, and P. Nepa, "Near-field Coupling in UHF-RFID Printer-Encoders," Proceedings of 2016 URSI International Symposium on Electromagnetic Theory (EMTS), Espoo, Finland, 15-18 August, 2016.

35. A. Michel, A. Buffi, P. Nepa, and G. Manara, "Optimal Antennas for RFID Printer-Encoders" 2016 IEEE International Symposium on Antennas and Propagation & USNC/URSI National Radio Science Meeting, Fajardo, Puerto Rico, 2016, pp. 1475-1476.

36. A. Michel, A. Buffi, P. Nepa and G. Manara, "Antennas for UHF-RFID Printer-Encoders," 2015 IEEE 15th Mediterranean Microwave Symposium (MMS), Lecce, 2015, pp. 1-4.

Remembering Prof. Valerian Tatarskii

Valery Zavorotny

University of Colorado Boulder/CIRES
216 UCB, Boulder, CO, 80309, USA (Retired)
E-mail: valery.zavorotny@colorado.edu

Abstract

Prof. Valerian Tatarskii is recognized in the field of radio science as one of the founders of the theory of wave propagation in random media. His outstanding seminal works made a global impact on studies of propagation and scattering of electromagnetic and acoustic waves in the atmosphere and the ocean. His papers and books remain a source of wisdom for scores of researchers in this field around the world. In this article, we pay special tribute to his exceptional career and contributions to science.

1. Introduction

Recently, in October of 2019, we celebrated Prof. Valerian Tatarskii's 90th birthday [1]. Unfortunately, on April 19, 2020, with deep sadness we learned about his passing in his home in Boulder, Colorado. V. I. Tatarskii received worldwide recognition as the founder of a new scientific direction, the theory of wave propagation in random media. The methods developed by him made it possible to solve a wide range of practical problems related to propagation and scattering of electromagnetic, sound, and seismic waves in the atmosphere, ionosphere, interplanetary and interstellar plasmas, the ocean, and the interior of the Earth. Prof. Tatarskii's innovative research was acknowledged as the authoritative and most widely referenced work in this field, making a global impact on physical science. He was one of the founders of the international journal *Waves in Random Media* which, together with Prof. Akira Ishimaru, laid the foundation for the current direction of this field. In this article, the main milestones of Prof. Tatarskii's life and scientific activities will be outlined, including the important publications and results.

2. Early Years of V. I. Tatarskii's Life

Valerian Tatarskii was born on October 13, 1929, in Kharkov, USSR, now Kharkiv, Ukraine. His father was an engineer who took part in the construction of various industrial facilities across the country in the years following the Russian Revolution. Valerian started school in Kharkov, but in1941 he and the Tatarskii family had to evacuate to the Siberian city of Krasnoyarsk, following the German Nazi invasion of the USSR. After the war, Valerian graduated from high school in Krasnoyarsk with a gold medal (the equivalent of valedictorian). In 1947, he was admitted to the Physics Department at Moscow State University (MSU).

3. V. I. Tatarskii's Education

While studying in the Physics Department at MSU (1947-1952), V. I. Tatarskii became interested by the problem of sound propagation in a turbulent atmosphere. Prof. V. A. Krasil'nikov, noticing the talented student's interest in scientific work, suggested that Valerian make this the basis of his master's thesis. It would be appropriate to mention here that V. A. Krasil'nikov was one of the first

Figure 1. Prof. Valerian Ill'ich Tatarskii in 2009.

Soviet scientists to study the phenomenon of light- and sound-wave propagation in the turbulent atmosphere. V. A. Krasil'nikov was the first to use the Geometrical Optics approximation in the interpretation of his experimental data on propagation of waves in random media [2-6]. Valerian Tatarskii, as his student, easily absorbed this new knowledge from his teacher. By the time of graduation, he successfully defended his thesis, which in turn became the basis of his first scientific publications [7, 8]. This set the direction for much of Tatarskii's subsequent research.

4. Beginning of the Scientific Career

In 1953, after graduating from MSU, Valerian Tatarskii joined the Laboratory for Turbulence Research at the Geophysical Institute of the USSR Academy of Sciences. There, under the leadership of A. M. Obukhov, V. I. Tatarskii continued to study the propagation and scattering of sound waves in a turbulent atmosphere. He later generalized this problem to the propagation of electromagnetic waves, which soon became his main scientific endeavor.

Here, it would be useful to briefly describe the state of this problem as it existed at that time. Early studies of light- and sound-wave propagation in random media in the Soviet Union were performed by V. A. Krasil'nikov and his colleagues. They used the Geometrical Optics approximation to explain their experimental data. This approximation works reasonably well when considering the propagation of waves in random media with characteristic scales that are much larger than the wavelength of the propagating waves and for relatively short paths [2-6]. In this case, wave scattering at large angles (let alone in the opposite direction) is extremely small. The medium that influences the forward propagation is therefore concentrated between the source and the observer points, along the geometrical-optics rays. This approach soon became very appealing, and was widely used for the interpretation of experiments performed over relatively short paths (see, e.g., [7-12] and elsewhere). Although decent agreement was observed between theoretical and experimental data for phase and angle-of-arrival fluctuations, there was no such agreement with respect to amplitude fluctuations.

In the 1940s and 1950s, Prof. Obukhov published two papers [14, 15], in which he applied the method of smooth perturbations to account for the diffraction effects in electromagnetic and acoustic wave propagation in a turbulent atmosphere. This method was independently developed by Prof. S. M. Rytov before WWII to describe the diffraction of light by ultrasound waves, and is today known as the Rytov approximation [16]. V. I. Tatarskii first met S. M. Rytov in 1955, and Rytov proved to be a significant and beneficial influence on Tatarskii's development as a scientist. The advances achieved by A. M. Obukhov and S. M. Rytov served as a starting point for Valerian Tatarskii to extend the analysis of wave propagation in random media beyond the Geometrical Optics approximation [17, 18]. Using Obukhov's spectral description of atmospheric turbulence and putting to wide use Rytov's method of smooth perturbations to allow for diffraction in the propagation of acoustic and light waves in a turbulent medium, he successfully solved a wide range of new, important, and practical problems. These results laid the basis for his PhD dissertation in 1957, and his first book, published in 1959 in Russian under the title *The Theory of Fluctuation Phenomena Upon Wave Propagation in a Turbulent Atmosphere*. In 1961, it was published abroad in English as *Wave Propagation in a Turbulent Medium* [19].

Continuing his work at the Institute of Atmospheric Physics – which split in 1956 from the Geophysical Institute – V. I. Tatarskii went on to explore more difficult problems of wave propagation in random media, and used increasingly powerful mathematical methods for their solution. V. I. Tatarskii recognized that applying methods developed in quantum field theory allowed him to go beyond the limits of the perturbation methods, and to obtain solutions applicable for a medium with strong fluctuations of the dielectric constant [20-22]. These developments became a valuable part of his DSci dissertation, which he defended in 1964, and for his second book, *Wave Propagation in a Turbulent Atmosphere*, published in 1967 [23]. This book also included other important results obtained by him at the IAP since the publication of his first book [19].

5. At the Frontier of Statistical Wave Propagation Theory

Both Geometrical Optics and Rytov's method of smooth perturbations are based on first-order perturbation theory. This limits their applicability to the regime of weak intensity fluctuations. However, electromagnetic waves can experience strong scintillations even in a medium with weak inhomogeneities of the dielectric constant, if it propagates over long enough paths. V. I. Tatarskii well understood the limitations of perturbation methods, and sought theories that would allow him to transcend the difficulty in describing the regime of strong scintillations. In the 1960s, he devoted significant efforts to constructing several such theories [24-26].

It should be mentioned that other researchers at that time were preoccupied with the same problem [27-30]. Strong and saturated scintillations in received radio signals had been already discussed for quite a long time in radio-astronomical and ionospheric studies. For the description of such scintillations, the model of a thin random phase screen was used with varied success. There were attempts made to employ this model for an extended random medium by replacing it with a equivalent phase screen. More successful was a numerical scheme in which the medium was replaced with a large number of phase screens. A similar approach, with some assumptions about the correlation between the scattered field and fluctuations of the medium, led L. A. Chernov to the local method of small perturbations, which allowed him to obtain closed equations for field statistical moments [27].

Around that time, V. I. Tatarskii realized that this approach was equivalent to describing this phenomenon by means of Leontovich's parabolic equation [31]. Combining this with a Markov process for the description of the random media, i.e., assuming that inhomogeneities were delta-correlated along the nominal propagation path, he proposed a very elegant method for the derivation of equations for the mean field and the second-order coherence function. He was also able to derive equations of the Einstein-Fokker-Planck type for the characteristic functional of the wave field, and equations for higher statistical moments [26, 32, 33]. What is important is that all of these equations are applicable for the full range of wave intensity fluctuations, from weak to strong. In the following years, these equations were studied analytically and numerically by scientists across the world for atmospheric and oceanic applications. This was the beginning of a new and important line of research.

In 1970, when V. I. Tatarskii was invited to publish an English edition of his book [23], he augmented it with new material from several papers [26, 32, 33]. These changes had to do with the propagation of short waves in a medium with random inhomogeneities approximated by a Markov random process. This book was published in English in 1971 under the title *The Effects of the Turbulent Atmosphere on Wave Propagation* [34]. It soon gained great popularity among specialists worldwide and became one of the classics in its field. It firmly established Prof. Tatarskii as one of the foremost experts in the field of wave propagation and scattering in random media. Domestic and foreign researchers recognized the important role of his books in their mastering of this very complex discipline. For example, the two-volume monograph by A. D. "Bud" Wheelon [35, 36] is preceded by the words, "These volumes are dedicated to Valerian Tatarskii who taught us all."

In all of these years, despite being a theoretician, he was also interested in experimental studies of light propagation through atmospheric turbulence. Tatarskii's involvement in experimental research helped him better understand the specifics and limitations of sensors, and to more accurately formulate a theoretical description of the wave propagation phenomena. Many of Tatarskii's theoretical predictions were validated by experiments conducted at the Obukhov Institute of Atmospheric Physics. In particular, he collaborated closely with Dr. A. S. Gurvich in studying the statistical characteristics of light and sound affected by turbulence, and later investigated laser-beam propagation in a turbulent atmosphere [37-39]. He participated directly in measurements and in planning measurements of statistical characteristics of signals propagating in a turbulent atmosphere and their subsequent interpretation. Valerian Tatarskii also established a very productive collaboration with Dr. V. I. Klyatskin, with whom he developed the above-mentioned Markov approximation for wave propagation in random media [32, 33, 40]. These studies were covered in a review [41].

Deriving the equations for statistical moments of the propagating wave was a very important step, but to solve those equations was no less of an important task. The equations for the first two moments, the mean field and the mutual coherence function, can be solved in a general form for various cases of medium statistics. However, the fourth moment, which is used to describe intensity fluctuations, does not have a full analytical solution for all scattering regimes. Nevertheless, researchers began to look for asymptotic solutions of these differential equations at a regime of saturated scintillations [42, 43].

I was a graduate student when I met Prof. Tatarskii at the Institute of Atmospheric Physics in 1970, when I asked V. I. Tatarskii to be my master's advisor. This request was granted, and since then my life and work became closely involved with Prof. Tatarskii. Soon after graduating from the Gorky State University, I joined the group of scientists at the IAP led by V. I. Tatarskii who worked on wave propagation in a turbulent atmosphere. To address the problem of calculating moments in the regime of strong scintillations, we decided to pursue an approach similar to that of quantum field theory, namely, Feynmann path integrals, or functional integrals, which represent a formal solution to both the Helmholtz and the parabolic equations [33]. Using that approach, we managed to evaluate the asymptotic behavior of the statistical moments of the *n*th order in a regime of strong scintillations [44]. That result became a basis of my PhD dissertation, which I completed under the supervision of Prof. Tatarskii. The same asymptotic result for higher statistical moments was obtained by I. G. Yakushkin, using the method of Green's functions [45], and by R. Dashen, using the Feynmann path-integral method [46]. Various aspects of using the Feynmann path-integral method for studying the statistics of scintillations were covered in V. I. Tatarskii's series of review papers [47-49].

6. Diversity of Research Interests

The scientific interests of V. I. Tatarskii in the 1970s and 1980s included not only the problem of strong fluctuations of wave parameters in a turbulent medium, but also other important problems of wave-propagation theory and related application topics. He was interested in studying the propagation of partially coherent light beams in a turbulent atmosphere [50]. V. I. Tatarskii with A. Vinogradov and Yu. Kravtsov discovered the enhancement effect of backscattering by bodies placed in a medium with random inhomogeneities [51]. The problem of wave propagation through absorbing one-dimensional random media was considered by him in [52], where the fluctuations of the dielectric permittivity were described by three distinct

Figure 2. Participants of the meeting in Tallinn (Estonia), September 1988: (first row) Yu. A. Kravtsov, M. S. Tatarskaya, V. I. Tatarskii, U. Mullamaa, A. Ishimaru, Mrs. Lang, A. Orekhova, Mrs. Renelde Flatte, V. V. Varadan, S. Flatte, A. S. Gurvich; (second row) V. V. Vorob'ev, V. I. Shishov, M. Nieto-Vesperinas, R. Hill, R. Lang, I. Besieris, Y. Kuga; (third row) Yu. N. Barabanenkov, I. G. Yakushkin, A. I. Saichev, V. Freilikher, V. L. Brekhovskikh, E. Bakhar, Mrs. Bakhar, L. Tsang, K. C. Yeh, V. I. Klyatskin; (fourth row) I. G. Granberg, C. Rino, G. Brown, V. U. Zavorotny, V. E. Ostashev, J. C. Dainty, V. N. Sekistov.

random processes. He took part in developing the multiple forward-scattering method that makes it possible to remove the restrictions imposed by the parabolic-equation method in the Markov approximation, namely, that the angles of forward scattering should be small [53, 54]. V. I. Tatarskii obtained modified equations for arbitrary statistical moments of waves propagating in random media in which structure parameters exhibit intermittency [55].

V. I. Tatarskii always had the surprising ability, on the one hand, to fearlessly use analytical methods from quantum field theory and, on the other hand, to find simple qualitative illustrations for applied methods and with their help to lucidly explain the results obtained using simple examples understood even by a lay person. The outstanding pedagogical talent of V. I. Tatarskii fully came to life in the second volume of the book (written together with S. M. Rytov and Yu. A. Kravtsov), *The Introduction to Statistical Radiophysics. Random Fields*, issued in the USSR in 1987 [56]. When translated into English and edited in four volumes under the title *Principles of Statistical Radiophysics* [57], the book enjoyed worldwide popularity among physicists in very different fields. It remains important up to the present day.

The range of scientific interests of V. I. Tatarskii was unusually wide. Besides classical problems of wave propagation in inhomogeneous media, Tatarskii's interests extended beyond this well-established field of physics, showing his diverse choice of research topics. He published significant results in the field of adaptive optics [58, 59], quantum mechanics [60], mathematical and statistical physics [61, 63], the theory of turbulence [62], and quantum statistical optics [65, 66].

7. V. I. Tatarskii as a Leader and Mentor

V. I. Tatarskii was not a purely armchair scientist. He proved to be a talented organizer and leader of scientific research. The teams headed by him have always had an atmosphere of enthusiastic scientific research. From 1978 to 1990, V. I. Tatarskii headed the laboratory, and then the department, at the Institute of Atmospheric Physics at the USSR Academy of Sciences. In 1990, he was invited to head a department at the Astro Space Center, newly created by the academician N. S. Kardashev at the P. N. Lebedev Physical Institute at the USSR Academy of Sciences (FIAN).

V. I. Tatarskii's students highly appreciated him as a remarkable tutor and mentor for whom their successes and failures were also his successes and failures. He was always engaged in the discussion of the problems he stated and helped in their solution. At the same time, he taught his students to be independent, and demanded that they bring the quality of their scientific work to world standards. Among the former students and followers of V. I. Tatarskii, there were many who continued their successful research activities in various fields of physics and mentored their own students.

8. The International Cooperation

In September 1988 in Tallinn (Estonia), V. I. Tatarskii, together with Prof. Akira Ishimaru from Washington State University, organized a meeting regarding the problems of propagation and scattering of electromagnetic waves in randomly inhomogeneous media. Its organization was the result of great interest among the international scientific community regarding this problem. This conference was the first of its kind held in the USSR. About three dozen foreign scientists who held leading positions in the global scientific community in this field received an invitation to participate. One of the consequences of this event was a decision to create a new international journal called *Waves in Random Media*. Four years later, a similar conference ("Wave Propagation in Random Media (Scintillation)") was held in Seattle at the University of Washington, under the chairmanship of V. I. Tatarskii and A. Ishimaru. It was attended by over two hundred speakers from 13 countries, including 30 scientists from the former Soviet Union. The invited talks presented at the conference were later published as a separate book [48]. The Scintillation Conference was a success, and it deepened cooperation and exchange of ideas among scientists working on the problems of wave propagation in random media. It promoted interdisciplinary approaches to solving problems of statistical optics, radio science, and acoustics.

9. Moving to the USA

In the early 1990s, V. I. Tatarskii was invited to the Laboratory of Wave Propagation of the National Oceanic and Atmospheric Administration (Boulder, Colorado), USA by its director, Dr. S. F. Clifford. He worked there until he retired from NOAA in 2006. Afterwards, he carried out research work at the company Radio-Hydro-Physics, LLC. This period of Tatarskii's life in Boulder was exceptionally productive. First, he continued working in his traditional fields of research: wave scattering and propagation in random media, and the theory of turbulence. He published several works on these topics (see, e.g., [67-73]). At the same time, his scientific interests began to encompass problems occurring in the theory of radio wave scattering by a rough sea surface. He obtained and published some important results, applying both analytical [74-81] and numerical methods [82-85] for solving those problems.

10. V. I. Tatarskii's Public Activities and Recognitions

The scientific and public activities of V. I. Tatarskii included his duties as a member of the Editorial Board of the *Journal of Soviet Physics, Uspekhi* (1985-1996), Vice Editor-in-Chief of the international journal *Waves in Random Media* (1991-1998), and a member of the editorial board of the international *Journal of Electromagnetic Waves and Applications* (2001-2008). V. I. Tatarskii was a corresponding member of the Russian Academy of Sciences (since 1976), an honorary member of the Optical Society of America (since 1994), and a member of the National Academy of Engineering, USA (since 1994).

In 1990, for their scientific achievements, V I Tatarskii and his colleagues (A. S. Gurvich, V. I. Shishov, S. M. Rytov, V. I. Klyatskin, Yu. A. Kravtsov, and, posthumously, L. A. Chernov) were awarded the State Prize of the USSR "for the study of the basic laws of wave propagation through turbulent media." That same year, he received a prestigious award from the Optical Society of America, the Max Born Medal, "for his outstanding seminal contributions to the theory of wave propagation through random media, particularly optical propagation through atmospheric turbulence, as well as for his fundamental contributions to the fields of statistical and quantum optics."

11. He Will be Remembered

In the memories of people who knew V. I. Tatarskii, he was known to be surprisingly modest, gentle, and a deeply intelligent person. Although scientific creativity was his main passion, he found time for a variety of hobbies. He loved listening to classical music; was an avid tourist, spending summer holidays kayaking with family and friends; and enjoyed skiing in the winter. He deeply cared for his wife, son, and grandchildren. All his friends and colleagues will remember Prof. V. I. Tatarskii as a remarkable scientist, mentor, and person. He will remain in the hearts of all who were fortunate enough to work and interact with him.

12. References

1. G. Brown et al., "Professor Valerian Ill'ich Tatarskii: An Appreciation," *Waves in Random and Complex Media*, **30**, 1, 2020, pp. 1-4.

2 V. A. Krasil'nikov, "Some Experiments on Sound Propagation in a Turbulent Atmosphere," *Doklady Akademii Nauk SSSR*, *Seriya Geofizicheskaya*, **46**, 1945, pp. 108-110 (in Russian).

3. V. A. Krasil'nikov, "On Amplitude Fluctuations of Sound Propagating in a Turbulent Atmosphere," *Doklady*

Akademii Nauk SSSR, *Seriya Geofizicheskaya,* **58**, 1947, pp. 1353-1356 (in Russian).

4. V. A. Krasil'nikov, "On Fluctuations of the Angle-of-Arrival in the Phenomenon of Twinkling of Stars," *Doklady Akademii Nauk SSSR, Seriya Geofizicheskaya,* **65**, 1949, pp. 291-294 (in Russian).

5. V. A. Krasil'nikov, "On the Influence of Index-of-Refraction Pulsations in the Atmosphere on the Propagation of Ultrasound Radio Waves," *Izvestiya Akademii Nauk SSSR, Seriya Geographicheskayai Geofizicheskaya*, **13**, 1949, pp. 33-57 (in Russian).

6. V. A. Krasil'nikov, "On Phase Fluctuations of Ultrasonic Waves Propagating in the Layer of the Atmosphere Near the Earth," *Doklady Akademii Nauk SSSR, Seriya Geofizicheskaya,* **88,** 1953, pp. 657-660 (in Russian).

7. V. I. Tatarskii, "Theory of Sound Wave Propagation in Turbulent Flow," *Zhurnal Experimental'noii Teoreticheskoi Fiziki*, **25**, 1, 1953, pp. 74-83 (in Russian).

8. V. I. Tatarskii, "Criterion of Applicability of Geometric Optics to Wave Propagation in a Medium with Weak Refractive Index Inhomogeneities," *Zhurnal Experimental'noii Teoreticheskoi Fiziki*, **25**, 1, 1953, pp. 84-86 (in Russian).

9. P. G. Bergman, "Propagation of Radiation in a Medium with Random Inhomogeneities," *Physics Reviews*, **70**, 7/8, 1946, pp. 486-492.

10. T. H. Ellison, "The Propagation of Sound Waves Through a Medium with Very Small Random Variations in Refractive Index," *Journal of Atmospheric and Terrestrial Physics*, **2**, 1, 1951, pp. 14-21.

11. L. A. Chernov, "Correlation of the Amplitude and Phase Fluctuations in Wave Propagation in Media with Random Inhomogeneities," *Akusticheskii Zhurnal*, **1**, 1954, pp. 1-89 (in Russian).

12. R. B. Muchmore and A. D. Wheelon, "Line-of-Sight Propagation Phenomenon – I. Ray Treatment," *Proceedings of the IRE*, **43**, 10, 1955, pp. 1437-1449.

13. L. A. Chernov, *Wave Propagation in a Turbulent Medium*, New York, McGraw Hill, 1960.

14. A. M. Obukhov, "Scattering of Sound in Turbulent Flow," *Doklady Akademii Nauk*, **30**, 7, 1941, p. 611 (in Russian).

15. A. M. Obukhov, "On the Influence of Weak Atmospheric Inhomogeneities on the Propagation of Sound and Light," *Doklady Akademii Nauk SSSR, Seriya Geofizicheskaya*, **2**, 1953, pp. 155-165 (in Russian) [English translation: A. M. Obukhov," Sound and Light Propagation in a Weakly Inhomogeneous Atmosphere," *Waves in Random Media*, **4**, 1994, pp. 9-19].

16. S. M. Rytov, "Diffraction of Light on Ultrasonic Waves," *Izvestia Akademii Nauk SSSR, Seriya Fizicheskaya*, **2**, 1937, pp. 223-259 (in Russian).

17. V. I. Tatarskii, "Phase and Amplitude Fluctuations of a Wave Propagating in a Weakly Inhomogeneous Medium," *Doklady Akademii Nauk SSSR*, **107**, 2, 1956, p. 245 (in Russian).

18. V. I. Tatarskii, "Wave Propagation in a Locally Isotropic Turbulent Medium with Smoothly Varying Characteristics," *Doklady Akademii Nauk SSSR*, **120**, 2, 1958, p. 289 (in Russian).

19. V. I. Tatarskii, *Wave Propagation in a Turbulent Medium*, New York, McGraw Hill, 1961 (New York, Dover, 1966).

20. V. I. Tatarskii and M. E. Gertsenshtein, "Propagation of Waves in a Medium with Strong Fluctuation of the Refractive Index," *Soviet Physics – JETP*, **17**, 1963, pp. 458-463.

21. V. I. Tatarskii, "Propagation of Electromagnetic Waves in a Medium with Strong Dielectric Constant Fluctuations," *Soviet Physics – JETP*, **19**, 4, 1964, pp. 946-953.

22. Yu. A. Ryzhov, V. V. Tamoikin, and V. I. Tatarskii, "Spatial Dispersion of Inhomogeneous Media," *Soviet Physics – JETP*, **21**, 2, 1965, pp. 433-438.

23. V. I. Tatarskii, *Wave Propagation in the Turbulent Atmosphere*, Moscow, Nauka Publishing House, 1967 (in Russian).

24. V. I. Tatarskii, "Strong Fluctuations of Light Wave Parameters in a Turbulent Medium, "*Soviet Physics – JETP*, **22**, 5, 1966, pp. 1083-1088.

25. V. I. Tatarskii, "The Strong Amplitude Fluctuations of a Wave Traveling in a Medium with Weak Random Inhomogeneities," *Radiophysics and Quantum Electronics*, **10**, 1, 1967, pp. 48-58.

26. V. I. Tatarskii, "Light Propagation in a Medium with Random Refractive Index Inhomogeneities in the Markov Random Approximation," *Soviet Physics – JETP*, 29, 6, 1969, pp. 1133-1138.

27. L. A. Chernov, "The Local Method of Computing Strong Fluctuations of the Field in the Problem of Wave Propagation in a Medium with Random Inhomogeneities," Proceedings of 6th All-Union Acoustic Conference, 1968.

28. L. S. Dolin, "Equations for the Statistical Moments of the Field in a Randomly Inhomogeneous Medium,"

Radiophysics and Quantum Electronics, **11**, 6, 1968, pp. 486-491.

29. V. I. Shishov, "Theory of Wave Propagation in Random Media," *Radiophysics and Quantum Electronics*," **11**, 6, 1968, pp. 500-505.

30. M. J. Beran and T. L. Ho, "Propagation of the Fourth-Order Coherence Function in a Random Medium (a Non-Perturbative Formulation)," *Journal of the Optical Society of America*, **59**, 9, 1968, pp. 1134-1138.

31. M. A. Leontovich, "On the New Method of Solving of the Radio-Wave Propagation Problem," *Izvestia Akademii Nauk SSSR, Seriya Fizicheskaya*, **8**, 1944, pp. 16-22 (in Russian).

32. V. I. Klyatskin and V. I. Tatarskii, "Strong Fluctuations of a Plane Wave Moving in a Medium with Weak Random Inhomogeneities," *Soviet Physics – JETP*, **28**, 2, 1969, pp. 346-353.

33. V. I. Klyatskin and V. I. Tatarskii, "The Parabolic Equation Approximation for Propagation of Waves in a Medium with Random Inhomogeneities," *Soviet Physics – JETP*, **31**, 2, 1970, pp. 335-339.

34. V. I. Tatarskii, *The Effects of the Turbulent Atmosphere on Wave Propagation*, Springfield, VA, National Technical Information Service, 1971.

35. A. D. Wheelon, *Electromagnetic Scintillation, 1. Geometrical Optics*, Cambridge, UK, University Press, 2001.

36. A. D. Wheelon, *Electromagnetic Scintillation, 2. Weak Scattering*, Cambridge, UK, University Press, 2003.

37. A. S. Gurvich and V. I. Tatarskii, "Coherence and Intensity Fluctuations of Light in the Turbulent Atmosphere," *Radio Science*, **10**, 1, 1975, pp. 3-14.

38. A. S. Gurvich, V. Kan, V. I. Tatarskii, and V. U. Zavorotny, "Four-Point Field Coherence Function in a Turbulent Medium," *Optica Acta*, **26**, 5, 1979, pp. 543-553.

39. V. I. Tatarskii, A. S. Gurvich, B. S. Elepov, Vl. V. Pokasov, and K. K. Sabel'feld, "Space Structure of Strong Intensity Fluctuations of Light in a Turbulent Medium," *Optica Acta*, **26**, 5, 1979, pp. 531-542.

40. V. I. Klyatskin and V. I. Tatarskii, "A New Method of Successive Approximations in the Problem of Wave Propagation in a Medium Having Random Large-Scale Inhomogeneities," *Radiophysics and Quantum Electronics*, **14**, 9, 1971, pp. 1100-1111.

41. V. I. Klyatskin and V. I. Tatarskii, "Diffusive Random Process Approximation in Certain Nonstationary Statistical Problems of Physics," *Soviet Physics Uspekhi*, **16**, 4, 1974, pp. 494-511.

42. K. S. Gochelashvili and V. I. Shishov, "Laser Beam Scintillation Beyond a Turbulent Layer," *Optica Acta*, **18**, 4, 1971, pp. 313-320.

43. I. G. Yakushkin, "Asymptotic Calculation of Field-Intensity Fluctuations in a Turbulent Medium for Long Paths," *Radiophysics and Quantum Electronics*, **18**, 11, 1975, pp. 1224-1229.

44. V. U. Zavorotnyi, V. I. Klyatskin, and V. I. Tatarskii, "Strong Fluctuations of the Intensity of Electromagnetic Waves in Randomly Inhomogeneous Media," *Soviet Physics – JETP*, **46**, 2, 1977, pp. 252-260.

45. I. G. Yakushkin, "Moments of Field Propagating in Randomly Inhomogeneous Medium in the Limit of Saturated Fluctuations," *Radiophysics and Quantum Electronics*, **21**, 8, 1978, pp. 835-840.

46. R. Dashen, "Path Integrals for Waves in Random Media," *Journal of Mathematical Physics*, **20**, 5, 1979, pp. 894-920.

47. V. I. Tatarskii and V. U. Zavorotny, "Strong Fluctuations in Light Propagation in a Randomly Inhomogeneous Medium," in E. Wolf (ed.), *Progress in Optics*, Amsterdam, Netherlands, Elsevier Science Publishers B.V., 1980.

48. V. I. Tatarskii, A. Ishimaru, and V. U. Zavorotny (eds.), *Wave Propagation in Random Media (Scintillation)*, Bellingham WA, USA, SPIE Press and Bristol, UK, the Institute of Physics Publishing, 1993.

49. M. I. Charnotskii, J. Gozani, V. I. Tatarskii, and V. U. Zavorotny, "Wave Propagation Theories in Random Media Based on the Path Integral Approach," in E. Wolf (ed.), *Progress in Optics*, Amsterdam, Netherlands, Elsevier Science Publishers B.V., 1993.

50. A. I. Kon and V. I. Tatarskii, "On the Theory of the Propagation of Partially Coherent Light Beams in a Turbulent Atmosphere," *Radiophysics and Quantum Electronics*, **15**, 10, 1972, pp. 1187-1192.

51. A. G. Vinogradov, Yu. A. Kravtsov, and V. I. Tatarskii, "Amplification Effect of Backscattering by Bodies Placed in a Medium with Random Inhomogeneities," *Radiophysics and Quantum Electronics*, **16**, 7, 1973, pp. 818-823.

52. V. I. Klyatskin and V. I. Tatarskii, "Statistical Theory of Wave Propagation Through Random Layered Media," *Radiophysics and Quantum Electronics*, **20**, 7, 1977, pp. 720-729.

53. V. E. Ostashev and V. I. Tatarskii, "A Series Based on Multiple Backscattering Problems of Wave Propagation in Inhomogeneous Media," *Radiophysics and Quantum Electronics*, **21**, 5, 1978, pp. 504-513.

54. V. E. Ostashev and V. I. Tatarskii, "Multiple Forward Scattering Method in Media with Random Inhomogeneities," *Radiophysics and Quantum Electronics*, **22**, 2, 1979, pp. 116-122.

55. V. I. Tatarskii and V. U. Zavorotny, "Wave Propagation in Random Media with Fluctuating Turbulent Parameters," *Journal of the Optical Society of America A*, **2**, 12, 1985, pp. 2069-2076.

56. S. M. Rytov, Yu. A. Kravtsov and V. I. Tatarskii, *The Introduction to Statistical Radiophysics. Part II. Random Field*, Moscow, Nauka Publishing House, 1987 (in Russian).

57. S. M. Rytov, Y. A. Kravtsov, V. I. Tatarskii, *Principles of Statistical Radiophysics*, *Volumes 1-4*, Berlin, Springer-Verlag, 1989.

58. V. I. Tatarskii, "Adaptive Systems and Coherence, II, "*Radiophysics and Quantum Electronics*, **24**, 7, 1981, pp. 872-882.

59. V. I. Tatarskii, "Quantum Noise in Adaptive Optical Systems, II," *Radiophysics and Quantum Electronics*, **25**, 9, 1982, pp. 731-742.

60. V. I. Tatarskii, "The Wigner Representation of Quantum Mechanics," *Soviet Physics Uspekhi*, **26**, 4, 1983, pp. 311-327.

61. V. I. Tatarskii, "Example of the Description of Dissipative Processes in Terms of Reversible Dynamic Equations and Some Comments on the Fluctuation Dissipation Theorem," *Soviet Physics Uspekhi*, **30**, 2, 1987, pp. 134-152.

62. M. M. Dubovikov and V. I. Tatarskii, "Calculation of the Asymptotic Form of the Spectrum of Locally Isotropic Turbulence in the Viscous Range," *Soviet Physics – JETP*, **66**, 6, 1987, pp. 1136-1141.

63. V. I. Tatarskii, "Criteria for the Degree of Chaos," *Soviet Physics Uspekhi*, **30**, 5, 1989, pp. 450-451.

64. V. P. Bykov and V. I. Tatarskii, "Causality Violation in the Glauber Theory of Photodetection," *Physics letters A*, **136**, 1(2), 1989, pp. 77-80.

65. V. I. Tatarskii, "Corrections to the Theory of Photocounting," *Physics Letters A*., **144**, 8(9), 1990, pp. 491-499.

66. V. P. Bykov and V. I. Tatarskii, "Perturbation Theory for Resolvents as Applied to Problems in Radiation Theory," *Soviet Physics Uspekhi*, **34**, 2, 1991, 167-184.

67. V. I. Tatarskii and M. M. Dubovikov, A. A. Praskovskii, and M. Yu. Karyakin, "Temperature Fluctuation Spectrum in the Dissipation Range for Statistically Isotropic Turbulent Flow," *Journal of Fluid Mechanics*, **238**, 1992, pp. 683-698.

68. V. I. Tatarskii, "Markovian Non-Gaussian Approximation for Light Propagation in a Random Medium," *Waves in Random Media*, **4**, 1994, pp. 511-519.

69. V. I. Tatarskii, "Characteristic Functional for One Class of Non-Gaussian Random Functions," *Waves in Random Media*, **5**, 1995, pp. 243-252.

70. V. E. Ostashev and V. I. Tatarskii, "Representation of the Helmholtz Equation Solution in the Form of a Series Based on Backscattering Multiplicity," *Waves in Random and Complex Media*, **5**, 1995, pp. 125-135.

71. V. I. Tatarskii and A. Muschinski, "The Difference Between Doppler Velocity and Real Wind Velocity in Single Scattering from Refractive Index Fluctuations," *Radio Science*, **36**, 6, 2001, pp. 1405-1423.

72. V. I. Tatarskii, "Theory of Single Scattering by Random Distributed Scatterers," *IEEE Transactions on Antennas and Propagation*, **53**, 10, 2003, pp. 2806-2813.

73. V. I. Tatarskii, "Use of the 4/5 Kolmogorov Equation for Describing Some Characteristics of Fully Developed Turbulence," *Physics of Fluids*,17, 2005, pp. 035110.

74. V. I. Tatarskii, "The Expansion of the Solution of Rough-Surface Scattering Problem in Powers of Quasi-Slopes," *Waves in Random Media*, **3**, 1993, pp. 127-146.

75. M. M. Charnotskii and V. I. Tatarskii, "Tilt-Invariant Theory of Rough-Surface Scattering," *Waves in Random Media*, **5**, 1995, pp. 361-380.

76. V. I. Tatarskii, "Formulation of Rough-Surface Scattering Theory in Terms of Phase Factors and Approximate Solutions Based on This Formulation," *Waves in Random Media*, **7**, 1997, pp. 557-578.

77. V. I. Tatarskii and M. I. Charnotskii, "On the Universal Behavior of Scattering from a Rough Surface for Small Grazing Angles," *IEEE Transactions on Antennas and Propagation*, **46**, 1, 1998, pp. 67-72.

78. I. M. Fuks, V. I. Tatarskii, and D. E. Barrick, "Behaviour of Scattering from a Rough Surface at Small Grazing Angles," *Waves in Random Media*, **9**, 1999, pp. 295-305.

79. V. I. Tatarskii, "Phase Factors Representation for Electromagnetic Scattering from a Rough-Surface Perfect Conductor," *Waves in Random Media*, **10**, 2000, pp. 339-358.

80. V. I. Tatarskii, "Use of Semi-Inversion Method for the Dirichlet Problem in Rough Surface Scattering," *Progress in Electromagnetic Research*, **PIER54**, 2005, pp. 109-135.

81. V. I. Tatarskii, “Equations for the Description of Wave Scattering by Multi-Valued Random Surfaces,” *Waves in Random and Complex Media*, **19**, 2009, pp. 480-500.

82. V. I. Tatarskii and V. V. Tatarskii, “Statistical Description of Rough-Surface Scattering Using the Quasi Small-Slope Approximation for Random Surfaces with a Gaussian Multivariate Probability Distribution,” *Waves in Random Media*, **4**, 1994, pp. 191-214.

83. V. I. Tatarskii and V. V. Tatarskii, “Non-Gaussian Statistical Model of the Ocean Surface for Wave-Scattering Theories,” *Waves in Random Media*, **6**, 1996, pp. 419-435.

84. V. I. Tatarskii and V. V. Tatarskii, “Statistical Non-Gaussian Model of Sea Surface with Anisotropic Spectrum for Wave Scattering Theory. Part I and II,” *Progress in Electromagnetic Research*, **PIER22**, 1999, pp. 259-313.

85. V. I. Tatarskii, “Multi-Gaussian Representation of the Cox-Munk Distribution for Slopes of Wind-Driven Waves,” *Journal of Atmospheric and Oceanic Technology*, **28**, 11, 2003, pp. 1697-1705.

URSI GASS 2023
August 19 (Sat) – 26 (Sat), 2023 SAPPORO, JAPAN

XXXVth General Assembly and Scientific Symposium of the International Union of Radio Science

August 19 – 26, 2023, Sapporo, Japan

www.ursi-gass2023.jp

Preliminary Call for Papers

The *XXXVth URSI General Assembly and Scientific Symposium (URSI GASS 2023)* is sponsored by The Institute of Electronics, Information and Communication Engineers (IEICE), the International Union of Radio Science (URSI), and the Science Council of Japan (SCJ), and will be held in Sapporo, Japan on August 19 – 26, 2023.

The scientific program will be organized covering the areas of URSI Commissions A to K and will comprise oral/poster sessions with invited and contributed papers, Commission Tutorials, General Lectures, and Public Lecture. In addition, there will be workshops, short courses, young scientist programs containing the Young Scientist Award and the Student Paper Competition, accompanying persons' programs, and industrial exhibition.

Prospective participants are invited to submit papers for inclusion in the scientific program. Detailed information will be posted on the URSI GASS 2023 website. Any topics related to URSI Commissions are welcome. In addition, papers addressing multidisciplinary aspects will be assigned to inter-Commission joint sessions.

COVID 19: URSI GASS 2023 is planned to be held as a totally physical event. Given the uncertainty on the vaccinations and on the status of the worldwide pandemic in 2023, however, it might be possible that the conference will be held in a hybrid format allowing both physical and remote participations.

Paper Submission

All papers should be submitted electronically via the link provided on the URSI GASS 2023 website, where the latest information on the submission procedures, templates, and sample formats will be posted. Accepted papers presented at URSI GASS 2023 may be submitted to IEEE for publication in IEEE Xplore, if the author wishes so.

Check www.ursi-gass2023.jp for regular updates.

Important Dates:

Paper submission site opens: **November 10, 2022**
Paper submission deadline: **January 25, 2023**
Notification of acceptance: **March 15, 2023**

URSI Commissions

Commission A: Electromagnetic Metrology
Commission B: Fields and Waves
Commission C: Radiocommunication and Signal Processing Systems
Commission D: Electronics and Photonics
Commission E: Electromagnetic Environment and Interference
Commission F: Wave Propagation and Remote Sensing
Commission G: Ionospheric Radio and Propagation
Commission H: Waves in Plasmas
Commission J: Radio Astronomy
Commission K Electromagnetics in Biology and Medicine

Young Scientist Award and Student Paper Competition

For the details on applications for the Young Scientist Award (YSA) and the Student Paper Competition (SPC), please visit the URSI GASS 2023 website.

Tayfun Akgül
Istanbul Technical University
Dept. of Electronics and Communications Engineering
Telecommunications Division
80626 Maslak Istanbul, Turkey
Tel: +90 212 285 3605; Fax: +90 212 285 3565
E-mail: tayfunakgul@itu.edu.tr.

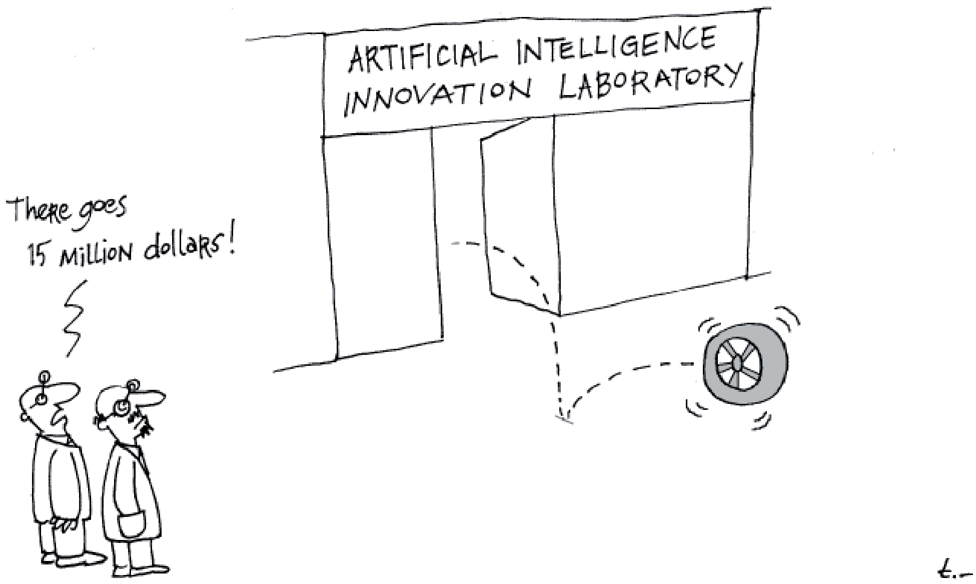

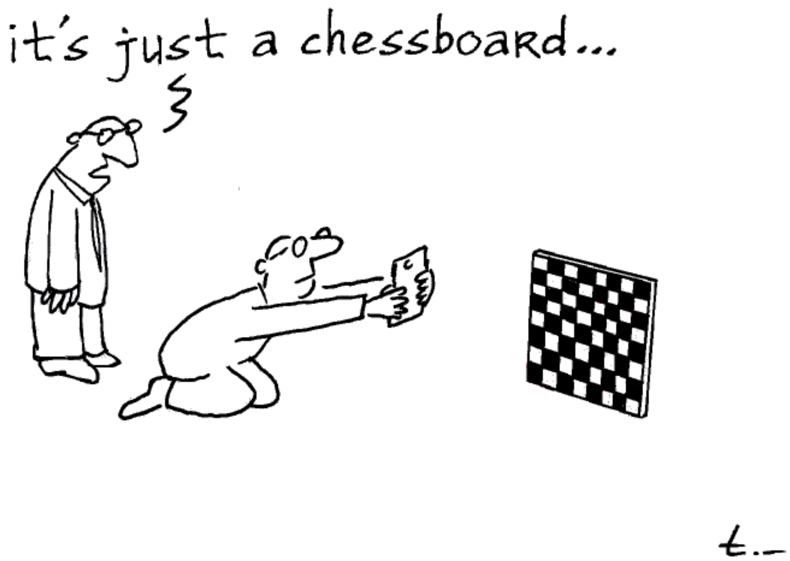

National Radio Science Meeting

January 10-13, 2023
University of Colorado at Boulder
Meeting website: www.nrsmboulder.org
USNC-URSI website: www.usnc-ursi.org

This open scientific meeting is sponsored by the U.S. National Committee (USNC) for the International Union of Radio Science (URSI). More information about USNC-URSI is available at *www.usnc-ursi.org.* Through technical co-sponsorship of the meeting by the IEEE Antennas and Propagation Society, authors will have their choice of submitting one-page abstracts that are not posted in IEEE Xplore, or two-page summaries that may be archived in IEEE Xplore. At least one author is required to register for each presented abstract or summary. While USNC-URSI encourages in-person attendance for all presenters, a hybrid meeting is planned to allow for authors to present remotely and for all attendees to participate fully in the conference. Papers must be presented for their corresponding summaries to be included in the proceedings and submitted to IEEE Xplore. Abstracts or summaries on any topic in the interest area of a Commission are welcome. Contact the appropriate USNC-URSI Commission Chair listed below or visit the meeting website for further information.

USNC-URSI Chair: Michael Newkirk, Michael.Newkirk@jhuapl.edu

USNC-URSI Secretary: Jamesina Simpson, Jamesina.Simpson@utah.edu

PLENARY SPEAKERS

Patricia Doherty, Boston College, URSI Vice-President & Women in Radio Science (WIRS) Invited Speaker

John Mather, NASA, Senior Project Scientist for the James Webb Space Telescope

ABSTRACT AND SUMMARY SUBMISSION

Abstract and summary preparation and submission instructions are found at the conference website, *www.nrsmboulder.org*. Authors may submit to special sessions in addition to the general topics listed below. A list of special sessions will be available on the conference website. Abstracts or summaries must be submitted by **Friday, September 16, 2022**. If you have any questions on abstract/summary submission or the technical program, please direct them to the USNC-URSI Secretary. Abstracts must have a minimum of 250 words and summaries are limited to two pages. Note that registration is required to present accepted papers and attend any session of the meeting.

ERNEST K. SMITH USNC-URSI STUDENT PAPER COMPETITION

Prizes will be awarded to three student papers. Awards will be made for First Prize in the amount of $1000, Second Prize $750, and Third Prize $500. The deadline for submission of ***full papers*** is the same as the regular submission deadline. Please see *www.nrsmboulder.org* for additional information, or contact the Student Paper Chair, Prof. Erdem Topsakal, Dept. of ECE, Virginia Commonwealth University, etopsakal@vcu.edu. Student papers will be presented at a separate session and awards will be presented during the conference. Student Paper Competition participants will have the option of submitting their papers for publication in a special section of the journal *Radio Science*.

Questions?
For questions concerning conference logistics, please contact Christina Patarino at:
Phone: (303) 492-5151
E-mail: nrsmboulder@colorado.edu

Abstract / Summary Submissions and Student Paper Competition Submissions are due by
September 16, 2022
Please visit *www.nrsmboulder.org*

In Memoriam: François Lefeuvre

It is with great sorrow that we, his friends and colleagues, announce the passing of François Lefeuvre on March 14, 2022.

Since his very first research position at the Ionospheric Research Group (GRI) in Saint-Maur des Fossés in 1969, to the position of Past President of URSI [2011-2014], François was constantly interested in the physics and analysis of waves in space plasmas. Throughout his scientific life, he published numerous high-level scientific publications and actively collaborated with scientists from many scientific centers all around the world. He was the principal investigator and co-investigator on numerous space projects, including probes or scientific satellites in various regions of our magnetosphere. As director of LPCE from 1994 to 2002, he actively contributed to the fame of this institute at international level.

François served extensively in URSI for 21 years. His contributions to URSI included multiple leadership positions and enduring collaboration projects. In the recent history of URSI, he was the only person to have completed nearly two full terms as President (2005-2008, 2009-2011), and to have been a member of the URSI board for 12 years.

The memory of François Lefeuvre, a prominent scientist and a remarkable person, will forever remain in the hearts of those who were lucky enough to work with him.

More can be learned about François Lefeuvre's scientific career at: https://www.ursi-france.org/ursi-france/evenements/journees-scientifiques/2017/francois-lefeuvre and in the paper written in tribute to François Lefeuvre published in the *Radio Science Bulletin* No. 360, March 2017, pp 69-74, available at https://www.ursi.org/content/RSB/RSB_360_2017_03.pdf.

Sebastien Celestin
University of Orleans
France Member of the Institut Universitaire de France (IUF)
LPC2E/CNRS 3A avenue de la Recherche Scientifique
45071 Orleans Cedex 2 France
E-mail: sebastien.celestin@cnrs-orleans.fr

In Memoriam: Gentei Sato

Dr. Gentei Sato (Figure 1) passed away peacefully at 4:30 pm, January 18, 2022. He was born in Miyagi Prefecture, Japan, on March 15, 1926. He received the BE and PhD degrees in Electrical Engineering from Tohoku University in 1947 and 1961, respectively.

Figure 1. Dr. Gentei Sato.

From 1947 to 1955, he was a Research Associate of the Communications Department of Tohoku University, and an Associate Professor at Tohoku University in 1956. From 1957 to 1964, he was the Head of the Research Laboratory, Yagi Antenna Co., Ltd., Saitama, Japan. From 1964 to 1992, he was a Professor at the Department of Electric and Electronic Engineering, Faculty of Science and Technology, Sophia University, Tokyo, Japan, and from 1992, a Professor Emeritus at the same university. At his passing he was a Representative Director of Antenna Giken Co., Ltd., Saitama, Japan, the company he helped to found in 1965.

His main fields of interest were terrestrial digital TV broadcasting for transmitting antennas (including the batwing antenna and the stacked-loop antenna), ultra-high-speed electronic scanning phased-array antennas (Wullenweber antenna), and microwave transmission devices (analog and digital phase shifters). He was the author of several books: "*Antenna Engineering*" (Sogo Denshi Publishing, 1969); "*Antenna Theory and Its Application*" (Mimatsu Data System, 1991); "*Data on Ultra High Speed Variable Transmission Devices and Its Application*" (Sogo Denshi Publishing, 1995); "*Modern Antenna Engineering*" (Sogo Denshi Publishing, 2004); "*The Tale of the Television Antenna Tower*" (Tokyo, Ribun, 2005); "*The Tale of the Antenna Tower*" (Tokyo, Ribun, 2009, in Japanese). He was the recipient of the best paper award of the Defense Technology Foundation in 1987. He published more than 500 papers in national and international conferences and journals.

Figure 2. The reception room in Dr. Sato's family home in Miyagi Prefecture.

Dr. Sato was a Life Fellow of the Institute of Electrical and Electronics Engineers; a member of the Institute of Electronics, Information and Communication Engineers of Japan; a member of the Institute of Image Information and Television Engineers of Japan; and a member of the Institute of Electronic Engineers of Japan.

His hobbies were Chinese poetry (especially, by Confucius and Du Fu); glider maneuvering; shooting; and photography. He wrote many books on his specialties.

After Prof. Sato and I moved to Sophia University, we started to invite prominent people from foreign companies and academic societies to give lectures. In particular, I still well remember that Prof. Shintaro Uda gave a valuable and interesting lecture on the invention of Yagi-Uda antennas. In addition, the names of people invited to his company (Antenna Giken Co., Ltd., Saitama, Japan) and/or to his parents' house (Miyagi Prefecture, Figure 2) included Prof. King, Prof. Wait, Prof. Harrington, Prof. Sarkar, Dr. Stone, Prof. Mei, Prof. Tai, Dr. Masters, Prof. Oliner, Dr. Licardi, Dr. Saad, Prof. Boerner, Prof. Mittra, Prof. Hall, Prof. Kraus, and Dr. Wheeler.

Prof. Gentei Sato was the head of Yagi Antenna Co., Sophia University, and Antenna Giken Co., so we worked together in various public and private sectors for more than forty years. He was of good character, never got angry, and I have nice memories of working with him.

He is survived by his wife, Mutsuko; two sons, Motoyuki and Tomonari; and a daughter, Kazuko.

Haruo Kawakami
Technical Advisor, Kato Electric Industry Co., Ltd.
E-mail: h.kawakami@ieee.org

In Memoriam: Oleg Alexandrovich Tretyakov

Oleg Alexandrovich Tretyakov (Figure 1), the Chair of Commission B of the URSI National Committee of Ukraine since 1993, a member of the IEEE, and Professor Emeritus of the Department of Theoretical Radiophysics, V. N. Karazin Kharkiv National University (KhNU), Ukraine, passed away on January 25, 2022, in Istanbul, at the age of 83. He died shortly after he was hospitalized and diagnosed with lung cancer on December 29, 2021.

Figure 1. Oleg A. Tretyakov on December 19th, 2016.

Oleg A. Tretyakov was born on February 4, 1938, in Artyomovsk (currently Bakhmut), Ukraine. He finished secondary school as a gold medalist in 1955. He received the MSc and the Candidate of Science (PhD equivalent) in Radio Physics, and the Doctor of Science (DSc) in Physics and Mathematics from the National University of Kharkov, Ukraine, in 1960, 1964, and 1973, respectively. He became a full Professor in the Department of Theoretical Radiophysics in 1975. He served as the Chair of the Doctoral Degree Specialized Committee from 1976 to 1997. In 1980, he was awarded a Diploma of the Supreme Council for the schooling of highly-skilled students. He was a devoted member of the Department of Theoretical Radiophysics at the KhNU for 25 years (from 1972 to 1997) as the Head of the Department, and for another 22 years as an emeritus faculty. He was on leave of absence from 1998 to 2020 to work as a Visiting Professor at the Electronics Engineering Department of the Gebze Technical University, Turkey.

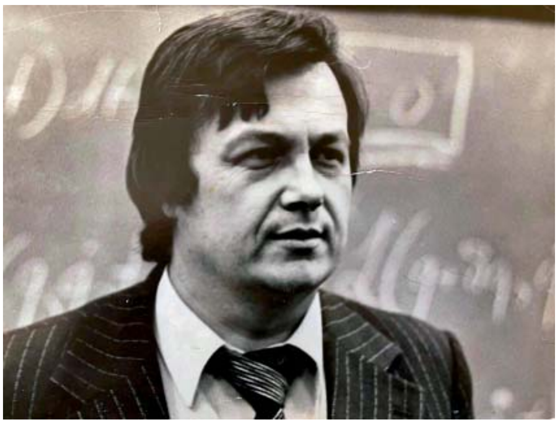

Figure 2. Oleg A. Tretyakov in the late 1970s.

In Ukraine, 22 candidates (PhD) and four doctors of science (DSc), and in Turkey, five PhD dissertations were defended under the supervision of Prof. Tretyakov. As a lecturer, he prepared the following lecture courses: Theoretical Mechanics, Electrodynamics, Quantum Mechanics; Evolutionary Approach to Electromagnetics; Fundamentals of Nonlinear Electrodynamics; and Nonlinear Electrodynamics. His brilliant teaching style remains the highest standard for all the teachers at the School of Radiophysics at KhNU (Figure 2).

As an invited lecturer, Prof. Tretyakov visited the Osaka Electro-Communication University (Osaka, 1970, 1980, 1992, 1993), Kyushu University (Fukuoka, 1980, 1993), and Kyoto University (Kyoto, 1992) in Japan; the Beijing University of Posts and Telecommunications (Beijing, 1985-86) in China (CIE); and the Technical University Hamburg-Harburg (Hamburg, 1997-98) in Germany. During his second visit to Japan in 1980, he obtained the decree of the Emperor of Japan concerning his ranking as a Full Professor of the Electro-Communication University in Osaka. He authored more than 250 scientific publications, published mainly in respectable international journals. Prof. Tretyakov also authored or co-authored two books (1993, 2006), and four monographs and book chapters (1989, 1993, 2002, 2021).

He was a co-editor of the *International Monograph Series on Advanced Electromagnetics* with the Science House Company Ltd., Tokyo, Japan. From 1995 to 2005, he was the Vice Editor-in-Chief, and later editorial board member, of the journal *Radio Physics and Radio Astronomy*, Ukraine. Prof. Tretyakov served on numerous technical program committees and steering committees of URSI and IEEE conferences (EMTS and MMET, respectively, and others).

Prof. Tretyakov had experience in solving diffraction problems by mathematically rigorous methods, wave scattering from rough surfaces, and wave propagation in random media, linear and nonlinear phenomena, and dynamic chaos in microwave oscillators and amplifiers. He founded the main direction of scientific research in the field of time-domain electromagnetics in the Theoretical Radiophysics Department at the KhNU. The direction was based on the Method of Modal Basis, proposed by him in the mid-1980s as a solid framework for analysis of

Figure 3. Oleg A. Tretyakov and his wife, Tetyana Tretyakova, lived in Istanbul from 1998 to 2022, until he passed away.

electromagnetic phenomena. The method was based on a modal expansion of the fields sought directly in the time domain, without exploiting any Fourier or other transform. As a result, the whole problem was split into two lower-dimensional problems: the problem in cross-section yielded the modal basis, and the problem in the longitudinal direction and time yielded the modal amplitudes. This method can be successfully applied to the rigorous analysis of transient signal propagation, propagation in transient media, and in nonlinear media. This approach, being analytical, allows obtaining rigorous solutions and deep physical insight into transient electromagnetic phenomena. A series of young scientists were attracted by this idea and are currently advancing the method.

His passion for science was exceptional and he kept contributing until the very end. After ending his contract with the university, Prof. Tretyakov continued his scientific work and remained active, devoting his time on his final paper, "A Novel Simple Format of Maxwell's Equations in SI Units," published in *IEEE Access* in June 2021. The paper was an extension of his recently published book chapter entitled "Innovative Tools for SI Units in Solving Various Problems of Electrodynamics" in the IET book *Advances in Mathematical Methods for Electromagnetics*. He was the sole advisor of the project titled "Analytical Solution for Radio Frequency Resonance Cavity Thrusters," sponsored by The Scientific and Technological Research Council of Turkey (TUBITAK) during 2021. His last invited conference talk was on "A New Simple Format of Maxwell's Equations in SI Units" at the opening plenary session of the 10th International Kharkiv Symposium on Physics and Engineering of Microwaves, Millimeter, and Submillimeter Waves (MSMW'20) on September 21st, 2020.

However, the life of O. A. Tretyakov was not only determined by radiophysics and electrodynamics. He loved to have coffee talks with his colleagues, sharing his life experiences, especially from his visits to Japan, from the Soviet Union period, and also from his China and the United States trips, with his own distinctive and unique sense of humor.

Recently, in his 2018 URSI AT-RASC conference paper, he honored his latest privileged group of former MSc and PhD students – Serkan Aksoy, Fatih Erden, Ozlem Akgun, Mehmet Kaya, Emre Eroglu, Ahmet Cosan; A. Yu. Butrym, Z. F. Nazirov, M. S. Antyufeyeva, Zheng YU, B. A. Kochetov, and M. N. Legenkiy – acknowledging them for their meaningful questions and interesting discussions during lecturing his course, "Evolutionary Approach to Electromagnetics," and especially for the fruitful collaborations afterwards. As students, colleagues, and friends, we not only lost a prominent scientist and mentor, but also a remarkable person. He was an inspiration and model for the several generations he mentored and encouraged throughout his career. His intellect, integrity, humor, professionalism, and humanity will be greatly missed.

Prof. Tretyakov is survived by his beloved wife Tetyana (Figure 3), his children, and grandchildren. His burial ceremony took place in Sisli, Istanbul, on January 28, 2022. He will be deeply missed by the fellows and colleagues who were lucky to work, discuss, or communicate with him. Expressions of condolence can be directed to me via e-mail at ferden@dho.edu.tr, and will be collected and handed over to his family.

Fatih Erden
National Defence University, Turkish Naval Academy
Department of Electronics Engineering
Tuzla, Istanbul, Türkiye
E-mail: ferden@dho.edu.tr

In Memoriam: Theodoros D. Tsiboukis

Prof. Theodoros D. Tsiboukis – EM scholar, friend and colleague of ours and of many others in URSI, IEEE, and around the world – passed away on April 11, 2021. He was born in Larisa, Thessaly, Greece, in 1948. He received the Diploma in Electrical and Mechanical Engineering from the National Technical University of Athens (NTUA), Greece, in 1971, and the Doctor Engineering in 1981 from the Aristotle University of Thessaloniki (AUTH), Thessaloniki, Greece. From 1981 to 1982, he joined the Electrical Engineering Department of the University of Southampton, England, as a Senior Research Fellow. In 1982, he joined the Department of Electrical and Computer Engineering (DECE) of AUTH, until 2015 when he retired as Professor Emeritus. During his tenure at DECE-AUTH, he served in many administrative positions, including 1993-1998 as Director of the Division of Telecommunications at the DECE, and from 1997-1998 as Chair of DECE. He was the Founder (1989) and the Head of the Applied and Computational Electromagnetics (ACEM) Laboratory until 2015.

Prof. Tsiboukis was a prolific scholar, authoring or co-authoring 13 books and monographs, two of them textbooks on undergraduate electromagnetics (one on statics and the other on dynamics), 16 book chapters, more than 170 refereed journal papers, and more than 200 international conference papers. His main research interests included computational electromagnetics, antennas, microwave engineering, material modeling, micro- and nano-electromechanical systems, and energy methods. In particular, he focused on electromagnetic field analysis by energy methods, computational electromagnetics (FEM, vector finite elements, MoM, FDTD method, integral equations, absorbing boundary conditions, perfectly matched layers), dual and variational methods, modern antenna systems, metamaterials, graphene, design of microwave systems, and design of MEMS/NEMS, reconfigurable devices, electromechanical actuators, and tunable composite media. He published in international archival publications including those of the IEEE, such as the *IEEE Transactions on Antennas and Propagation*, *IEEE Transactions on Magnetics, IEEE Transactions on Microwave Theory and Techniques, Proceeding of the IEEE*, and numerous others.

He served as a reviewer on numerous refereed international journals and conferences, especially those of the IEEE, technical panels, editorial boards, and organizing committees of conferences, symposia, and workshops. He was the Principal Investigator (PI) of several research projects, and the PhD advisor of 15 PhD students and a multitude of diploma theses. He was a member of diverse scientific societies (including the IEEE), associations, chambers, and institutions. He was also the recipient of a plethora of awards and distinctions, including the Panhellenic Mathematical Society Award, EMC Europe 2004 Best Paper Award, CEM 2014 Best Paper Award, and others.

He is survived by his wife Yioula, son Dimitris, daughter Natali, grandson Aggelos, brothers Ioannis and Athanasios, relatives, friends and colleagues.

He will be missed greatly by all that he touched, collaborated, directed, educated, and mentored for his gentle and sincere demeanor, abundant joy and love of life, and fundamental and everlasting scholarly contributions in electromagnetics and electrical engineering in teaching, research, and service.

May His Memory Be Eternal (ΑιωνίαΤουΗΜνήμη).

Constantine A. Balanis
School of Electrical, Computer and Energy Engineering
Arizona State University
Tempe, Arizona, 85287-5706, USA
E-mail: balanis@asu.edu

John N. Sahalos
University of Nicosia, Cyprus and
Aristotle University of Thessaloniki
Thessaloniki, 54124, Greece
E-mail: sahalos@auth.gr

IEEE International Symposium on Antennas & Propagation

& USNC-URSI Radio Science Meeting

JULY 23-28, 2023 • Portland

You are cordially invited to the *2023 IEEE International Symposium on Antennas and Propagation and USNC-URSI Radio Science Meeting – AP-S/URSI 2023*, from *July 23–28, 2023*, at the *Oregon Convention Center and Hyatt Regency*, in Portland, Oregon, USA, *the City of Roses*. This conference is cosponsored by the IEEE Antennas and Propagation Society (AP-S) and the US National Committee (USNC) for the International Union of Radio Science (URSI). It is intended to provide an international forum for the exchange of information on state-of-the-art research on antennas, propagation, electromagnetic engineering, and radio science. The symposium and meeting will include a wide range of technical sessions, invited talks, special sessions, student paper and design competitions, short courses, tutorials, exhibits, professional meetings, tours, and networking events. All events will be held in person, however there will an option to join some business meetings remotely.

The paper submission deadline is January 27, 2023. Conference website: https://2023.apsursi.org

Steering and Organizing Committee

General Chairs
Jamesina J. Simpson
jamesina.simpson@utah.edu
Reyhan Baktur
reyhan.baktur@usu.edu

Finance Chair
Satish Sharma
ssharma@sdsu.edu

Tech. Prog. Chairs
Andy Chrysler
chryandr@isu.edu
Cindy Furse
cfurse@ece.utah.edu
Karl Warnick
warnick@ee.byu.edu

URSI Tech. Prog. Chair
Jonathan Chisum
jchisum@nd.edu

Special Sessions Chair
Dan Sievenpiper
dsievenpiper@eng.ucsd.edu

Sponsors & Exhibits Chairs
Fikadu Dagefu
fikadu.t.dagefu.civ@army.mil
Luis Gomez
ljgomez@purdue.edu
Tutku Karacolak
tutku.karacolak@wsu.edu
Praveen Sekhar
praveen.sekhar@wsu.edu
Neill Kefauver
w.neill.kefauver@lmco.com
Kevin Geary
kgeary@hrl.com
James Schaffner
jhschaffner@hrl.com

Short Courses and Workshops Chairs
Ata Zadehgol
azadehgol@uidaho.edu
George Trichopoulos
gtrichop@asu.edu

Student Paper Competition Chairs
Magda El-Shenawee
magda@uark.edu
Ahmed Hassan
hassanam@umkc.edu
Amanda Malone
amanda.malone@ieee.org

Student Design Contest Chairs
Ting-Yen Shih
tshih@uidaho.edu
Glauco Fontgalland
fontgalland@dee.ufcg.edu.br

Young Professionals Chairs
Payam Nayeri
payam_nayeri@ieee.org
Peiyuan Qin
peiyuan.qin@uts.edu.au

Local Arrangements Chairs
Tutku Karacolak
tutku.karacolak@wsu.edu
Praveen Sekhar
praveen.sekhar@wsu.edu

Publicity and Social Media Chairs
Emily Porter
emily.porter@austin.utexas.edu
Negar Tavassolian
ntavasso@stevens.edu

Women in Engineering and Radio Science Chairs
Asimina Kiourti
kiourti.1@osu.edu
Maria Pour
maria.pour@uah.edu

URSI/AP-S Liaison
Jamesina J. Simpson
jamesina.simpson@utah.edu

Social Programs and Hospitality
Joanne Wilton; Susan Stone; Judy Long

International Advisory Committee
Fan Yang
fan_yang@tsinghua.edu.cn
David Davidson
david.davidson@curtin.edu.au
Peter De Maagt
peter.de.Maagt@esa.int
Buon Kiong Lau (Vincent)
bkl@eit.lth.se
Özlem Aydin Civi
ozlem@metu.edu.tr
Paolo Nepa
paolo.nepa@unipi.it
Marco A. Ridenti
arideni@ita.br
Dirk de Villiers
ddv@sun.ac.za

https://2023.apsursi.org

James C. Lin
University of Illinois at Chicago
851 South Morgan Street, M/C 154
Chicago, IL 60607-7053 USA
E-mail: lin@uic.edu

Safety Guidelines and 5G Communication RF Radiation

James C. Lin

University of Illinois at Chicago
851 S. Morgan St. (M/C 154)
Chicago, IL 60607 USA
E-mail: lin@uic.edu

The health and safety implications of fifth-generation (5G) cellular-communication technology have been under scrutiny while the rollout is well underway worldwide. Advocates of 5G mobile technology hail 5G as a faster and more-secure technology than its predecessor 3G and 4G systems. The major enabling infrastructure uses millimeter-wave (mm-wave) and phased-array technologies to achieve line-of-sight directivity, high data rates, and low latency. A central vulnerability or security threat is that it may allow spying on users. Nevertheless, this is a system architecture and technology or regulatory issue, but not a biological or health safety matter.

1. 5G Cellular Mobile Technology

5G cellular mobile technology is a telecommunication technology that is multilayered in frequency allocation and varied in operational scope and performance. It includes an extremely wide range of multiple radio-frequency (RF) bands. Its frequency coverage may be roughly separated into two ranges: the sub-6 GHz bands, and 24 GHz to 60 GHz frequencies that reach well into the mm-wave region. The frequency ranges have often been further divided into low-band 5G, mid-band 5G, and high-band 5G. Low-band 5G starts at about 400 MHz, and often uses existing or previous 3G or 4G frequencies or newly opened frequencies to operate: for example, the latter may overlap with the existing 4G band. 5G rollout began with the mid-band that includes the popular frequencies between 3 GHz and 4 GHz. However, the primary 5G technological advances are associated with the high-band 5G, promising performance bandwidths as high as 20 GHz and multiple-input, multiple-output strategies using 64 to 256 antennas at short distances, and offering performance up to 10 times the current 4G networks.

From the perspective of frequency allocation, 5G encompasses an enormous range, from 3 GHz to 60 GHz and beyond, in one giant skip from 4G. Even with current technological advances, the demand and performance challenges clearly vary immensely from the low to high bands. The performance bandwidth of 20 GHz obviously is not viable or supportable at low-band. By design default or spectrum necessity, the bandwidth performance will only be accomplished by leapfrogging to the high-band 5G. The higher 5G mm-wave bands where the wider spectrum is accessible primarily at shorter range will lead to massive proliferation of many micro-cells, because existing cell towers are unsightly and too big for the urban settings where mm-wave phased-arrays will mostly be deployed. For health safety matters, it is not obvious whether the biological responses to high-band 5G radiations would be akin to earlier generations or low-band 5G radiations, given the distinctive characteristics of mm-wave and its interaction with the complex structure and composition of pertinent superficial biological cells and tissues, such as the cornea of the eye and nerve-rich human skin, the large, protective organ of the body.

2. Recent Updates of Safety Recommendations

The two most widely promulgated RF safety guidelines or standards have recently published revisions of their respective 1998 and 2005 versions [1, 2]. The updated ICNIRP guidelines and IEEE standards appear to cater to industry wishes: they are strongly linked to thermal effects associated with measurable temperature elevations. The updates also seem to have been synchronized to accommodate the 5G rollout.

The World Health Organization's (WHO's) International Agency for Research on Cancer (IARC) classified exposure to RF radiation as a possible carcinogen to humans in 2011. The IARC had evaluated then-available scientific studies and concluded that, while evidence was incomplete and limited – especially regarding results from animal experiments – epidemiological studies of humans reported that increased risks for gliomas (a type of malignant brain cancer) and acoustic neuromas (or acoustic schwannomas, a non-malignant tumor of Schwann-cell-sheathed auditory nerves on the side of the brain) among heavy or long-term users of mobile telephones are sufficiently strong to support a classification of possibly carcinogenic in humans for exposure to RF radiation from mobile phones [3, 4].

It is noteworthy that the coveted animal experiments were indeed published in 2018. Specifically, the National Toxicology Program (NTP) of the US National Institute of Environmental Health Science (NIEHS) reported observations of two types of cancers in laboratory rats exposed, life long, to RF radiation used for 2G and 3G mobile telephone operations [5]. It was the largest health-effect study ever undertaken by NIEHS/NTP. Among other observations, it concluded that there was statistically significant and clear evidence that the RF radiation had led to the development of malignant schwannoma (a rare form of tumor) in the heart of male rats whose body temperature did not exceed 1°C. Further, there was also evidence for the same schwannoma risk among female rats. NTP also noted that there were unusual patterns of cardiomyopathy, or damage to heart tissue, in both RF-exposed male and female rats when compared with concurrent control animals. In addition, based on statistical significance, the pathology findings showed indications of some evidence for RF-dependent carcinogenic activity in the brain of male rats, specifically glioma. However, the findings for female rats were deemed as providing only equivocal evidence for malignant gliomas when compared with concurrent controls.

Furthermore, shortly after the NTP report, the Cesare Maltoni Cancer Research Center at the Ramazzini Institute in Bologna, Italy, published the results from its comprehensive study on carcinogenicity in rats exposed (either lifelong or prenatal until death) to 3G, 1800 MHz RF radiation [6]. The study involved whole-body exposure of male and female rats under plane-wave equivalent or far-zone exposure conditions. The authors estimated that the whole-body SARs were 0.001 W/kg, 0.03 W/kg, and 0.1 W/kg during exposures of 19 h/day for approximately two years. A statistically significant increase in the rate of schwannomas in the hearts of male rats was detected for whole-body 0.1 W/kg RF exposure. It is important to note that the NTP and Ramazzini RF exposure studies presented similar findings in heart schwannomas and brain gliomas. Two relatively well-conducted RF exposure studies employing the same strain of rats thus showed consistent results in significantly increased cancer risks.

While recognizing that the two afore-mentioned studies used large numbers of animals, best laboratory practice, and animals exposed for the entirety of their lives, the recent updates preferred to quibble with alleged "chance differences" between treatment conditions and the fact that the measured animal body core temperature changes reached 1°C. In doing so, it may have overlooked the absurdity of inferring a 1°C body core temperature rise as being carcinogenic. Furthermore, it totally ignored the implications of RF agents or have chosen to sidestep them through such pretexts as that the evidence or findings did not provide credible indication of adverse effects caused by chronic RF exposures.

3. High Band 5G mm-Waves

For high-band 5G, the distinctive characteristics of mm-wave and its interaction with the complex function and structure of relevant biological tissues associated with the cornea of the eye and the large protective organ of the skin are of special concern.

The human skin tissue is about 2 mm in thickness. It is not homogeneous, but consists of three major layers of stratum corneum, epidermis, and dermis. It has a total mass of about 3 kg, and covers nearly the entire body surface (about 1.85 m^2). It is differentiated according to its location on the body, and it can vary in thickness depending on what part of the body it is covering. On the back, it may be greater than 2.0 mm thick, and on the eyelids, it can be less than 0.35 mm thick. The skin is also an important sensory organ, endowed with nerve endings that are sensitive to touch, pain, and warmth. Anatomically, it is the largest organ of the human body. Its various constituent cells and tissues help to keep microbes out, hold body fluids in, and prevent dehydration.

The power reflection coefficients of the skin for mm-wave decreases from 60% to 20% as frequency increases, while the power transmission coefficient increases from 50% to 65%. The penetration depth, where the power deposition is reduced by an exponential factor (e^{-2}) of a planar mm-wavefront, decreases from 1.2 mm to 0.4 mm for skin, and the induced energy deposition increases with mm-wave frequency [7]. However, at the highest frequencies the energy deposition in the deeper regions inside the skin is lower, because of the reduced penetration depth at these frequencies [8].

Studies on mm-wave interactions aimed both toward biological effects and medical applications began nearly 50 years ago, most notably in Russia or the former Soviet Union. A comprehensive review of research on biological effects of mm-wave from some the earlier studies showed that at incident power densities of $100\ \mathrm{W/m^2}$ or less, mm-wave can affect cell growth and proliferation, enzyme activity, genetic status, function of excitable membranes, peripheral receptors, and other biological systems [9]. However, a common concern has been the lack of clarity in reported experimental protocols, rigor in statistical analysis, inadequate in-situ dosimetry, absence of sham-exposure and temperature controls, as well as paucity of reported details.

A recent paper provided an updated summary of results published from Russia since 1997, including a few related studies from elsewhere [10]. The review focused on experimental findings of mm-wave effects at subcellular and cellular levels, including cell proliferation and gene expression. It also contained effects on excitable tissues and immune systems, and responses on the eyes and skin. It concluded that available data showed incident mm-wave power densities below $100\ \mathrm{W/m^2}$ does not produce any harmful effect on eyes, but exposures at higher levels may result in adverse effects that dependent on the frequency and duration of exposure. Likewise, studies have shown absence of genotoxic effects in skin cells or changes in gene expression for low-power exposures without significant temperature elevations. However, the results on proliferative effects for cells of different types are contentious.

Furthermore, while some recent studies did not show non-thermal changes in electrical activity and structure of excitable cells, the rate of mm-wave power deposition was noted to play a significant role in eliciting the electrical response of nerve cells. Millimeter waves have been reported to produce systemic effects in humans and animals that involve hypoalgesia and endogenous opioids, and can affect the behavior of the immune and nervous systems around $100\ \mathrm{W/m^2}$. There are suggestions that systemic responses are initiated by stimulation of free nerve endings in the skin, followed by modulation of central neural activity resulting in biological effects.

Recently, several reviews were published based mostly on data from papers written in English [11-13]. A 2019 review [11] included 45 in-vivo studies conducted using laboratory animals and other biological preparations, and 53 in-vitro studies involving primary cells and cultured cell lines. The review was based on published papers through the end of 2018 using 6 GHz to 100 GHz as the RF source frequency. However, because fewer studies were reported at 30 GHz or below and at frequencies higher than 90 GHz, the review mainly covered published studies conducted in the mm-wave frequency range from about 30 GHz to 65 GHz.

This industry-supported review noted that aside from the wide frequency ranges, the studies were diverse in both subject matter and end points investigated. Biological effects were observed to occur both in-vivo and in-vitro for different biological endpoints studied. Indeed, the percentage of positive responses at non-thermal levels in most frequency groups was as high as 70%. (Higher mm-wave intensities, up to $200\ \mathrm{W/m^2}$, did not seem to cause any greater responses.) For example, in the 53 in-vitro studies involving primary cells ($n = 24$) or cell lines ($n = 29$), approximately 70% of the primary cell studies and 40% of the cell-line investigations showed effects that were related to mm-wave exposure. However, the protocol applied for control of biological-target or culture-medium temperature during mm-wave exposure was uncertain in a large fraction of these studies.

An overview of the total published scientific literature on the possible effects of mm-waves on skin and skin cells in 2020 counted only 99 experimental studies [12]. Many of these were focused on thermal stress and pathophysiology associated with exposure to high power densities.

More recently, a review from the Australian Government included 107 experimental studies (91 in-vitro, 15 in-vivo, and one human) that investigated various biological effects of mm waves, including genotoxicity, cell proliferation, gene expression, cell signaling, membrane function, and other effects [13]. It asserted that the review of experimental studies provided no confirmed evidence that low-level mm waves were associated with biological effects relevant to human health. It suggested that many of the studies reporting effects came from the same research groups and the results have not been independently reproduced. Most of the studies employed low-quality methods of exposure assessment and control, so the possibility of experimental artifact could not be excluded. Furthermore, many of the effects reported may have been related to heating from high power deposition so the assertion of a low-level effect is questionable in many of the studies.

To date, there was no reported epidemiological study that investigated mm waves and their potential health effects.

While there are about 100 published laboratory

Table 1 Thermal Effect Based Guidelines or Standards for Short-Term (6 or 30 min) Exposure

Spectrum Range	Key ΔT Parameter	ΔT	Average Mass/Area	Average Time	Health Effect Level	Safety Factor*	General Public Level	Safety Factor*	Worker** Level
100 kHz-300 GHz	Body Core	1 °C	WBA***	30 min	4 W/kg	50	0.08 W/kg	10	0.4 W/kg
100 kHz – 6 GHz	Local Head-Torso	2 °C	10 g	6 min	20 W/kg	10	2 W/kg	2	20 W/kg
	Local Limbs	2 °C	10 g	6 min	40 W/kg	10	4 W/kg	2	40 W/kg
> 6 GHz – 300 GHz	Local Head-Torso	5 °C	4 cm^2	6 min	200 W/m^2	10	20 W/m^2 (in 4 cm^2)	2	100 W/m^2
30 GHz – 300 GHz	Local Limbs	5 °C	2 cm^2	6 min	400 W/m^2	10	40 W/m^2 (in 1 cm^2)	2	200 W/m^2

*Reduction Factor; **Workers - Occupational or Controlled Exposure; *** WBA - Whole Body Average

investigations of all types, the reported biological responses were thus inconsistency in the association between biological effects and mm-wave exposure. Indeed, the types of reported laboratory investigations were small, limited, and diverse, considering the wide 5G mm-wave frequency domain. The jury on biological effect or health impact is still out on 5G mm waves. Moreover, there is a lack of ongoing controlled laboratory investigations. To help improve the situation, new laboratory investigations should provide experimental designs with statistical validity that support methods, procedures, and protocols amenable to independent replication, and must include quantitative exposure, dosimetry, and temperature determination and control.

4. Anomalies in Recently Updated Safety Recommendations

The recently updated safety guidelines and standard make recommendations to purportedly protect against established adverse health effects in humans resulting from exposure to electromagnetic fields in the frequency range between 6 GHz to 300 GHz. In fact, these are recommendations for short-term exposures of 6 min to 30 min, based on limiting whole-body temperatures from rising above 1°C or tissue temperatures to 5°C (Table 1).

If the responsible entities believe what appears to be their position concerning experimental results from rats from NIEHS/NTP that a whole-body temperature rise of 1°C is carcinogenic, then the safety factors of 10 for the public or 50 for workers would be marginal and practically meaningless from the perspective of "safety" protection (more so above 6 GHz).

It is noteworthy that the average power density thresholds under controlled laboratory conditions for microwave auditory effect in human subjects with normal hearing for 10 μs to 32 μs pulses are about 14 kW/m^2 in the near field of 1250 MHz to 3000 MHz [8]. In other words, the 14 kW/m^2 per pulse peak power density generates a barely audible sound level of 0 dB. To generate sound at 60 dB, or the audible level for normal conversation, requires 1000-fold higher power density per pulse. To generate a tissue-injuring level of sound at 120 dB would take another 1000-fold increase in required peak power density, or 14 GW/m^2 per pulse. Such a high-power microwave pulse-generated acoustic pressure wave can be initiated in the brain and then reverberate inside the head to potentially, if not surely, cause serious injury of white and grey brain matters along with other neural elements [6]. Yet the corresponding theoretical temperature elevation would be about 1°C, which would be "safe" by current protection guidelines. Of course, the clinical implications are uncertain at present, and would demand future study for clarification.

As shown in Table 1 for mm waves, the reference local tissue temperature rise in the head, torso, and limbs of humans is 5°C. This level of temperature rise would bring the tissue temperature from a normal value of 37°C to a hyperthermic 42°C. A 42°C tissue temperature is known to be cytotoxic with exponential cell-killing capacities. It is used as the basis for clinical cancer therapy in hyperthermia treatment for cancer protocols [14-16]. The recently updated safety recommendations provide a reduction factor of 10 for the public's "safety" and a "safety factor" of two in the case of workers. The efficacy of these updated safety recommendations is borderline, and the updated recommendations are meaningless from the perspective of "safety" protection.

In summary, the safety recommendation updates were based primarily on limiting the tissue-heating potentials of RF radiation to elevate body temperatures. There are significant anomalies in the recently updated safety recommendations. However, aside from the above-mentioned anomalies, the existing scientific data is too limited, especially at mm wavelengths, for any reliable assessment or conclusion with any certainty. Some of the updated safety recommendations are marginal, questionable, and lack scientific justification from the perspective of "safety" protection.

5. References

1. IEEE, "Standard for Safety Levels with Respect to Human Exposure to Electric, Magnetic, and Electromagnetic Fields, 0 Hz to 300 GHz," *(Revision of IEEE Std C95.1-2005/Incorporates IEEE Std C95.1-2019/Cor 1-2019)*, October 4, 2019, pp. 1-312.

2. ICNIRP, "Guidelines for Limiting Exposure to Electromagnetic Fields (100 kHz to 300 GHz)," *Health Phys.*, **118**, 5, 2020, pp. 483-524.

3. R. Baan, Y. Grosse, B. Lauby-Secretan, F. El Ghissassi, V. Bouvard, L. Benbrahim-Tallaa, N. Guha, F. Islami, L. Galichet, and K. Straif, WHO International Agency for Research on Cancer Monograph Working Group, "Carcinogenicity of Radiofrequency Electromagnetic Fields," *The Lancet Oncology*, **12**, 2011, pp. 624-626.

4. IARC Working Group on the Evaluation of Carcinogenic Risks to Humans, "Non-Ionizing Radiation, Part 2: Radiofrequency Electromagnetic Fields," *IARC Monogr. Eval. Carcinog. Risks Hum.*, **102**, 2, 2013, pp. 1-460.

5. US National Toxicology Program, "Technical Report on the Toxicology and Carcinogenesis Studies in HSD: Sprague-Dawley SD Rats Exposed to Whole-Body Radio Frequency Radiation at a Frequency (900 MHz) and Modulations (GSM and CDMA) Used by Cell Phones," NTP, Raleigh, NC, Tech. Rep. 595, 2018.

6. L. Falcioni et al., "Report of Final Results Regarding Brain and Heart Tumors in Sprague-Dawley Rats Exposed from Prenatal Life Until Natural Death to Mobile Phone Radiofrequency Field Representative of a 1.8 GHz GSM Base Station Environmental Emission," *Environ. Res.*, **165**, August 2018, pp. 496-503.

7. J. C. Lin, *Electromagnetic Fields in Biological Systems*, Boca Raton, FL, CRC Taylor/Francis, 2011, pp. 1-57.

8. J. C. Lin, "5G Communication Technology and Coronavirus Disease," *IEEE Microwave Magazine*, **21**, 9, September 2020, pp 16-19.

9. A. G. Pakhomov, Y. Akyel, O. N. Pakhomova, B. E. Stuck, M. R. Murphy, "Current State and Implications of Research on Biological Effects of Millimeter Waves: A Review of the Literature, *Bioelectromagnetics*, **19**, 7, 1998, pp. 393-413.

10. S. I. Alekseev and M. C. Ziskin, "Biological Effects of Millimeter and Submillimeter Waves," in B. Greenebaum and F. Barnes (eds.), *Handbook of Biological Effects of Electromagnetic Fields, Fourth Edition*, Boca Raton, FL, CRC Press, 2019, Chapter 6, pp. 179-242.

11. M. Simkó and M. O. Mattsson, "5G Wireless Communication and Health Effects – A Pragmatic Review Based on Available Studies Regarding 6 to 100 GHz," *Int. J. Environ. Res. Public Health*, **16**, 18, September 2019, pp. 3406.

12. D. Leszczynski, "Physiological Effects of Millimeter-Waves on Skin and Skin Cells: An Overview of the To-Date Published Studies," *Reviews on Environmental Health*, **35**, 4, 2020, pp. 493-515.

13. K. Karipidis, R. Mate, D. Urban, et al., "5G Mobile Networks and Health – A State-of-the-Science Review of the Research into Low-Level RF Fields Above 6 GHz," *J. Expo Sci. Environ. Epidemiol.*, **31**, July 2021, pp. 585-605.

14. D. J. Watmough and W. M. Ross (eds.), *Hyperthermia*, Glasgow, Blackie, 1986, pp. 42-75.

15. J. C. Lin, "Hyperthermia Therapy," in J. G. Webster (ed.), *Encyclopedia of Electrical and Electronics Engineering, Volume 9*, New York, Wiley, pp. 450-460.

16. NIH/NCI, "Hyperthermia to Treat Cancer," https://www.cancer.gov/about-cancer/treatment/types/hyperthermia#hyperthermia-treatment-research, accessed on September 27, 2021.

EuCAP 2023
Florence, March 26-31, 2023

17th EUROPEAN CONFERENCE ON ANTENNAS & PROPAGATION

EuCAP 2023

Call for Papers

Florence
Italy
27 – 31 March 2023

17th European Conference on Antennas and Propagation

THE CONFERENCE

EuCAP is Europe's largest and most significant conference on antennas and propagation attracting more than 1400 participants from academia and industry, and more than 50 industrial exhibitors worldwide. It is an excellent forum for exchanging new technical-scientific achievements, demonstrating state-of-the-art technology, and establishing and strengthening professional networks.

EuCAP 2023 will give the opportunity to address some of the main challenges of our time for technical-scientific research in Antennas, Electromagnetics, Propagation and Measurements.

FORMAT OF THE CONFERENCE

The conference will comprise:

- Plenary sessions with invited and keynotespeakers
- Oral sessions (both convened and regular)
- Poster sessions
- Short courses
- Industrial and scientific workshops
- Industrial exhibition

APPLICATION TRACKS

Aiming at increasing the interaction between academia and industry, the conference will featuresession tracks focused on front-line applications; see the backside.

BEST PAPER AWARDS

A Best Student Paper Award and Best Paper Awards in the four categories Antennas, Electromagnetics, Propagation, and Measurement are planned at EuCAP2023.

GRANTS

A limited number of grants covering both travel and registration will be offered to selected authorsof high-quality papers. Please see the conference homepage for more information (www.eucap2023.org).

AMTA EUROPE

The Antenna Measuremen Techniques Association (AMTA) is strongly involved in the conference.
AMTA will contribute with invited speakers, provide special sessions, cooperate in the application tracks, and sponsor the technical tours.

EXHIBITION AND SPONSORSHIP

The conference will provide numerous opportunities for exhibitors and sponsors, according to their strategic visibility and publicity targets.
Coffee breaks and lunches will be served in the exhibition area to increase the interaction between participants and exhibitors. Please see the conference homepage for more information.

FLORENCE

Florence is a perfect location since it represents modernity in a historical environment, offering all the facilities of a modern city but in a renaissance environment rich in suggestive scenarios. This feature, the lively cultural atmosphere, the excellent Italian food, and the Mediterranean spring climate will offer an unforgettable experience to all the participants.

Information for Authors

Authors are invited to submit papers in PDF format, with a minimum length of two and a maximum length of five A4 pages.

The paper must contain enough information for the Technical Programme Committee and reviewers to assess the quality ofthe work in a single acceptance/ rejection review process. It will be possible to revise accepted papers in line with the reviewers' comments.

Submit your paper online at www.eucap2023.org no later than **14 October 2022**.
The submission requires an EDAS® account, which is free.

Presented papers will be includedin IEEE Xplore, if the authors choose this option during the submission process. Compliancewith the IEEE format is mandatory in this case.

At least one of the authors of eachpaper must register as a delegate attending the conference.
A delegate cannot register more than two papers in their nameas "presenting author."

Important Dates
Deadline: 14 October 2022
Notification: 19 December 2022
Revised paper: 17 January 2023

Firm Deadline
For EuCAP 2023, there will be no extension of the paper sub-mission deadline; late or updatedsubmissions will not be accommodated after the deadline.

Asta Pellinen-Wannberg
Umeå University, Department of Physics and
Swedish Institute of Space Physics
S-90187 Umeå, Sweden
Tel: +46 90 786 7492
E-mail: asta.pellinen-wannberg@umu.se

Introduction by Associate Editor

This time I am happy to introduce a young female scientist from India. I met Dr. Rashmi Joshi on one of my last conferences before retirement, the 14th Spacecraft Charging Technology Conference at ESTEC in Noordwijk, Netherlands, in April 2016. This turned out to be Rashmi's first conference visit abroad. My colleague, Dr. Carol Norberg, and I had attended the conference to present our papers and learn about the latest advances within the areas of expertise of the other participants in preparation for teaching graduate school classes about the space environment around Earth. We were impressed by young Rashmi, who gave a very well prepared talk about spacecraft-charging research in India. She also presented several posters about solar panels and arc flashes.

When we asked Rashmi about the conference dinner, she was skeptical because it would be late, and the bus did not pass her hotel. She had promised to call back home to India every evening after arriving at the hotel. When Carol and I promised to be her bodyguards and escort her to the hotel in the evening, her husband was happy to trust us. We had together a very nice dinner in a cozy restaurant. Indeed, the entrance to Rashmi's hotel was a little bit secluded and dark.

Read Rashmi's moving story about her multiple life cycles already at a young age. She also gives her wise reflections about girls' conditions for education and later career opportunities in a traditional Indian household.

Working Mother from India: Redefining Traditions

Rashmi Shah (maiden name: Joshi)

Quest Global India Private Limited
Bengaluru, India
E-mail: rashmi.joshi.2189@gmail.com

Looking back on my nine years of professional career, I am much satisfied to have touched manifold verticals. From working with the Indian government to working in the private sector, from delving into research and into academics, it has been a diverse experience. Currently, I am associated with a foreign MNC (multi-national corporation) that has been established in India for a couple of decades. In this article, I wish to share my experience and various challenges at different stages of my career.

From Childhood Until Doctoral Degree

My parents migrated from a mountainous Himalayan region (Pithoragarh) towards the other end of India (Jamnagar – Gujarat) to set up a good income and nurture posterity in the best possible way. My father had always taken calculated risks in his life, which directly or indirectly have positively affected the upbringing of my siblings and myself. Thanks to my parents, I could follow a conventional roadmap for my studies. After completing my graduation and post-graduation in Instrumentation and Control Engineering, I had an opportunity to work with the Institute for Plasma Research as a Junior Research Fellow. To be truthful, in India, the post-graduate students who opt for research studies receive way less compensation compared to those who pursue their careers in the corporate sectors. Here, I thank my PhD supervisor, Dr.-Ing Suryakant B. Gupta, for guiding me through the dilemma of pursuing a PhD or continuing my career in the corporate sector.

Finally choosing the former, I delved into it and also got fruitful results. I could publish my work in IEEE *Transactions* and had a chance to visit the European Space Agency (ESA) at Noordwijk, The Netherlands, for one of the conferences on space research. It was my first international trip, and I was the only Indian attendee in the conference. As even my supervisor could not attend it, I grabbed the opportunity to represent my team in the forum. Yes, we were the only team in India who was involved in space-plasma interaction experiments, which was one of the crucial sessions in the conference. I received recognition in my society for receiving a doctorate degree at the age of 29. I was the first one in my family to complete a PhD so young.

I received my doctoral degree from Nirma University and Institute for Plasma Research in 2018. This was based on a thesis titled "Diagnostics of ESDs on Satellite Solar Panels."

I was involved in a diverse project that had a physicist, a mechanical engineer, and myself working towards the same goal. Each one had their own area for contributions, where I was responsible for development of the data-acquisition software and analyzing captured electrostatic-discharge (ESD) events occurring on satellite solar-panel coupons under simulated geo-synchronous-Earth-orbit (GEO) and low-Earth-orbit (LEO) environments. The project was sponsored by the Indian Space Research Organization (ISRO) to identify the root cause for reportedly observed failures in various satellite components operating at higher voltages. The space environment is unfavorable for high-power-generating satellites. On-orbit measurements claimed the presence of low-density plasma in low Earth orbit and dense electron clouds in geo-synchronous Earth orbit. These are responsible for charging satellite components at different potentials based on their surface material properties. The proximity between two surfaces charged at different potentials results in an ESD or arc. An arc is defined as a rapid displacement of charge, either by a punch-through effect, flashover propagation, or release of a blow-off current between surfaces and the surrounding environment (nanosecond to microsecond). The resultant ESD may trigger a secondary arc that can destroy the solar-panel circuit and severely damage the substrate. There was therefore a need to test the performance of these solar arrays in a ground-simulation facility.

Solar-panel coupons obtained from ISRO were exposed to an adverse space environment that was artificially created inside the vacuum chamber in a laboratory to obtain arcs for analysis. Various electrical and optical arc parameters were measured using a dedicated real-time controller and a *LabVIEW* environment. Complete automation and easy data manipulation based on various diagnostics techniques were developed in-house. Primary data acquisition consisted of capturing the discharge current that was in the range of microseconds and the voltage waveform that triggered other data-acquisition sequences. Diagnostics of high-voltage and current signals generated during arc (discharge) may provide details about some arc-mitigation techniques as a desired outcome of the research. Various arc properties such as the arc velocity, neutralization velocity, and surface flashover were derived from these signals.

Apart from this, automated ESD location-predictor software was developed during my PhD research. This algorithm can predict the arc-current waveform at different locations on the solar coupon. These predicted waveforms showed good agreement with those experimentally obtained. A database consisting of such waveforms can be used to identify the location of the discharge (arc) on any two-dimensional surface. The technique used for predicting the arc-current waveform was developed using *LabVIEW VISION* during my PhD research.

Balancing Office Work and Baby at Home

After submitting my thesis, I joined Bombardier Transportation India Private Limited as a Control Software Engineer. In India, the balance between office work and home responsibilities is not easy for a woman. Although we have a high percentage of female students in STEM, moving ahead and make a career in this is not common. Most females prefer to be homemakers after marriage or after having a child. There is also a general understanding in the society that men are the primary earning members in the household, and it is okay for a woman to stay at home and be completely involved in social and family responsibilities. This is the main reason that women do not explore their strengths in the professional world.

I am in my early 30s and a mother of a 2.5-year-old (Figure 1). I belong to a traditional Indian family, where three or more generations stay under the same roof, and it is a woman's accountability to satisfy the emotional needs of everyone in the family. As quoted by someone, "One woman, many roles" truly applies here. At times, playing the roles of a wife, mother, daughter, and daughter-in-law, women tend to forget about their own desires. From going through childbirth to being the primary parent for the child's basic needs, women shoulder major responsibilities. All

Figure 1. Rashmi with her daughter, Pihu.

of these exist during the most productive years of one's life span. In my case, I could continue my pregnancy only until the 29th gestation week and gave birth to Pihu (my daughter), who was just 900 grams back then. It was the most difficult phase of our life, and we were clueless on methods for her upbringing.

At that point in time, I could understand that although God puts us with difficult situations, He also ensures that we are courageous enough to overcome them. I experienced that a mother is strongest when it comes to her child. It was not easy for me to take care of my daughter after an emergency C-section. However, I was fortunate enough to have extensive support from my mother-in-law (which continues!). After spending six weeks in NICU, we could bring our daughter home and soon after, the world was hit by the global pandemic coronavirus.

We have been working from home since March 2020 (soon to be two year). This gave me a chance to witness the day-to-day growth of my daughter more closely than many working mothers. With God's grace, Pihu, my tiny preemie, is blossoming into a beautiful flower.

Message

I feel that for all the women around the world it has never been easy to be financially independent. Only a good education and career helps us to achieve this. Here, financial independence is not the final goal; however, it is the major milestone in becoming emotionally independent. We cannot choose the family we are born into; however, we need to wisely choose a life partner and the family we are getting married into. A good and supportive husband is often not by luck. Indeed, a woman's husband can be her strength or can work towards rusting her talents. Women need to be outspoken about the difficulties they face at home and encourage men to share them. In many cases, men are not asked to share household responsibilities even by their mothers during their teen-hood, due to which they are not capable of understanding the difficulties faced by their working wife. Parents need to analyze their methods for raising their children without any gender discrimination.

On the other hand, girls/women should start identifying their strengths and work on them. Working in an office makes no difference in incorporating values or being attached to your children. Indeed, working mothers signify power and wisdom, especially towards their daughters. In my case, although as a working wife and mother I can spare less time for my husband and daughter, I always prefer it to be quality time. Somewhere, I feel that I am demonstrating for my daughter the importance of achieving life goals, being financially as well as emotionally independent.

CALL FOR PAPERS

ICEAA
IEEE APWC

Cape Town, South Africa, September 5-9, 2022

FORMAT > Hybrid. A hybrid virtual plus in-person format will be followed.

ICEAA '22
IEEE APWC '22

5 - 9 September 2022
Cape Town, SOUTH AFRICA

www.iceaa-offshore.org

ICEAA 2022	**IEEE APWC 2022**
International Conference on Electromagnetics in Advanced Applications	IEEE-APS Topical Conference on Antennas and Propagation in Wireless Communications

The 23rd edition of the ICEAA and 11th edition of the IEEE APWC will take place jointly on 5-9 September 2022 in Cape Town, South Africa. A hybrid virtual plus in-person format will be followed to accommodate pandemic uncertainties. The conferences are technically sponsored by the Politecnico di Torino and by Stellenbosch University. The conferences consist of invited and contributed papers, and share a common organization, registration fee, submission site, workshops and short courses, banquet, and social events. Papers may be submitted to the IEEE Xplore Digital Library.

Information for Authors

Authors must submit an extended abstract or a summary paper electronically by March 20, 2022. Authors of accepted contributions must submit the executed copyright form and registration electronically by June 1, 2022. Each registered author may present up to two papers, with the second paper incurring an additional fee. All papers must be presented by one of the authors. Please refer to the website for submission instructions and further details.

Deadlines (2022)

Paper or extended abstract submission	March 20
Notification of acceptance	May 10
Presenter registration	June 1

Inquiries

Prof. Roberto D. Graglia
Chair of Organizing Committee
DET - Politecnico di Torino
Torino, ITALY
roberto.graglia@polito.it

Prof. Piergiorgio L. E. Uslenghi
Chair of Scientific Committee
ECE - University of Illinois at Chicago
Chicago, Illinois, USA
uslenghi@uic.edu

Prof. Matthys M. Botha
Chair of Local Organizing Committee
DEEE – Stellenbosch University
Stellenbosch, SOUTH AFRICA
mmbotha@sun.ac.za

ICEAA Topics

- Adaptive and reconfigurable antennas
- Complex media
- Electromagnetic applications to biomedicine
- Electromagnetic applications to nanotechnology
- Electromagnetic education
- Electromagnetic measurements
- Electromagnetic modeling of devices and circuits
- Electromagnetic packaging
- Electromagnetic properties of materials
- Electromagnetic theory
- EMC/EMI/EMP
- Finite methods
- Frequency selective surfaces
- High power electromagnetics
- Integral equation and hybrid methods
- Intentional EMI
- Inverse scattering and remote sensing
- Metamaterials and metasurfaces
- Microwave antennas, components and devices
- Optoelectronics and photonics
- Phased and adaptive arrays
- Plasma and plasma-wave interactions
- Printed and conformal antennas
- Radar cross section and asymptotic techniques
- Radar imaging
- Radio astronomy (including SKA)
- Random and nonlinear electromagnetics
- Reflector antennas
- Technologies for mm and sub-mm waves

APWC Topics

- Active antennas
- AI in electromagnetic applications
- Antennas and arrays for security systems
- Channel modeling
- Channel sounding techniques for MIMO systems
- Cognitive radio
- Communication satellite antennas
- DOA estimation
- EMC in communication systems
- Emergency communication technologies
- Indoor and urban propagation
- Low-profile wideband antennas
- MIMO systems
- Mobile networks
- Multi-band and UWB antennas and systems
- OFDM and multi-carrier systems
- Propagation models
- RFID technologies
- Signal processing antennas and arrays
- Small mobile device antennas
- Smart antennas and arrays
- Space-time coding
- Vehicular antennas
- Wireless communications
- Wireless mesh networks
- Wireless power transmission and harvesting
- Wireless security
- Wireless sensor networks

Nosherwan Shoaib
Research Institute for Microwave and Millimeter-Wave Studies (RIMMS)
School of Electrical Engineering and Computer Science (SEECS)
National University of Sciences and Technology (NUST)
H-12, Islamabad, Pakistan
E-mail: nosherwan.shoaib@seecs.edu.pk

Young Scientist and Student Paper Activities at URSI GASS 2021

It can be said with no doubt that the COVID-19 pandemic has disrupted in-person conference activities worldwide. Similarly to 2020, the year 2021 was a challenging year, with COVID-19 measures across the globe posing severe restrictions on people moving around and meeting in person. In this context, the URSI General Assembly and Scientific Symposium (GASS) 2021 was conducted in hybrid mode. The Young Scientist (YS) Awards were also granted and the Student Paper Competition (SPC) was held. In this ECR column we feature two short reports on the Young Scientist Awards and the Student Paper Competition. These reports were kindly provided by the Young Scientist Panel, consisting of Phil Wilkinson (Chair), Peter van Daele, Stefan J. Wijnholds, and Inge Lievens; and Sembiam R. Rengarajan (Chair of the Student Paper Competition), respectively.

1. Young Scientist Awards at the URSI GASS 2021

1.1 Background

The Young Scientist (YS) Awards are presented at URSI flagship meetings – these being the General Assemblies of URSI, the URSI Atlantic Radio Science Conferences (AT-RASC), and the URSI Asia-Pacific Radio Science Conferences (AP-RASC) – to recognize an international group of individuals who have made innovative contributions and discoveries in multidiscipline research related to the fields of URSI.

In general, the three URSI flagship meetings are held in a three-year cycle to review current research trends, present new discoveries, and make plans for future research and special projects in all areas of radio science, especially where international cooperation is desirable. Young researchers can apply for a Young Scientist Award at any of these three URSI flagship meetings. A Young Scientist Award is primarily a recognition of the scientific value of the work presented in the paper submitted by the young researcher. The award links to financial support through waiving registration fees, in some cases also providing accommodation or even travel support when originating from specific and selected countries.

To qualify for an award the applicant:

- must be less than 35 years old on September 1 of the year (2021) of the URSI General Assembly and Scientific Symposium;
- should have a paper, of which he or she is the principal author, submitted and accepted for oral or poster presentation at a regular session of the General Assembly and Scientific Symposium.

Applicants should also be interested in promoting contacts between developed and developing countries. Applicants from all over the world are welcome, including from regions that do not (yet) belong to URSI. All successful applicants are expected to participate fully in the scientific activities of the URSI flagship meetings.

Applications are assessed by the URSI Young

Scientist Panel, taking into account the national ranking of the application and the technical evaluation of the paper by the relevant URSI Commission. During the selection process, application or granted Young Scientists Awards at the occasion of previous URSI flagship meetings are not considered, except in the final stage when a proper balance is sought among Commissions and geographical locations.

After the call for the Young Scientist Awards of the URSI GASS 2021, 181 applications from 30 countries were received through an online application procedure.

1.2 Selection Process

The selection process was carried out in four steps:

1. The URSI Secretariat checked eligibility (first author, age limit, submission of required documents, acceptance of paper, etc.). One candidate was removed from the list in this step, as the candidate was not eligible.

2. The Chair, Vice Chair, and ECRs of each of the 10 URSI Commissions were asked to rank the applicants who submitted a paper in one of the sessions organized in their Commission, purely based on the scientific merit of the work presented in the paper.

3. In parallel, the Member Committees were asked to rank the applicants originating from their country or region based on local, practical, technical, or other issues.

4. The rankings by the Commissions and the Member Committees were combined in a score by the Young Scientist Panel to come to a final selection, considering a proper balance over the 10 URSI Commissions, a proper geographical balance, as well as a gender balance. During this final step, it was always ensured that the selected awardee had a paper of significant technical value, and in some specific cases the Young Scientist Panel also considered the comments provided by the reviewers during the reviewing process for all submitted papers at the GASS 2021. One candidate had submitted two papers, and was scored based on the best-ranked paper.

Finally, the Young Scientist Panel submitted a list of 95 awardees to the URSI Board. After careful consideration, the URSI Board approved the proposed selection and all awardees were contacted. The deadline for acceptance of the Young Scientist Award was set as 15 May 2021.

1.3 Young Scientist Awardees

Al-Behadili, Hasanain	Iraq
Barman, Kheyali	India
Biswas, Sanat K	India
Bonnafont, Thomas	France
Capannolo, Luisa	USA
Caramazza, Laura	Italy
Chakraborty, Rohit	India
Chakraborty, Sumanjit	India
Chakraborty, Arnab	India
Chartier, Alex	USA
Chen, Ke	China
Chen, Rui	Saudi Arabia
Colella, Micol	Italy
D'Agostino, Simona	Italy
Dalarsson, Mariana	Sweden
Das, Bakul	India
Das, Barnali	India
De, Arijit	India
Deb, Priti	India
Dinleyen, Serhat	Turkey
Dutta, Shweta	USA
Fathnan, Ashif	Indonesia
Faul, Fabian	Germany
Fetescu, Mirela	The Netherlands
Galiffi, Emanuele	UK
Gao, Yuan	China
Geng, Yangliao	China
Goode, Ian	Canada
Guha, Bijay	India
Hanzelka, M.	Czech Republic
Hsieh, Yikai	Japan
Ištuk, Niko	Ireland
Jana, Debasis	India
Kakoti, Geetashree	India
Kalita, Jyotirmoy	India
Kapusuz, Kamil	Belgium
Katsko, Sofiia	Ukraine
Kishimoto, Seiya	Japan
Kossenas, Konstantinos	UK
Kuniyil, Viswanathan	India
Labate, Giuseppe	Italy
Lasisi, Shakirudeen	UK
Liu, Ming	China
Liu, Xiaokang	Italy
Liu, Zhuoyang	China
Liu, Sen	Japan
Lodi, Matteo Bruno	Italy
Ma, Qianli	USA
Martynova, V.	Russian Federation
Mathur, Phalguni	India
Maxim, S.	Russian Federation
Methapettyparambu, J.	France
Mishra, Vigyanshu	USA
Moss, Vanessa	Australia
Motroni, Andrea	Italy
Mukherjee, Anwesha	India
Nanni, Jacopo	Italy
Niotaki, Kyriaki	France
Palazzi, Valentina	Italy
Palmer, Elizabeth	USA
Pavone, Santi Concetto	Italy
Pignalberi, Alessio	Italy
Plavin, A.	Russian Federation

Pu, Wei	UK
Rajwade, Kaustubh	UK
Raveendran, Athira	India
Rodini, Sandra	Italy
Ryabkova, M.	Russian Federation
Said Camilleri, Jeantide	Malta
Sao Jose, Artur	France
Shirokov, E.	Russian Federation
Shoaib, Nosherwan	Pakistan
Singh, Amit Kumar	India
Singh, Kuldeep	India
Sinha, Shipra	India
Slevin, Edward	USA
Surco Espejo, Teddy	Brazil
Thomas, Evan G.	USA
Thummaluru, S. Reddy	India
Urbani, Michele	Spain
Vakalis, Stavros	USA
Vital, Dieff	USA
Wang, Xuchen	Finland
Wang, Zhaoyang	Switzerland
Xu, Hanyang	China
Yang, Ying	China
Yepes, Cristina	Italy
You, Li	China
Zhang, Hao	China
Zhang, Xingqi	Ireland
Zhang, Xiao-Jia	USA
Zhou, Fuhui	China
Zhou, Yiwen	New Zealand
Zhu, Liang	USA
Zubair, Muhammad	Pakistan

1.4 Statistics on Diversity

Table 1 provides an overview of the distribution by Commission, indicating the applications received, the selected awardees, and the acceptance rate.

Commis-sion	Total App.	Selected	Acc. Rate
A	9	3	33.3%
B	53	27	50.9%
C	9	6	66.7%
D	17	9	52.9%
E	5	4	80.0%
F	27	13	48.1%
G	17	10	58.8%
H	17	9	52.9%
J	9	6	66.7%
K	16	8	50.0%
Total	**179**	**95**	**53.1%**

Table 1. The distribution of Young Scientist awardees by Commission

Region	Total App.	Selected	Acc. Rate
Asia-Pacific	10	6	60.0%
China	22	10	45.5%
Europe	64	39	60.9%
India	49	21	42.9%
Middle East	7	5	71.4%
Americas	27	14	51.9%
Total	**179**	**95**	**53.1%**

Table 2. Geographical distribution of Young Scientist awardees

To provide an overview of the geographical spread of the Young Scientist Awardees, each of them was assigned to a region as shown in Table 2. To allow a better interpretation, some countries from which a large number of Young Scientists originated were listed separately from their region (in this case, China (CIE), China (SRS), and India).

Based on the information provided by the applicants, the gender balance shown in Table 3 was obtained.

1.5 Follow-Up on Young Scientist Selection

The names, as well as pictures, affiliations and a link to the submitted papers, are available on the URSI Web site. Starting from the first day of the GASS 2021, an extra link was provided to each of the presentations by the Young Scientists until the end of the view-on-demand period of the pre-recorded presentations. The Young Scientist certificates were handed over to the Young Scientists at the GASS 2021 for those who were physically present in Rome, and were mailed to those who could not be present.

The applicants received free registration, and if they were physically present on site, financial support for board and lodging at the General Assembly and Scientific Symposium. The Young Scientists who were present in Rome were also invited to the Young Scientist Party. As the GASS 2020 Young Scientists were deprived from any financial reward linked to their award, the URSI Board decided that if they attended the GASS 2021, the GASS 2020 Young Scientist Awardees could register as students (with reduced fee) and were welcome to join the GASS 2021 Young Scientist Party.

Gender	Total App.	Selected	Acc. Rate
Male	120	64	53.3%
Female	59	31	52.5%
Total	**179**	**95**	**53.1%**

Table 3. Gender Balance of Young Scientist awardees

1.6 Conclusion

This report provided a summary of the process and the outcome of the selection for the GASS 2021 Young Scientists. Being aware of the specific situation with respect to the postponement of the GASS 2020 as a physical conference and the fact that GASS 2021 was a hybrid meeting, the URSI Board took specific measures to try to keep the Young Scientists program active, as this is one of the pillars and activities within URSI that distinguishes us from other scientific unions. By providing these awards and publicizing this information and these awards through the Web site and social media, the URSI Board has the intention to keep young researchers interested in URSI and to keep the events organized and supported by URSI.

The Board thanks all the individuals involved in this program and selection process, and congratulates all Young Scientist Awardees.

2. Student Paper Competition at the URSI GASS 2021

George Uslenghi, General Chair of the URSI General Assembly in Chicago in 2008, was instrumental in motivating URSI to initiate the URSI international Student Paper Competition (SPC) and in encouraging the United States National Committee for URSI (USNC-URSI) to fund the prizes. The Student Paper Competition at the URSI General Assembly and Scientific Symposium (GASS) 2021 was once again financially sponsored by the United States National Committee (USNC) for URSI. This was the eighth international URSI Student Paper Competition sponsored by the USNC-URSI: six at URSI GASS and two at AT-RASC.

There were 46 eligible applicants for the Student Paper Competition. The rules for the Student Paper Competition were published on the URSI GASS 2021 Web site, and they are repeated here.

The rules for the Student Paper Competition were as follows:

- The first author and presenter must be a full-time university student.

- The topic of the paper must be related to the field of one of the ten URSI Commissions.

- A full paper, not longer than 10 pages and not shorter than four pages in single-column, single-spaced format, meeting the requirements of the Student Paper Competition paper URSI template, must be submitted by January 31, 2021.

- Each student is allowed to submit one paper only for the Student Paper Competition.

- The student must also submit either an Extended Abstract or a Summary Paper version of the paper at the same time the full paper is submitted.

- Applicants to the 2020 GASS Student Paper Competition will not be eligible to participate with the same paper.

- Submissions should be made through the URSI GASS 2021 online paper submission system, with the appropriate box (indicating the Student Paper Competition) being checked during the paper submission.
- The full paper will be evaluated within the competition and will not be published to ensure that there are no subsequent prior-publication issues for those students who wish to submit the work to a journal. This means that the ten-page paper will not be included in the conference proceedings. Only the shortened version will appear in the conference proceedings.

- A paper that is submitted to a journal before submission to the student competition is ineligible. However, students are encouraged to submit their papers to a journal after January 31, 2021.

- A letter from the student's advisor on university letterhead must be uploaded with the full paper. The letter must state that the author is enrolled as a full-time university student in a degree program. If the paper is coauthored, the letter must state that all coauthors played only an advisory role. No other students are permitted as coauthors.

Commission Chairs or their representatives served as the jury in the process of selecting the finalists, and later in selecting the cash prize winners. Each member of the jury recommended three expert reviewers for each paper submitted in his or her Commission. Each reviewer provided a thorough review of each paper. The criteria used by reviewers were the quality, originality, and scientific merit of the paper. Each reviewer gave an overall score between 1 and 5, 5 being the best. The top 18 papers were subsequently selected based on the average reviewers' score for each paper. These 18 papers had an average score of 4.25 or better. The jury then ranked these papers from 1 to 18, 1 being the best. The jury had access to reviewers' comments and scores. Ten finalists were chosen based on the ranking of the jury and they were invited to present their papers. All the finalists were recognized at the awards banquet.

Because of the COVID-19 pandemic, the URSI GASS 2021 was organized in hybrid mode, allowing the Student Paper Competition finalists to present in person or virtually. Each finalist had 20 minutes for the presentation of the paper and five minutes for questions and answers. The finalist presentations were ranked based on clarity of the presentation, adherence to time, accessibility to the broad audience of the ten URSI Commissions, and the ability to answer questions on the work.

The top five award winners were:

1. First Prize ($1500): Edward Slevin, Georgia Institute of Technology, Atlanta, GA, USA, "Wideband VLF/LF Transmission from an Electrically-Small Antenna by Means of Time-Varying Non-Reciprocity via High-Speed Switches" (Commission B).

2. Second Prize ($1250): David Rodriguez, Politecnico di Torino, Torino, Italy, "Microwave Brain Imaging System Validation via Realistic Experiments" (Commission B).

3. Third Prize ($1000): Barnali Das, National Centre for Radio Astrophysics, TIFR, Pune, India, "Coherent Radio Emission from Main Sequence Pulsar: Introducing a New Stellar Diagnostic" (Commission J).

4. Fourth Prize ($750): Sandra Rodini, University of Pisa, Pisa, Italy, "A Contactless Measurement of the Surface Impedance of a Thin Sheet of Material" (Commission D).

5. Fifth Prize ($500): Clément Henry, Politecnico di Torino, Torino, Italy, "On the Solution of the Brain-to-Skull Contrast Breakdown with a New Integral Scheme: Mathematical Framework and Medical Application Scenarios" (Commission B).

The following finalists, in alphabetical order, received honorable mention:

6. Miroslav Hanzelka, Institute of Atmospheric Physics, Czech Academy of Sciences, Czech Republic, "Assessing the Measurability of Perturbations in Electron Velocity Distribution Caused by Nonlinear Interaction with Chorus Subpackets" (Commission H).

7. Devojyoti Kansabanik, National Centre for Radio Astrophysics, TIFR, Pune, India, "Unraveling the Eclipse Mechanism for Black Widow Pulsar J1544+4937 Using Broad Band Radio Spectrum" (Commission J).

8. Makoto Kitahara, Tokyo Metropolitan University, Tokyo, Japan, "Investigation on the Human Body Exposure to the Magnetic Fields Owing to Wireless Power Transmission System with the Sandwiched Structure" (Commission D).

9. Shakirudeen Lasisi, University of Nottingham, Nottingham, UK, "On the Inclusion of Thin Sheets in the Global Multi-Trace Method" (Commission B).

10. Shipra Sinha, Indian Institute of Geomagnetism, Mumbai, India, "Cosmic Noise Absorption Characteristics During the Impulse-Induced Supersubstorm of 21st January 2005" (Commission H).

Several people were thanked for contributing to the success of the Student Paper Competition. Inge Lievens provided support throughout this process, often working in the evenings and weekends. Koyama Yasuhiro, Nuno Borges Carvalho, Naoki Shinohara, Kazuya Kobayashi, John Volakis, Yves Louet, Amir Zaghloul, Apostolo Georgiadis, Arnaud Vena, Asghari Hossein, Frank Gronwald, Virginie Deniau, Chaouki Kasmi, V. Chandrasekar, Patricia Doherty, Janos Lichtenberger, Jyrki Manninen, Richard Bradley, Joe Wiart, and Koichi Ito provided valuable services as the jury. Numerous reviewers provided expert reviews of all papers. Peter Van Daele, Alain Sibille, and Carlo Carobbi helped with the organization of the Student Paper Competition. Inge Heleu prepared and sent the certificates to the awardees. Ana Ferreras and James Manning of the National Academies of Sciences, Engineering, and Medicine in the United States processed the checks for the top five awardees.

IUCAF Annual Report for 2021

1. Introduction

The Scientific Committee on Frequency Allocations for Radio Astronomy and Space Science, IUCAF, was formed in 1960 by its adhering Scientific Unions, IAU, URSI, and COSPAR, at the behest of URSI. The IUCAF brief is to study and coordinate the requirements of radio-frequency spectrum allocations for passive radio sciences – radio astronomy, space research, and remote sensing – and to make these requirements known to the national and international bodies that regulate the use of the radio spectrum.

IUCAF operates as an Affiliated Body of the International Science Council (https://council.science/what-we-do/affiliated-bodies/). IUCAF is a Sector Member of the International Telecommunication Union's Radiocommunication Sector (ITU-R), with observer status at the Space Frequency Coordination Group (SFCG) (see https://www.sfcgonline.org/home.aspx). IUCAF is online at http://www.iucaf.org.

2. Membership and Member Affiliations with Other Bodies

There was no change in the composition of IUCAF during 2021. IUCAF is still seeking a replacement IAU committee member for one that resigned in 2018. At the end of 2020, the IUCAF membership from the three adhering Unions was as shown in Table 1. Additionally, the Counselor for ITU-R Study Group 7 (Science Services), Mr. Vadim Nozdrin, is an ex-officio member by virtue of his ITU-R position, as specified in IUCAF's Terms of Reference. IUCAF also has an informal group of correspondents, in order to improve its global geographic representation and for consultation on specific issues, for instance concerning astronomical observations in the optical and infrared domains.

URSI	Dr. Haiyan Zhang	China
	Dr. Steven Reising	USA
	Dr. Ingemar Häggström	Sweden
	Dr. Anastasios Tzioumis	Australia
	Dr. Wim van Driel	France
IAU	Dr. Harvey Liszt (Chair)	USA
	Dr. Masatoshi Ohishi	Japan
	Dr. Adrian Tiplady	South Africa
COSPAR	Dr. Yasuhiro Murata	Japan

Table 1. The IUCAF membership from the three adhering Unions at the end of 2020.

IUCAF members also participate in the activities of other bodies. Tiplady is a member of CRAF, the European Committee on Radio Astronomy Frequencies of the European Science Foundation (https://www.craf.eu/). Zhang is Chair of the Radio Astronomy Frequency Committee in the Asia-Pacific region (RAFCAP), whose members also include Ohishi and Tzioumis (see http://www.atnf.csiro.au/rafcap/). Tzioumis is Chair of ITU-R Working Party 7D (Radio Astronomy). Ohishi, IUCAF's Immediate Past Chair, is the official liaison between the IAU and the ITU, and is the immediate past President of IAU Commission F3 (Astrobiology). He is Head of the Spectrum Management Office at the National Astronomical Observatory of Japan. Van Driel was until recently the Secretary of IAU Commission B4 on Radio Astronomy and a member of its Organizing Committee. Liszt is a member of the American Astronomical Society's Committee on Light Pollution, Radio Interference and Space Debris, and the IAU Executive Committee on WG Dark and Quiet Sky Protection, and served on the Steering Committee of the IAU Inter-Division Commission C.B4 on Protection of Existing and Potential Observatory Sites.

3. IUCAF Terms of Reference (Revised 2015)

A revision to the statement of IUCAF's composition, operating practices, and Terms of Reference (TOR), originally dating to 1972 when IUCAF was the Inter-Union Committee on Allocation of Frequencies, was approved by ICSU's Executive Board in 2015 (http://www.iucaf.org/IUCAF_Terms_Of_Reference.pdf).

4. International and Regional Spectrum Management Meetings Attended by IUCAF Members During 2020

Radio-frequency spectrum management meetings were moved online during 2021. IUCAF participated in the international and regional regulatory meetings shown in Table 2.

IUCAF submitted three documents containing four compatibility studies to these ITU-R Working Party meetings:

To WP1A, Document 1A/143 (https://www.itu.int/md/R19-WP1A-C-0143/en) "Proposed revisions to preliminary draft new Report ITU-R SM. [WPT.BEAM.IMPACTS] – Impact studies and human hazard issues for wireless power transmission via radio frequency beam,"

03/01-03/12	Working Party 5D (IMT=Mobile Telecom)	ITU-R
04/12-04/16	Working Party 7D (Radio Astronomy)	ITU-R
05/10-05/21	Working Party 5B (Radar and airborne mobile)	ITU-R
05/20-05/21	Committee on Radio Frequencies – CORF	US NAS
05/25-06/02	Working Party 1A (Spectrum engineering)	ITU-R
06/07-06/18	Working Party 5D	ITU-R
09/16-09/23	Working Party 7D	ITU-R
10/04-10/15	Working Party 5D	ITU-R
11/03-11/12	Working Party 1A	ITU-R
11/29-12/10	Working Party 5B	ITU-R

Table 2. The international and regional regulatory meetings in which IUCAF participated.

concerning potential interference from out-of-band emissions into the spectrum band 23.6 GHz to 24 GHz that is reserved for passive radio science, originating in proposed use of an ISM band at 24.1 GHz for wireless device charging.

To WP5B, Document 5B/418 (https://www.itu.int/md/R19-WP5B-C-0418/en) "Proposed update on working document towards a preliminary draft new Report ITU-R [NON-SAFETY AMS CHARACTERISTICS AND SHARING NO STUDIES] related to agenda item 1.10 - Technical characteristics, operational scenarios, spectrum needs, coexistence, and sharing studies of non-safety aeronautical mobile systems in the frequency bands 15.4-15.7 GHz and 22-22.21 GHz," detailing interference from proposed airborne wireless mesh networks into the adjacent bands at 15.35 GHz to 15.4 GHz (reserved for passive radio science) and 22.21 GHz to 22.5 GHz (allocated to radio astronomy).

To WP5D, Document 5D/788 (https://www.itu.int/md/R19-WP5D-C-0788/en) "Proposed update on the working document towards sharing and compatibility studies of HIBS under agenda item 1.4 - Compatibility between HIBS and the radio astronomy service operating in the frequency band 2 690-2 700 MHz," detailing interference from proposed use of IMT base stations on high-altitude platform systems circulating at 20 km altitude.

Members also participated in national spectrum-management proceedings, working in their capacities as spectrum managers at their respective observatories.

5. IUCAF Business Meetings

IUCAF business was discussed by e-mail as matters arose during the year 2021.

6. Finances

The IUCAF budget is held and managed by URSI. Sustaining financial contributions of €5,000, €2,000, and €1,000 were gratefully received from IAU, URSI, and COSPAR, respectively, for calendar year 2021.

7. The IUCAF Role

IUCAF is a global forum where spectrum management concerns of passive radio science in all ITU-R Regions are regularly addressed in a comprehensive manner. The group is expert in the underlying science, in the spectrum-management needs of the science, and in the workings of the spectrum-regulatory regime that allocates spectrum and makes the rules for radio-spectrum use. IUCAF has supported radio astronomy and passive radio science in Geneva since its inception in 1960, when the first spectrum band was allocated for exclusive use by passive research.

IUCAF's 60th birthday was observed in 2020 at the Fifth International IUCAF School on Spectrum Management in Stellenbosch, South Africa, which was described in the 2020 Annual Report. IUCAF's early history was recounted by Dr. Brian Robinson in "Frequency Allocation: The First Forty Years" (*Annual Reviews of Astronomy and Astrophysics*, **37**, 1999, pp. 65-96, available at https://tinyurl.com/y5vsgb6x).

The practice of reserving narrow portions of the radio-frequency spectrum for radio astronomy expanded after 1960, so that bands shared by radio astronomy and satellite remote sensing now provide crucial information used to improve weather forecasting and to quantify the effects of climate change. On this basis, IUCAF also provides an interface between the radio-astronomy and satellite-remote-sensing communities via the Space Frequency Coordination Group. IUCAF is currently participating in the SFCG's Lunar Martian Spectrum Group that is planning the use of radio communications on and around the Moon, and most especially, in the Shielded Zone of the Moon: the volume of space that is shielded from view of the Earth and protected for scientific use by international treaty, in the form of the ITU-R Radio Regulations.

8. Contact with ISC, the IUCAF Sponsoring Unions (IAU, URSI, COSPAR), and Other International Organizations

IUCAF maintains regular contact with its adhering Unions and the parent body, ISC. These organizations play a strong supporting role for IUCAF, the members of which are thereby greatly encouraged.

The major international conference, "Dark and Quiet Skies II for Science and Society" (http://research.iac.es/congreso/quietdarksky2021/), sponsored by the IAU, the UN Office of Outer Space Affairs, the Government of Spain, and the Instituto de Astrofisica de Canarias, was about to occur in person on La Palma during October 3 to 7, 2021, when eruption of a volcano on the island (!) forced the organizers to move the meeting online at the last minute. Over 1000 registrants attended online in numbers of a few hundred on each of five days, the last of which was largely devoted to radio astronomy. IUCAF members Liszt and Ohishi represented radio astronomy on the Scientific Organizing Committee, and supervised the update of the radio-astronomy working group report (https://noirlab.edu/public/products/techdocs/techdoc051/) that was presented on the final day of the recent meeting. The D&QS II meeting produced documents for consideration at the 2022 session of the Scientific and Technical Subcommittee (STSC) of the Committee on Peaceful Uses of Outer Space (COPUOS), as noted on their website at https://www.unoosa.org/oosa/en/ourwork/copuos/stsc/2022/index.html.

The Dark and Quiet Skies meetings were of special importance because they formulated recommendations outside the usual ITU-R regulatory regime that protects only the very small amount of radio spectrum that is formally allocated to astronomy and other passive science. The Dark and Quiet Skies meetings considered risks to astronomy of all kinds across the electromagnetic spectrum, and concluded that satellites in low Earth orbit should refrain from illuminating radio telescopes and radio-quiet zones at all radio frequencies, with specific recommendations to accomplish this goal.

IUCAF participated remotely in the 2021 URSI GASS. The URSI Council requested an updated report covering the period since 2017, and it can be accessed at https://www.cv.nrao.edu/~hliszt/URSI/IUCAF-ReportToCouncil_2017-2021.docx.

The IUCAF Chair delivered a presentation on spectrum matters.

9. 94 GHz Coordination Agreement with the European Space Agency (ESA)

Since 2005, NASA JPL has operated the 94.05 GHz CloudSat cloud-profiling radar in the middle of a broad swath of spectrum that is allocated to and heavily used by radio astronomy. The powerful kW beam of this nadir-pointing radar saturates any receiver over which the satellite passes during its 16-day repeating orbital cycle, independent of the radio-astronomy antenna pointing. More seriously, the radar could burn out the radio-astronomy receiver in the worst case. A variety of modifications to radio-astronomy operations and instruments have been made on this account, especially for moveable-array antennas that are transported in a zenith-pointing orientation with their super-cooled electronics operating. The unstable operations of this aging satellite have necessitated several last-moment accommodations on the part of radio astronomy.

To forestall this situation when ESA, with participation from the Japanese Space Agency, JAXA, launches the EarthCare mission in 2023 with an even-higher-power 94 GHz radar, IUCAF has for many years participated as an observer in meetings of the Space Frequency Coordination Group (SFCG), where EarthCare and other high-power radars were discussed. This 15-year effort bore fruit in April 2021, when ESA and IUCAF signed a Memorandum of Understanding under which the EarthCare radar will be silenced when its beam passes close enough to a radio-astronomy antenna that the radio-astronomy receiver could be damaged.

IUCAF is grateful to ESA for agreeing to modify the EarthCare radar's operation, to JAXA for designing the radar in such a way that such an accommodation was possible, and to NASA, which facilitated coordination by providing calculations and other support at SFCG.

The agreement may be accessed at the IUCAF website (http://www.iucaf.org/).

10. Outreach, Training, and the Sixth International IUCAF School on Spectrum Management for Radio Astronomy

IUCAF maintains its World Map of Radio Astronomy Sites and Radio Quiet Zones that has been viewed 70,000 times since its creation in 2008 (see http://tinyurl.com/yrvszk). IUCAF continued to distribute its exceptionally popular IUCAF-logo fidget-spinner, thanks to a continuing grant from an anonymous donor. IUCAF is in the early planning stage for the Sixth International School on

Spectrum Management for Radio Astronomy that will occur in the Asia Pacific Region in 2025. Presentations from the Fifth School in Stellenbosch in 2020, and earlier IUCAF schools, are available on the IUCAF website (http://www.iucaf.org/)

11. IUCAF Concerns in 2021 and Beyond

Until recently, improved access to spectrum for science ran through the radio-frequency spectrum regulatory regime, by procuring and protecting allocated spectrum. However, the tables have turned. Allocations to science are fixed while the radio spectrum fills in with new radio communication systems, such as high-power radars onboard satellites, collision avoidance radars on cars, 5G mobile phones, and broadband WiFi. Radio-spectrum regulators authorize satellite mega-constellations in low Earth orbit that have turned the dark and quiet night sky into a circus of artificially-generated radiation. Satellite trails from reflected sunlight are increasingly affecting optical/infrared astronomy, even from the Hubble Space Telescope that currently shows satellite trails in some 8% of its images. It was just such considerations, and the inability to raise them at ITU-R, which motivated IUCAF involvement in the Dark and Quiet Skies meetings. Concerns originating with radio communications and radio-spectrum management have now spilled over into far wider concerns for the health of the environment that radio-spectrum regulators are ill-equipped to handle.

Closer to home, succession planning and matters of engagement continue to be of concern. Many nations with major investments in radio astronomy and strong histories of participation are not currently represented by astronomers in spectrum management, despite IUCAF prodding.

12. Acknowledgements

IUCAF is grateful for the organizational and financial support that has been given by ICS, IAU, URSI, and COSPAR over the past 60 years, especially the URSI Secretariat. IUCAF also recognizes the support given by radio-astronomy observatories, universities, and national funding agencies to individual IUCAF members, allowing them to participate in the vital work of the committee. IUCAF especially appreciates the contributions of the organizations and individuals who made the last spectrum-management school such a resounding success in 2020, just as the world was about to shut down.

Harvey Liszt, Chair
Charlottesville, Virginia, USA
E-mail: hliszt@nrao.edu, iucafchair@iucaf.org

INTERNATIONAL SYMPOSIUM ON ELECTROMAGNETIC THEORY (URSI EMTS 2023)

22-26 May 2023, Vancouver, BC, Canada

First Call for Papers

The International Symposium on Electromagnetic Theory (EMTS 2023) will be held from 22-26 May 2023 at the University of British Columbia in Vancouver, BC, Canada. The third largest metropolitan area in Canada, Vancouver is known for its stunning natural beauty, cosmopolitan atmosphere, friendly people, and attractions like Stanley Park, English Bay, Granville Island, the North Shore mountains, and Whistler. Vancouver International Airport (YVR) is only 20 minutes by car from UBC.

Organized by Commission B (Fields and Waves) of the International Union of Radio Science (URSI), EMTS 2023 is sponsored by the Canadian National Committee of URSI (CNC-URSI) and technically co-sponsored by the IEEE Antennas and Propagation Society. Since it was first organized in Montreal in 1953, this is the 24th event in the triennial series of EMTS symposia,

EMTS 2023 will focus on electromagnetic fields and their applications. The conference will offer plenary talks by distinguished speakers, regular oral and poster sessions, a one-day summer school (May 22), and several scientific and industrial tours and workshops. A number of Young Scientist Awards that cover the registration fee and accommodation during the conference will be offered. In addition, business meetings, receptions, and a conference banquet will be organized.

Contributions on any aspect within the scope of Commission B are solicited. Some suggested topics are listed below. The authors may submit an extended abstract of at least 250 words in length in single-column format not exceeding one page or a two to four-page summary in IEEE two-column format. Special-session topics will be listed later on the conference website. All submissions will be reviewed by the Commission B Technical Advisory Board. Accepted and presented summaries may be submitted to IEEE Xplore while the extended abstracts will not be published in IEEE Xplore.

General Chair: Prof. David Michelson, *The University of British Columbia,* davem@ece.ubc.ca

Technical Program Chair: Prof. John Volakis, *Florida International University*, jvolakis@fiu.edu

Special Sessions Chair**:** Prof. Lot Shafai, *University of Manitoba*, lot.shafai@umanitoba.ca

Important Dates

- Paper submission site opens: August 15, 2022
- Deadline for paper submission: **December 15, 2022**
- Notification of acceptance: January 10, 2023
- Early-bird and author registration ends: March 31, 2023

Suggested Topics

1. Electromagnetic theory
- Analytical and semi-analytical methods
- Mathematical methods in electromagnetics
- Scattering and diffraction
- Inverse scattering and imaging
- Propagation and materials in electromagnetics
- Quantum techniques
- AI/ML and optimization methods

2. Computational methods
- Integral equation methods
- Partial differential equation methods
- High-frequency and hybrid methods
- Fast solvers and high-order methods
- Time-domain techniques
- Computational algorithms
- Nonlinear electromagnetics

3. Materials and wave-material interaction
- Metamaterials and metasurfaces
- New materials for electromagnetics.
- Plasmonics and nano-electromagnetics
- Electromagnetic bandgaps and other periodic structures
- Optical devices
- EMC and EMI
- Electromagnetics in biology and medicine

4. Antennas and propagation
- Antenna theory
- Antenna measurements
- Multi-band and wideband antennas
- Antenna arrays and MIMO systems
- Wireless communication systems
- Guided waves and structures
- Random media and rough surfaces
- Millimeter wave/5G propagation
- Millimeter-wave antennas
- MIMO for 5G /6G communication
- Vehicular, marine and automotive RF links

5. Other topics
- Wireless data and power transfer
- Wireless sensors for IoT
- History of electromagnetics
- Education in electromagnetics

www.emts2023.org

URSI Accounts 2021

Introduction by the URSI Secretary General

The basis of the income for URSI lies in the contributions by the URSI Member Committees, contributing in line with their "unit of contribution" and in line with their impact in Council. In addition to these contributions, and in order to be able to face new challenges, explore new possibilities or covering increased costs, efforts have been made to explore possible new resources from meetings through the establishment of yearly URSI Flagship meetings. These Flagship meetings constitute, in a three-year cycle, the URSI General Assembly and Scientific Symposium (GASS), the Atlantic Radio Science Conference (AT-RASC) and the Asia-Pacific Radio Science Conference (AP-RASC). Besides the indications that this will be of a financial benefit in the future, this has also fulfilled one of the main objectives of URSI, namely serving our community. From a scientific point of view, these yearly Flagship have been a major success and encouraging from a financial point of view.

The COVID-19 pandemic has disrupted the normal way of operations for URSI, as has been the case for many amongst us on a personal level as well as on a professional level. This pandemic, from which we are now gradually recovering, has forced us, just as other organizations, to re-consider the concept used for our Flagship meetings. These scientific conferences, being one of the cornerstones of URSI activities in bringing researchers, young scientists, and experts together in a multidisciplinary way from all over the world to interact, discuss and plan future activities, had disappeared and were re-invented in a "corona-proof" concept. Now that the "in-person" meetings are possible again, we have been experiencing the eagerness of people and colleagues to come back to these conferences and again, share and discuss experiences. The COVID-19 pandemic has taught us how much we rely on human contact and personal interactions in our professional as well as private lives.

The pandemic however changed the format in which we organize the conferences and how we offer access to participants from our community. The hybrid format, used by many conferences nowadays, by which both on-site as well as online participation is possible, is becoming a standard but organizers are still struggling in finding the right formula for ensuring the proper added value for online participants as social activities, poster sessions, interactive sessions, Q&A sessions... are more difficult or even impossible to implement. Many of these features require dedicated software, extra audiovisual equipment, additional staff... and consequently, rapidly increasing costs for organizing a conference. This will be a major challenge in trying to make our URSI Flagship meetings into profitable events.

All of the initiatives taken over the past few years, such as the Flagship meetings, the Radio Science Letters, the Young Scientists Programme, the individual membership… all contribute to the creation of an URSI community and serve our colleagues, scientists, young researchers... but consume part of the assets accumulated over many years. URSI has indeed accumulated substantial reserves in the past, allowing us to invest, but as the recent years and events illustrate, this should be handled with great care and cautiousness, to not compromise the long-term future of URSI.

As you may realize from the balance shown below, there seems to be an increase in the income and expenditure of URSI comparing to the previous years. However, this is only because of the fact that the secretariat now also actively supports organizers of URSI-supported conferences, besides the URSI Flagship meetings, with software and staff for paper submission and registration. This implies that registration for those conferences pass through URSI accounts but are immediately transferred back to the organizers. This process relates to the new and updated way URSI supports conferences and meetings, which was decided upon at the 2017 GASS in Montreal but gradually implemented, with some delay due to the COVID-19 pandemic. It creates an additional workload on the URSI Secretariat but has again been proven to be a valuable service to our community.

Besides the need to carefully take care of the financial aspect in running an organization such as URSI, it is also necessary to stress the tremendous amount of voluntary work done by all the URSI officers, Commission representatives and individuals within the URSI community supporting URSI. This commitment of our scientific community to URSI is crucial in the success of URSI and cannot be underestimated. It remains to be said that only thanks to this commitment, URSI is still in a financially healthy situation and able to perform its main objective: attracting researchers, with emphasis on young researchers helping them to successfully launch their careers, giving them the opportunity to present their work and facilitating their participation in a free exchange of scientific results in a worldwide community of radio scientists.

Prof. Peter Van Daele
Secretary General of URSI

Balans URSI			2021	2020	2019	2018
ASSETS						
	Installations, Machines & Equipment		0,00	0,00		2.633,83
	Dollars en andere					
		Fortis - USD rekening	3.000,94		118,98	137,46
		Fortis - CAD rekening	0,00	0,00	0,00	64.622,60
		Fortis - GBP	34.342,10		0,00	0,00
		Fortis - JPY	0,00		0,00	0,00
		Paypal USD	15.589,00		0,00	0,00
			52.932,04		118,98	64.760,06
	Euro’s					
		Banque Degroof	0,00	0,00	0,00	0,00
		Fortis Zichtrekening	241.078,68			46.871,42
		Fortis Spaarrekening	692,87	692,87	692,87	692,87
		BNP Paribas 001-6726585-02	7,33			32.049,25
		BNP PARIBAS 001-8740096-84	0,27	0,57	0,57	0,00
		Paypal	1.581,52	691,32	691,32	0,00
			243.360,67			79.613,54
	Investments					
		Demeter Sicav Shares/DPAM BL EMU	0,00	0,00	0,00	22.681,79
		Rorento units/ Robeco GLBL Total Return	0,00	0,00	0,00	111.995,67
		Aqua Sicav/ DPAM MML MON	0,00	0,00	0,00	63.785,56
		Effectenportefeuille BNP Paribas				381.000,00
						579.463,02
		652 Rorento units on behalf of Van Der Pol Fund	0,00			11.833,55
						591.296,57
	Petty Cash		182,96	208,39	208,39	126,49
	Total Assets					738.430,49
	Less Creditors					
		IUCAF	42.024,86			34.750,50
		ISES	5.053,53			5.053,53
		RFI	5.588,11	0,00	0,00	0,00
			-52.666,50			-39.804,03
		Van der pol medal fund	0,00			-11.833,55
		Basu medal fund	0,00			-4.216,35
		Paid Remuneration	9.293,94			6.752,90
NET TOTAL OF URSI ASSETS						689.329,46
The net URSI Assets are represented by:						
	Closure of Secretariat					
		Provision for closure of secretariat	135.000,00			115.000,00
			135.000,00			115.000,00
	Scientific Activities Fund					
		Provision for Scientific activities	60.000,00			60.000,00
		Provision for Routine Meetings	15.000,00			20.000,00

Provision for publications	40.000,00			40.000,00
Provision for administration	105.000,00			105.000,00
Provision for I.C.S.U / ISC dues	6.000,00			6.000,00
	226.000,00			231.000,00
Flagship Meetings				
Provision for GASS	120.000,00			120.000,00
Provision for AT-RASC	120.000,00			30.000,00
Provision for AP-RASC	30.000,00			30.000,00
Total allocated URSI assets	631.000,00			526.000,00
Unallocated Reserve Fund	716.274,59			163.329,46
				689.329,46
Statement of Income and expendatiture for the year ended 31 December				
INCOME				
Contr. nat. members (year -1)	8.614,00			35.918,00
Contr. nat. members (year)	184.945,22			177.890,30
Contr. nat. members (year +1)	21.900,00			8.510,00
Income general assembly 2014	0,00	0,00	0,00	0,00
Income GASS	104.110,78	0,00		168.100,25
Income AT - RASC	0,00	0,00	0,00	254.405,98
Income AP - RASC	0,00	0,00	0,00	0,00
Support Conf. Org. - general	0,00		0,00	0,00
Support Conf. Org. - ECIO	0,00	0,00		0,00
Support Conf. Org. - BSS	0,00	0,00		0,00
Support Conf. Org. - ECOC	234.250,20		0,00	0,00
Support Conf. Org. - Benelux Forum	0,00	0,00		0,00
Support Conf. Org. - RFI	0,00	0,00	0,00	0,00
Publications	4.656,55		0,00	0,00
Bank interests	0,00	0,00	0,00	0,00
Other Income	8.053,74			7.432,40
Total Income	566.530,49			652.256,93
EXPENDITURE				
A1) Scientific Activities	267.596,20			391.797,22
General Assembly	48.102,50			16.789,02
Mid Term Meetings 2015				
AT RASC	7.718,29			339.052,60
AP RASC	7.718,29			28.806,01
Support Conference organistation	200.806,54			0,00

Schientific meetings: symposia/col-loqiua	3.250,58			5.239,93
Represantation at scientific meetings	0,00	0,00		1.909,66
Other				
A2) Routine Meetings	0,00			285,20
Brueau/Executive committee	0,00			285,20
Other				
A3) Publications	52.900,96			34.105,06
B) Other Activities	6.055,00			5.821,00
Contribution to I.C.S.U / I.S.C.	4.055,00			3.821,00
Contribution to other I.C.S.U. /I.S.C. bodies	2.000,00			2.000,00
C) Administrative Expenses	177.264,53			128.537,62
Salaries, Related Charges	138.473,68			99.535,91
General office expenses/administra-tion	2.286,68			1.693,71
Travel and representation expenses	390,00			5.918,34
Insurances/Communications/Gifts	10.828,54			8.013,33
Office Equipment				
Audit / Accountancy fees	7.624,01			6.170,42
Tax / Legal advice	1.357,85		0,00	0,00
Bank charges	4.868,12			5.888,99
Depreciation	0,00			1.316,92
Loss on Investments (realised/unre-alised)	11.435,65	0,00	0,00	0,00
Total Expenditure	503.816,69			560.546,10
Excess of Expenditure over Income	62.713,80	-198,53		91.710,83
Currency differences	-292,63			-7.185,67
Positive Currency differences	8.266,49	0,00	8,83	4.392,33
Currency translation diff. (USD=>EURO) - Others				
Accumulated Ballance at 1 Januari				600.411,97
				689.329,46
ADDITIONAL INFORMATION				
Rates of exchange				
January 1				
USD - 0,8243 EUR				
CAD - 0,6849 EUR				
GBP - 1,1128 EUR				
JPY - 0,0079 EUR				
December 31				
USD - 0,8830 EUR				

CAD - 0,6849 EUR				
GBP - 1,1911 EUR				
JPY - 0,0077 EUR				
Balthasar Van der Pol Fund				
652 Robeco Global (formerly Rorento Shares):				
Market value on December 31	0,00			37.457,40
(Aquisition Value: USD 14.175,00/EUR 11.833,55)				
Book Value on December 31	0,00			11.833,55
Market Value of investments on December 31				
DPAM EMU (formerly Demeter Sicav Shares)	0,00	0,00	0,00	94.832,10
Robeco Global (formerly Rorento Units)(1)	0,00	0,00	0,00	720.720,00
DPAM MML MON (formerly Aqua-Sicav)	0,00	0,00	0,00	89.156,20
Bonds	0,00			381.000,00
	0,00			
Book Value on December 31				591.296,57
(1) Including the 652 Rorento Shares of v d Pol Fund				
APPENDIX				
Detail of Income and Expenditure				
I. INCOME				
Other Income				
Other Income - Bonds	8.053,74			7.432,40
	8.053,74			7.432,40
II. EXPENDITURE				
General Assembly				
GASS Organisation	12.991,20			15.025,34
Van der pol Medal	432,25	0,00	0,00	0,00
GASS - Basu Award	417,14	0,00	0,00	0,00
GASS - President’s Award	208,12	0,00	0,00	0,00
GASS - Young Scientists	0,00	0,00	0,00	0,00
GASS - Officials	15.854,98	0,00	0,00	0,00
Support Commissions	18.198,81	236,00	0,00	1.763,68
	48.102,50			16.789,02
AT RASC				
AT RASC Organisation	7.718,29			228.957,77
AT RASC Young Scientists	0,00	0,00	0,00	25.930,98
AT RASC Officials	0,00	0,00	0,00	41.744,55
Support Commissions	0,00	0,00	0,00	42.419,30
	7.718,29			339.052,60

AP RASC					
	AP RASC Organisation	7.718,29			28.806,01
	AP RASC Young Scientists	0,00	0,00	0,00	0,00
	AP RASC Officials	0,00	0,00		0,00
	Support Commissions	0,00	0,00		0,00
		7.718,29			28.806,01
Support Conference Organisation					
	Support Conference Organisation	750,00	0,00	0,00	0,00
	Support Conf. Org. - ECOC	200.056,54			0,00
	Support Conf. Org. - Benelux Forum	0,00	416,44		0,00
		200.806,54			0,00
Routine Meetings					
	Routine meetings: board meeting	0,00			285,20
		0,00			285,20
Symposia/Colloquia/Working Groups					
	Meeting support Commission B	0,00	0,00		0,00
	Meeting support commission F	0,00	0,00	0,00	0,00
	Meeting support commission G	0,00			0,00
	Meeting support commission H	0,00		0,00	1.700,00
	Meeting Support Commission J	0,00	0,00		0,00
	Meeting supp centr fund (Student award MC)	3.250,58			3.539,93
		3.250,58			5.239,93
Contribution to other ICSU bodies					
	Contribution to other I.C.S.U. /I.S.C. bodies	2.000,00			2.000,00
		2.000,00			2.000,00
Publications					
	Publications / Website	52.900,96			34.105,06
		52.900,96			34.105,06

URSI Conference Calendar

July 2022

COSPAR 2022
44th Scientific Assembly of the Committee on Space Research (COSPAR) and Associated Events
Athens, Greece, 16-24 July 2022
Contact : GREECE COSPAR 2022 Secretariat, Fax: +30 2103643511, E-mail: info@cosparathens2022.org , https://www.cospar-assembly.org/assembly.php

September 2022

EMC Europe 2022
Gothenburg, Sweden, 5-8 September 2022
Contact : EMC Europe 2022 Secretariat: info@emceurope2022.org, Conference Chair: Prof. Jan Carlsson jan.carlsson@emceurope2022.org, https://www.emceurope2022.org/

ICEAA - IEEE APWC
Cape Town, South Africa, 5-9 Sept 2022
Contact : E-mail: iceaa22@iceaa.polito.it; https://www.iceaa-offshore.org/

December 2022

URSI - RCRS 2022
IIT, Indore, India 01 - 04 December, 2022
2022 URSI Regional Conference on Radio Science
Contact: Dr Abhirup Datta, Convener, URSI-RCRS 2022, E-mail: abhirup.datta@iiti.ac.in, https://sites.google.com/iiti.ac.in/rcrs2022

August 2023

URSI GASS 2023
XXXVth URSI General Assembly and Scientific Symposium 2023
Sapporo, Hokkaido, Japan, 19 - 26 August 2023
Contact: URSI Secretariat, c/o INTEC, Tech Lane Ghent Science Park - Campus A, Technologiepark-Zwijnaarde 126, B-9052 Gent, Belgium, E-mail info@ursi.org

August 2025

AP-RASC 2025
Asia-Pacific Radio Science Conference 2025
Sydney, Australia, August 2025
Contact: Prof. Paul Smith, Macquarie University, Australia, E- mail paul.smith@mq.edu.au

A detailed list of meetings is available on the URSI website at http://www.ursi.org/events.php

Information for Authors

Content

The *Radio Science Bulletin* is published four times per year by the Radio Science Press on behalf of URSI, the International Union of Radio Science. The content of the *Bulletin* falls into three categories: peer-reviewed scientific papers, correspondence items (short technical notes, letters to the editor, reports on meetings, and reviews), and general and administrative information issued by the URSI Secretariat. Scientific papers may be invited (such as papers in the *Reviews of Radio Science* series, from the Commissions of URSI) or contributed. Papers may include original contributions, but should preferably also be of a sufficiently tutorial or review nature to be of interest to a wide range of radio scientists. The *Radio Science Bulletin* is indexed and abstracted by INSPEC.

Scientific papers are subjected to peer review. The content should be original and should not duplicate information or material that has been previously published (if use is made of previously published material, this must be identified to the Editor at the time of submission). Submission of a manuscript constitutes an implicit statement by the author(s) that it has not been submitted, accepted for publication, published, or copyrighted elsewhere, unless stated differently by the author(s) at time of submission. Accepted material will not be returned unless requested by the author(s) at time of submission.

Submissions

Material submitted for publication in the scientific section of the *Bulletin* should be addressed to the Editor, whereas administrative material is handled directly with the Secretariat. Submission in electronic format according to the instructions below is preferred. There are typically no page charges for contributions following the guidelines. No free reprints are provided.

Style and Format

There are no set limits on the length of papers, but they typically range from three to 15 published pages including figures. The official languages of URSI are French and English: contributions in either language are acceptable. No specific style for the manuscript is required as the final layout of the material is done by the URSI Secretariat. Manuscripts should generally be prepared in one column for printing on one side of the paper, with as little use of automatic formatting features of word processors as possible. A complete style guide for the *Reviews of Radio Science* can be downloaded from http://www.ips.gov.au/IPSHosted/NCRS/reviews/. The style instructions in this can be followed for all other *Bulletin* contributions, as well. The name, affiliation, address, telephone and fax numbers, and e-mail address for all authors must be included with All papers accepted for publication are subject to editing to provide uniformity of style and clarity of language. The publication schedule does not usually permit providing galleys to the author.

Figure captions should be on a separate page in proper style; see the above guide or any issue for examples. All lettering on figures must be of sufficient size to be at least 9 pt in size after reduction to column width. Each illustration should be identified on the back or at the bottom of the sheet with the figure number and name of author(s). If possible, the figures should also be provided in electronic format. TIF is preferred, although other formats are possible as well: please contact the Editor. Electronic versions of figures *must* be of sufficient resolution to permit good quality in print. As a rough guideline, when sized to column width, line art should have a minimum resolution of 300 dpi; color photographs should have a minimum resolution of 150 dpi with a color depth of 24 bits. 72 dpi images intended for the Web are generally *not* acceptable. Contact the Editor for further information.

Electronic Submission

A version of Microsoft *Word* is the preferred format for submissions. Submissions in versions of T_EX can be accepted in some circumstances: please contact the Editor before submitting. *A paper copy of all electronic submissions must be mailed to the Editor, including originals of all figures.* Please do *not* include figures in the same file as the text of a contribution. Electronic files can be send to the Editor in three ways: (1) By sending a floppy diskette or CD-R; (2) By attachment to an e-mail message to the Editor (the maximum size for attachments *after* MIME encoding is about 7 MB); (3) By e-mailing the Editor instructions for downloading the material from an ftp site.

Review Process

The review process usually requires about three months. Authors may be asked to modify the manuscript if it is not accepted in its original form. The elapsed time between receipt of a manuscript and publication is usually less than twelve months.

Copyright

Submission of a contribution to the *Radio Science Bulletin* will be interpreted as assignment and release of copyright and any and all other rights to the Radio Science Press, acting as agent and trustee for URSI. Submission for publication implicitly indicates the author(s) agreement with such assignment, and certification that publication will not violate any other copyrights or other rights associated with the submitted material.

Become An Individual Member of URSI

The URSI Board of Officers is pleased to announce the establishment of categories of individual membership of URSI. The purpose of individual membership of URSI is to secure professional recognition of individual radioscientists and to establish their better connection with the URSI Board of Officers, Scientific Commissions, and URSI Member Committees. Three categories of individual membership (URSI Corresponding Member, URSI Senior Member and URSI Fellow) have been established.

URSI Corresponding Membership is the first step into the URSI community and provides:

- Access to the proceedings of URSI Flagship Conferences via the Web site
- Notifications of new editions of URSI publications.

In addition, URSI Senior Members and URSI Fellows benefit from the following:

- Reduced registration fees at URSI Flagship Meetings.
- Reduced registration fees at some meetings organized by partnering organizations such as (but not limited to) IEEE AP-S and EuCAP.
- A page charge reduction from 175 USD to 150 USD for papers published in the URSI journal, Radio Science Letters.
- An invitation to receive their individual membership certificate at an URSI Flagship meeting.

Fellowship is by invitation only; Senior Membership can be by invitation or application. Corresponding Membership is a streamlined, instant process. Details, and an online application for URSI Senior Membership, are available at http://www.ursi.org/membership.php#tab-sectionA1.